



Emissions and impact on air quality of PM and BC in Saporanga, Rio Grande do Sul - field campaign and model assessment 2014

report elaborated by

Fundação Estadual de Proteção Ambiental Henrique Luiz Roessler

Prefeitura Municipal de Saporanga

Universidade Federal de Pelotas

Centro Mario Molina Chile

Swedish Meteorological and Hydrological Institute

August 13, 2015

CONTENT

CONTENT	2
1 EXECUTIVE SUMMARY	3
2 INTRODUCTION	7
3 METHODS	11
3.1 METEOROLOGICAL INFORMATION	12
3.2 AIR QUALITY DATA	14
3.3 EMISSION INVENTORY	19
3.4 REGIONAL DISPERSION MODELING	31
3.5 LOCAL DISPERSION MODELING	33
4 RESULTS	35
4.1 METEOROLOGICAL MEASUREMENTS	35
4.2 AIR QUALITY MONITORING RESULTS	38
4.3 REGIONAL DISPERSION MODELING	54
4.4 LOCAL DISPERSION MODELING	58
4.5 INTEGRATED ANALYSIS OF EMISSIONS AND IMPACT	65
5 CONCLUSIONS	74
6 RECOMMENDATIONS	75
7 ACKNOWLEDGEMENTS	77
8 REFERENCES	77

Project team and co-authors:

- Cecilia Bennet and Lars Gidhagen (SMHI)
- Márcio D'Avila Vargas, Flávio Wiegand and Ismael Luís Schneider (FEPAM)
- Daniela Saft, Andrea Diana Oberherr, Fabiana Haubert and Cláudio Kreuning (Prefeitura Municipal de Sapiranga)
- Anderson Spohr Nedel, Marcelo Alonso and Glauber Mariano (UFPeI)
- Patricia Krecl (UTFPR)
- Matías Tagle, Ximena Díaz and Pedro Oyola (Centro Mario Molina Chile)

Contact: Lars Gidhagen (lars.gidhagen@smhi.se)

1 Executive summary

Atmospheric particles of inhalable size, often quantified as the mass of particles with a diameter less than 10 (PM10) or 2.5 (PM2.5) micrometer, have been associated with health effects in urban populations. Except for the health impact, the particles include light-absorbing soot – in what follows referred to as black carbon (BC) – which is an important short-lived climate pollutant (SLCP) that contributes to global warming.

Sweden and Brazil have signed a Memorandum of Understanding to cooperate in the fields of environmental protection, climate change and sustainable development. Within this framework, the Swedish Meteorological and Hydrological Institute (SMHI) and Fundação Estadual de Proteção Ambiental Henrique Luiz Roessler (FEPAM), have initiated a technical cooperation to assess the sources of particle and black carbon emissions in Brazilian cities. This report documents the results of a pilot project focusing the emissions of PM2.5 and BC in the city of Saporanga and the impact of those emissions on air pollution levels. The pilot project also received strong support and collaboration from Universidade Federal de Pelotas, Universidade Tecnológica Federal do Paraná (UTFPR), Centro Mario Molina Chile and the Prefeitura Municipal de Saporanga.

We applied an integrated approach that combines monitoring of air pollution levels, building-up of an emission inventory of relevant species, and modeling the dispersion of atmospheric pollutants. The monitoring campaign was conducted from July 31 to August 29, 2014 in Saporanga and included measurement of chemical composition and physical properties of fine particles at three fixed stations - one in the city center and the other two in residential areas - and two meteorological stations were deployed to register weather conditions.

In parallel an emission database was created. Traffic volumes were determined on major roads, through traffic counts and by using statistics from road tolls. In order to quantify the use of residential wood combustion, a survey was performed among all school children, in total 7876 responded to a questionnaire about the use of wood combustion in their homes. Particle emissions from major industrial and commercial sources were estimated from activity data shared by local institutions/persons and emission factors found in the literature.

Dispersion modeling was performed on three scales: The regional model delivered the particles transported from sources outside Saporanga, mainly from urban emissions in the Porto Alegre Metropolitan area and from vegetation fires north of the city. An urban scale model simulated the impact of local sources in and close to Saporanga and a street canyon model was used to capture the traffic impact in the city centre.

Results

Levels of fine particles in Sapiranga are comparable or slightly higher than those reported from the Metropolitan area of Porto Alegre. There is no limit value for fine particles in Rio Grande do Sul, but the annual average PM_{2.5} levels determined in Sapiranga are at the limit value for the São Paulo legislation (20 µg/m³). Therefore it is of interest to identify the main sources to the fine particle pollution in Sapiranga.

The measurements and model simulations show that the background air arriving to Sapiranga is, as an average over a year, responsible for 65-70% of the pollution within the city. Sources outside Sapiranga are found in particular in the urbanized areas between Porto Alegre and Sapiranga, but there are also frequent vegetation fires to the north of the city that generates significant particle pollution during parts of the year. In Sapiranga center (station T) wood combustion, used in connection with commercial/industrial activities as well as for heating and cooking in residential areas, contribute to about 22% and local traffic exhaust for the remaining 9% of the measured PM_{2.5} level. In some residential areas, exemplified with São Luiz where station L was located, RWC is the dominating local source to PM_{2.5} (25% contribution to measured PM_{2.5} level for RWC, 32% for all local wood combustion sources). The RWC contribution is even more accentuated during winter conditions; for example in August 2014 it rose to 43% at station L. The mobile monitoring campaign indicates that conditions can be similar in other residential areas of Sapiranga. The strong spatial and temporal variations in the use of RWC contribute to a wide interval in the estimated emissions of PM_{2.5} and BC (Table ES1).

Table ES1. Estimated annual average emissions of PM_{2.5} and BC in Sapiranga for 2014 (tons/year)

Source	PM _{2.5}	BC	BC/PM _{2.5} ratio	comments
brick production	20	1.4	7%	<i>outside the city</i>
charcoal production	202	14.1	7%	<i>outside the city</i>
traffic exhaust	12	7.8	65%	<i>inside the city</i>
residential wood combustion	4-26	0.3-1.8	7%	<i>inside the city</i>
restaurants	42	2.9	7%	<i>inside the city</i>
Industry	83	5.8	7%	<i>inside the city</i>
Total inside city:	140-163	16-18		
Total Sapiranga:	363-385	32-34		

Estimated source contributions are illustrated in Figure ES1.1 (PM_{2.5}) and ES1.2 (BC).

For BC the annual mean levels are estimated to be between 1.5 to 2.5 µg/m³, with a more dominating contribution from traffic exhausts, although RWC also contributes significantly in residential areas like at station L.

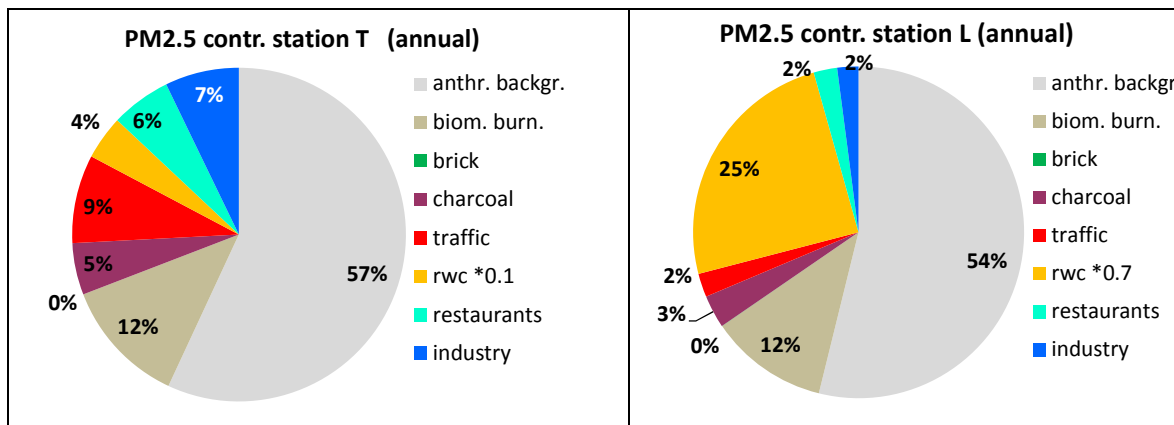


Figure ES1.1 Estimated contributions of different PM2.5 sources for the year 2014, according to the integrated analysis of monitor data and model simulations. Simulated annual average for PM2.5 were 18.6 $\mu\text{g}/\text{m}^3$ (station T) and 19.7 $\mu\text{g}/\text{m}^3$ (station L).

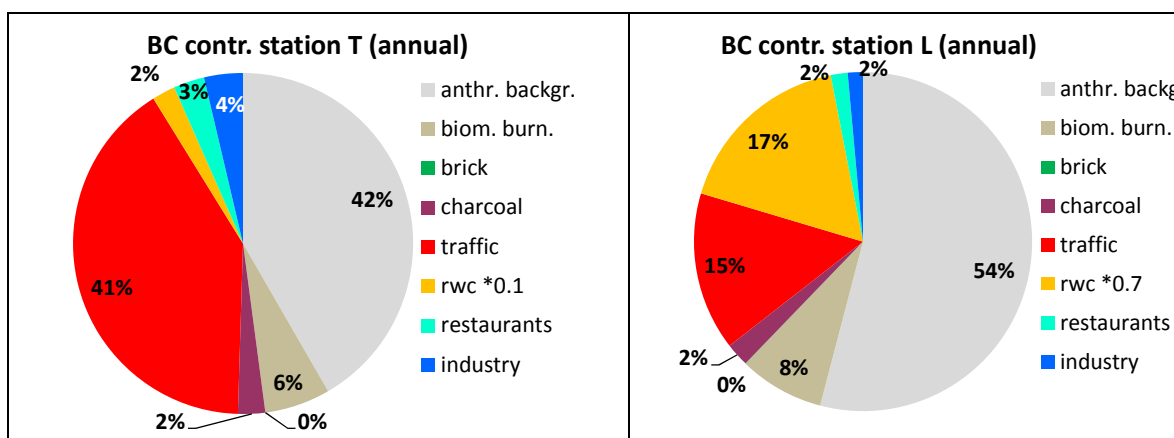


Figure ES1.2 Estimated contributions of different BC sources for the year 2014, according to the integrated analysis of monitor data and model simulations. Annual mean BC levels were estimated to 2.3 $\mu\text{g}/\text{m}^3$ at station T and 1.8 $\mu\text{g}/\text{m}^3$ at station L.

Recommendations

The main objectives with the Sapiranga pilot project were to estimate the emissions of fine particles and black carbon, and determine the impact of those emissions on the air quality in the city. With those results as a basis, there are possibilities to identify actions and measures that can reduce both emissions and pollution levels. The report discusses some areas where actions could contribute to lower the air pollution levels in Sapiranga.

1. Actions in the Porto Alegre Metropolitan area: About half of the air pollution in Sapiranga is caused by sources in Porto Alegre, Novo Hamburgo and other urbanized areas outside Sapiranga itself. Prioritized actions in the Rio Grando do

Sul state should focus a renewal of the heavy duty diesel vehicle fleet, the most polluting industrial sources, especially metallurgic industry, waste burning, and open biomass burning.

2. Industrial/commercial sources in Sapiranga: All of those, representing charcoal and brick production as well as restaurants, use wood combustion with a rather old technology and without cleaning the exhaust gases. Improved operation with higher energy efficiency and use of dry wood could have positive effects on the emissions and should be requested. Wherever possible a change to cleaner fuels should be encouraged.
3. Residential sources: Burning of waste and garden residues outside in gardens or streets could be an important source of pollutants and should be minimized. The use of residential wood combustion for heating and cooking is fairly common in many residential areas. Actions to improve the operation and technology of those fireplaces, as well as to replace the wood combustion with cleaner fuels like gas and electricity, would imply efficient ways to reduce particle pollution in the city.
4. Road traffic: The use of older diesel vehicles is known to be a large source of particles and especially Black Carbon. A brand new heavy duty vehicle emits about 2% of an old vehicle and the emission reduction among vehicles produced before the year of 1999, as compared to those produced after 1999, is at least 50%. If all heavy duty vehicles from before 1999 were replaced by vehicles from 2000 the reduction of the traffic PM emission would be 40%, if they were replaced by vehicles produced after 2012 the reduction would be 80%.

2 Introduction

Atmospheric particles of inhalable size, often quantified as the mass of particles with a diameter less than 10 (PM10) or 2.5 (PM2.5) micrometer, are linked to strong health effects on urban populations. Except for the health impact, the particles include light-absorbing soot – in what follows referred to as black carbon (BC) – which is an important short-lived climate pollutant (SLCP) that contributes to global warming.

The transport sector, in particular through diesel fueled heavy duty vehicles, constitutes an important source for particles and soot in ambient air. Another important source is residential wood combustion for cooking and space heating. Apart from these two sources, represented in many Swedish and Brazilian cities, combustion processes like burning of agricultural waste, forest fires and industrial processes with poor technology can also deteriorate the air quality as a consequence of their high particle emissions. For all these combustion sources, and in particular for those that impact urbanized areas, there are strong synergy effects won on health and climate by reducing PM and BC emissions.

The Swedish Ministry of Environment maintains and searches for bilateral cooperation with environmental authorities in other countries. In November 2013, a Memorandum of Understanding to cooperate in the fields of environmental protection, climate change and sustainable development was signed between the Swedish and Brazilian Ministries of Environment. One of the listed areas of cooperation is air pollution monitoring and control, as well as pollution abatement and prevention of black carbon and tropospheric ozone.

Sweden and Chile have been cooperating to improve the air quality in Santiago and other Chilean cities over the last two decades. During 2013 the Swedish Ministry of Environment funded a bilateral cooperation between the Swedish Meteorological and Hydrological Institute (SMHI) and the Chilean Ministry of Environment focusing on emissions and impact of PM and BC from residential wood combustion in Southern Chile. The funding to SMHI included the task to seek similar air quality cooperation with Brazil. During a workshop held in August 2013, a cooperation project was formulated between SMHI and the regional environmental authority in Rio Grande do Sul State, Fundação Estadual de Proteção Ambiental Henrique Luiz Roessler (FEPAM). Together SMHI and FEPAM formulated a pilot project to assess emissions and impact of PM and BC within a typical mid-sized city in the region, Sapiranga. The results of this pilot project are presented in this report. The Sapiranga project also involved the Prefeitura Municipal de Sapiranga and air quality experts from the Universidade Federal de Pelotas (UFPEL), Universidade Tecnológica Federal do Paraná (UTFPR) and Centro Mario Molina Chile.

General objectives

- Cooperation on methodologies to quantify atmospheric emissions and assess the impact on air pollution levels of particles (PM_{2.5} and black carbon) in Brazilian cities.
- Support Brazilian authorities in their effort to reduce the exposure to high PM levels and to adhere to the *Climate and Clean Air Coalition* (CCAC) initiatives aiming at reducing short-lived climate pollutant emissions like black carbon.

Specific objectives

- To perform an assessment of PM and BC emissions in the city of Sapiranga.
- To determine present concentration levels and contributions from local and regional sources.

Sapiranga city

Sapiranga city is located in the Rio dos Sinos Valley some 60 km northeast of Porto Alegre, capital city of Rio Grande do Sul State. The region belongs to the Atlantic Forest bioma and consists of an extensive area of lowlands between the Shield of Rio Grande do Sul (towards Uruguay) and the escarpments of the Basalt Plateau towards the north (limiting to the Santa Catarina State). Some Sapiranga facts are found in Table 2.1.

Table 2.1: Facts for Sapiranga city (Instituto Brasileiro de Geografia e Estatística, 2014)

State:	Rio Grande do Sul
Inhabitants:	79 152
Area:	138 km ²
Demographic density:	542 inhabitants per km ²
Human Development Index (HDI):	0.711
Gross Domestic Product (GDP):	R\$ 992 millions
GDP per capita:	R\$ 12 800
Export (2010):	US\$ 164 millions
Employments:	24 900 persons
Employments within industry sector:	16 430 persons

Sapiranga, with a highest altitude of 650 m, has a moderately warm climate with an annual mean temperature of 20 °C and a seasonal difference of about 10 °C (Fig. 2.1). Precipitation is present all through the year with an annual precipitation between 1400 and 1600 mm. The climate is characterized as **Cfahn** according to the Köppen classification, which means moderately warm without dry season, with high temperatures during summer

and mild winters with frequent forming of mist. The seasonal variations are presented in Fig. 2.2.

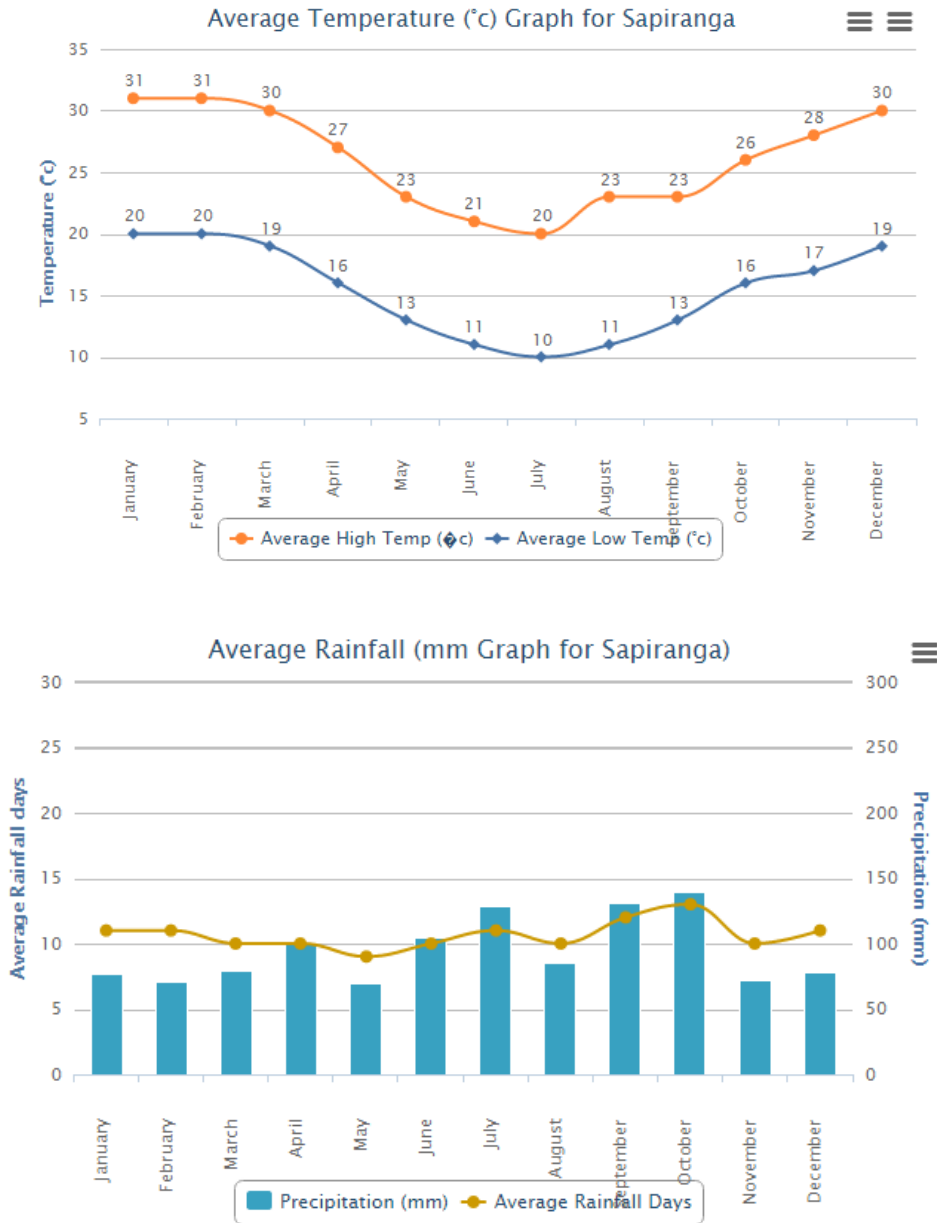


Figure 2.2: Climatological conditions in Sapiranga expressed as monthly mean values

The origins of Sapiranga city date back to the early nineteenth century, when the lands of the then colony of San Leopoldo began to be occupied by German immigrants which gave Sapiranga a rural character. Today Sapiranga is predominantly urban with an important center for footwear industry. The city still includes rural areas dedicated to forestry (mostly

black acacia) and the production of other commodities of agricultural and horticultural origin (English yam, rice, cassava and fruit varieties).

One aspect that differentiates the Sapiranga municipality in the Brazilian context is the frequent use of bicycles. The Municipal Department of Transit estimates that more than 40,000 bikes circulate in Sapiranga, contributing to the city being referenced as the "city of bicycles".

Overview of reported tasks

This report describes the results obtained during 2014 which include a monitoring campaign, the development of an emission inventory for primary particulate matter and dispersion modeling calculations. More specifically we will report the following tasks:

- A two month campaign to generate local meteorological information from the city.
- A one month monitoring campaign to measure PM mass and number concentration levels together with some PM constituents, i.e. BC, elemental carbon (EC), organic carbon (OC) and elemental composition.
- Regional dispersion modeling to describe background PM levels in the air masses arriving to Sapiranga.
- Build-up of an emission inventory for major PM sources located inside Sapiranga.
- Urban and local dispersion modeling based on local meteorology and with input from PM sources identified in the emission inventory.
- An integrated analysis based on the information generated by the different activities.

3 Methods

This section describes the methods used for monitoring the air pollution levels, building-up an emission inventory and the dispersion modeling employed to calculate the atmospheric dispersion of the emitted pollutants. The basic approach used to estimate the PM2.5 and BC emissions together with their impact on air quality is illustrated in Fig. 3.1:

1. Use local activity data and emission factors from the literature to create an emission inventory for the sources that are expected to contribute most to PM2.5 and BC levels (traffic, wood combustion, industry etc)
2. Conduct a monitoring campaign to collect PM2.5 and BC concentrations in areas where different sources are expected to dominate. In parallel perform regional dispersion modeling to look for long range transport signals that can contribute to the total concentrations as registered by Sapiranga monitors. Perform concurrent measurements of local meteorology.
3. Use dispersion models with input of local meteorology and atmospheric emissions from the inventory (1) to create maps showing the theoretical effect of the emissions in the inventory. Compare model results with monitored data and conclude on the magnitude of the emissions. Major differences should imply modifications of emissions until an acceptable resemblance between simulated and monitored levels are obtained. In this way we can assess and control the quality of the emission inventory.



Figure 3.1 Concept for validating emissions (see point 1-3 above)

After having a credible emission inventory it is possible to perform scenario modeling, which means changes in the emissions inventory that reflect certain actions, e.g. improved technology for dominating sources or replacement of polluting activities that contributes to PM2.5 and BC reductions. The model will give quantitative estimates of the effect of different actions. The present report describes the work conducted in 2014 and does not include scenario modeling.

An overview over the monitoring activities is given in Fig. 3.2. The two meteorological stations were located above roofs. The T (traffic) station was located on a balcony facing the city centre street with most traffic. The stations L (residential area with wood combustion) and B (background) were both measuring at roof level.

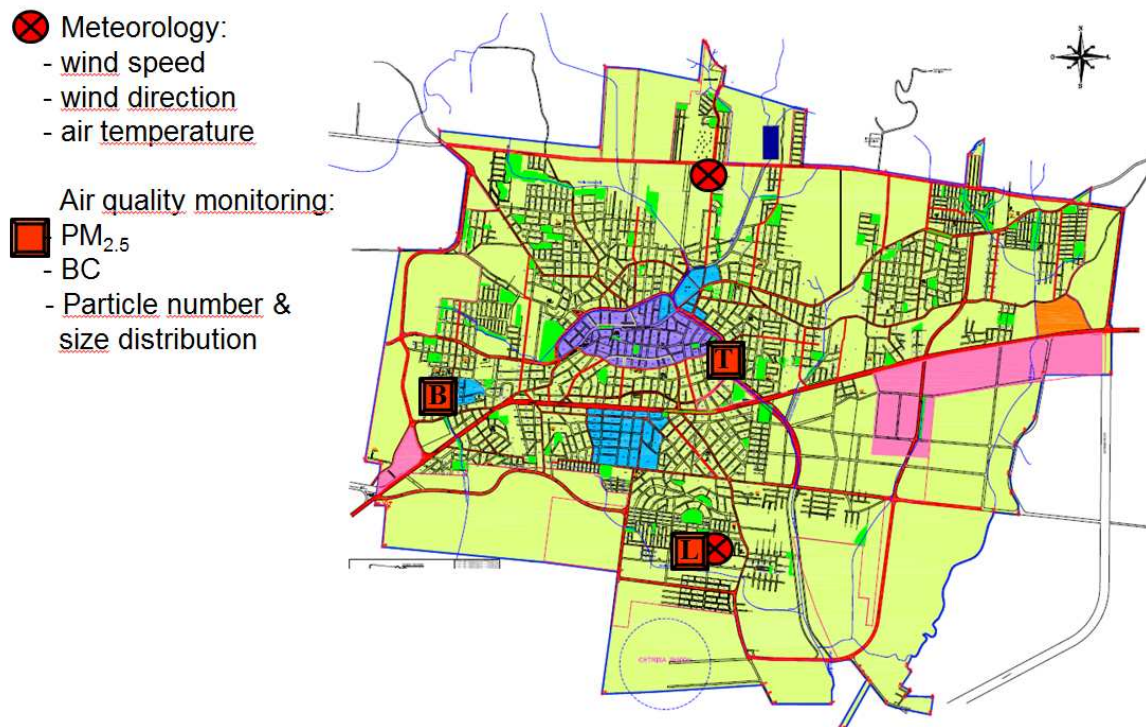


Figure 3.2 Map over Sapiranga showing locations for air quality monitoring (stations T, L and B) and stations for meteorological measurement.

3.1 Meteorological information

Two automatic stations *Wireless Davis Vantage Pro2* were installed at rooftop level in Sapiranga. One station was installed on a 5 m high pole at the roof of the Fire Department, in the north region, and another one was located together with the air quality monitoring station L in an urban area in the south of the city (Fig. 3.2). Weekly maintenance was conducted to download data and change batteries. The measurement period was from June 16 to September 08. The meteorological stations recorded 15-minute measurements of wind direction and speed, air temperature, barometric pressure, relative humidity and precipitation (Table 3.1.1).

There is also a permanent meteorological station in “Campo Bom” belonging to the National Institute of Meteorology (INMET), from which data are publically available online. The station is situated about 12 km SW of Sapiranga (Fig. 3.1.2). Besides the basic meteorological fields of automatic equipment, the “Campo Bom” station also reports radiation (in kJ/m²). Some synoptic cloudiness data were also gathered from Porto Alegre.



Figure 3.1.1 Locations of automatic meteorological stations: Fireplace Department (right) and Station “L” (left).

Table 3.1.1 Meteorological data specifications.

Variable	Resolution	Range	Nominal Accuracy (+/-)
Barometric pressure	0.1 hPa	540 to 1100 hPa	1.0 hPa
Precipitation rate	0.2 mm	up to 2438 mm/hr	greater of 5% or 1 mm/hr
Temperature	0.1°C	-40°to +65°C	0.5°C
Humidity	1%	1 to 100%	3% RH; 4% above 90%
Wind Direction	1°	0 to 360°	Intervals of 22.5°
Wind Speed (large cups)	0.4 m/s	1 to 80 m/s	greater of 1 m/s or 5%

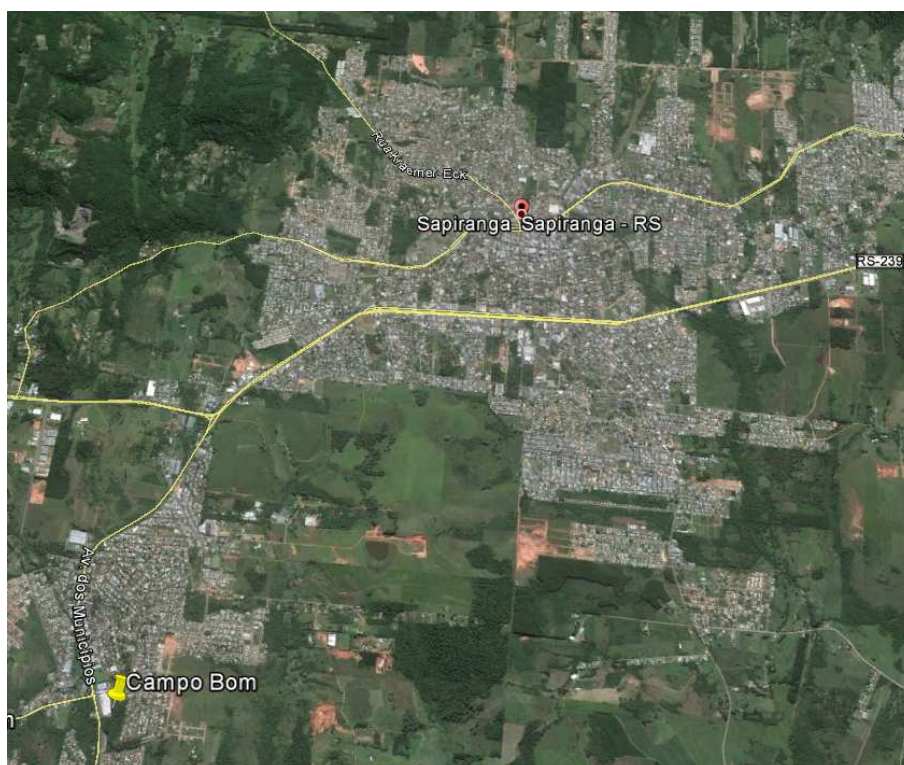


Figure 3.1.2 Location of the Campo Bom meteorological station (lower left).

3.2 Air quality data

PM2.5 monitoring was accomplished with three types of instruments:

- Harvard Impactor (2 units, station T and L, the reference instruments for PM monitoring during this campaign)
- DustTrak (2 units, station T, L and B plus event mapping at ~20 stations)
- BAM monitor (1 unit, station B)

BC was measured with micro-aethalometers at station T and L plus mapped at ~20 stations covering the entire Sapiranga city. EC/OC and elemental composition were analyzed from Harvard Impactor filters at station T and L. Particle number size distributions were monitored at the sampling sites T, L and B.

Harvard Impactor

PM2.5 samples for subsequent elemental analysis and mass concentration were collected in parallel on 37 mm teflon filters and 37 mm quartz filters on a daily basis, using Harvard Impactors operated with an air flow of 4 liters per minute (LPM). In this instrument, the

ambient air is pumped through a nozzle, where the air flow and particles are accelerated. The air flow is directed towards an impaction plate and diverted along a defined path. The particles are diverted along the air flow, with the deflection angle depending on the mass of the particle and its velocity. Heavier particles deviate less and hit the plate, while the lighter particles flow until being collected on the filter. In this study we used a nozzle designed to measure particles less than or equal to $2.5\ \mu\text{m}$ in aerodynamic diameter when operated at a flow of 4 LPM (Marple et al., 1987). The air flow rate was checked daily with a digital flowmeter (Challenger, BGI).

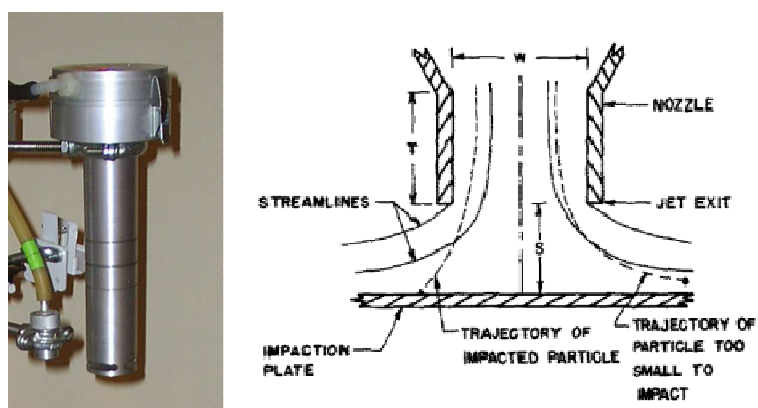


Figure 3.2.1 Harvard Impactor device for PM_{2.5} (left). Operating diagram of an impactor (right), Marple et al., 1976.

For mass determination, the filters were analyzed by a gravimetric procedure at the Environmental Chemistry Laboratory of Harvard School of Public Health (HSPH). The quantification of chemical elements was determined using X-Ray Fluorescence Spectroscopy (XRF) on Teflon filters, at the same laboratory. The XRF analyses were performed by a PANalytical Epsilon 5 XRF analyzer, which reports elemental concentrations for 51 elements, ranging from sodium (Na) through lead (Pb). For further analysis, we considered only those elements whose measured values were at least 2 times the reported uncertainty on at least 80% of the samples.

Samples for EC and OC analysis were collected on pre-fired (850 °C, 3 h) quartz fibre filters and were analyzed by a thermal-optical transmittance method (TOT) following a NIOSH temperature protocol at HSPH. Quartz filters were kept under low temperature and light conditions, until they were analyzed at laboratory.

The Harvard Impactor is not a designated class II equivalent PM_{2.5} sampler by the U.S EPA. Centro Mario Molina Chile has performed two intercomparisons between filter measurements made with the Harvard Impactor and US E.P.A approved samplers (Beta Attenuation Monitor, MetOne). Both comparisons were conducted in Chile (2010 and 2012) and showed good similarity for the concentration ranges found in Sapiranga.

The PMF (Positive Matrix Factorization) is a receptor model based on least-square techniques, which was developed by Dr. Paatero (University of Helsinki). The receptor models use statistical methods to identify and quantify sources of air pollutants at a receptor site. Unlike models of photochemical and air quality dispersion, receptor models do not use emissions, meteorological data or chemical mechanisms of transformation to estimate the contribution of the sources receptor concentrations. These models are therefore a natural complement to other models of air quality and are used to identify sources that contribute to air quality problems. The U.S EPA has developed the PMF 5.0 software which uses a kind of factor analysis of particles' elemental composition. The structure of the PMF allows maximum use of available data set and better treatment of missing data, or data that are below the detection limits.

We used the XRF values and analytical uncertainties of each element (obtained from Harvard XRF analysis) as input to the PMF. Data processing was performed for different factors that we later identified as PM emission sources based on the literature.

DustTrak aerosol monitor

We used the DustTrak equipment (model 8520, TSI) to continuously monitor PM_{2.5} mass concentrations at the two fixed stations. The instrument was operated at a flow rate of 1.7 LPM with an impactor to remove particles larger than 2.5 μm (shown in Fig. 3.2.2). To determine particle concentration it uses the light scattering method. According to this method particles that pass through a laser beam scatter the light in an amount that is proportional to the diameter of the particles. The equipment has a light sensor that allows not only counting the amount of particles but also detect the intensity of the scattered light. In this way, the instrument calculates the total volume of particles in an air sample. To calculate accurate concentrations of particulate matter, DustTrak concentrations were corrected by comparing the average concentrations registered by the DustTrak against measurements performed with the Harvard Impactor during the same time period (24 hours), see Figures 4.2.6-7 for more details. A second DustTrak unit was used for mobile measurements, however the data collected with this instrument could not be corrected using parallel measurements with the Harvard Impactor instrument.



Figure 3.2.2 DustTrak device used for PM_{2.5} continuous measurement.

BAM

The Continuous Particulate Monitor BAM-1020 (Met One Instruments, Inc.) was used in Station “B” to capture the background contribution. This equipment automatically measures and records airborne particulate mass concentrations using the principle of beta ray attenuation. The measurements are based on high-energy electrons emitted by C^{-14} which are sent through a spot of filter tape at which ambient air particles are collected. This sensor collected PM_{2.5} data from July 21 to August 28. Figure 3.2.3 shows the BAM-1020 installation.



Figure 3.2.3 BAM-1020 installed in Station “B”, rack inside the building with the instrument (left) and the outside inlet with the head separating the PM_{2.5} fraction (right).

Scanning Mobility Particle Sizer (SMPS)

Concentrations of total number and size distribution of atmospheric nanoparticles were measured with a Scanning Mobility Particle Sizer model 3910 (TSI Inc.), scanning every 60 s and using a 0.75 LPM inlet flow and a 0.25 LPM condensation particle counter (CPC) flow. This equipment uses isopropyl alcohol as condensation liquid and registers across 13 channels the particles between 10 and 420 nm in diameter. Sampling was conducted at 3 locations:

- Site L: 19 h of sampling, during weekdays and day period, between July 9 and August 27, 2014. Measurements were made at a height of 2 m above ground level.
- Site T: 197 h of sampling, including weekdays and weekends, during day and night period, between 07 and 18 August 2014. Measurements were made at a height of 5 m above street level.
- Site B: 130 h of sampling, during weekdays, including day and night period, between 01 and 12 September 2014. Measurements were made at a height of 2 m above ground level.

For each sampling site, hourly averages for number concentration and size distribution of atmospheric nanoparticles were calculated. Spearman correlations were performed between the hourly particle number concentration (PNC) and meteorological variables to identify factors that predominantly acted in the formation of nanoparticles. Statistical analyses were performed using the software SPSS Statistics 22.

To evaluate the modal distribution of the particle number concentrations, a parameterization of the particle size number distribution (PND) was applied that uses a multi-lognormal function as described in Hussein et al. (2005). The PND is assumed to consist of several lognormal modes according to the equation

$$B(D_p)|_{\text{measured}} \rightarrow \frac{dN}{d(\log(D_p))} = \sum_{i=1}^n \frac{N_i}{\sqrt{2\pi \log(\sigma_{g,i})}} \exp \left[-\frac{(\log(D_p) - \log(\bar{D}_{pg,i}))^2}{2 \log^2(\sigma_{g,i})} \right]$$

$$= \sum_{i=1}^n N_i A_i(D_p, \bar{D}_{pg,i}, \sigma_{g,i})$$

where B is the measured particle number size distribution of a certain particle diameter D_p (nm). The three parameters that characterize an individual mode i are: the mode number concentration N_i (cm^{-3}); the mode geometric variance $\sigma_{g,i}^2$ (dimensionless) and the mode geometric mean diameter $\bar{D}_{pg,i}$ (nm). n is the number of individual modes.

Microaethalometer

The microaethalometer (model AE51, AethLabs, Fig. 3.2.4) is a portable monitor that measures the rate of change of light absorption due to the continuous deposition of aerosol on a filter. The measurements are performed at a wavelength of 880 nm and are interpreted as the mass concentration of black carbon. The field measurements were performed at a temporal resolution of 1 min, with a flow rate of 0.1 LPM and a size-selective inlet to remove particles with diameter larger than 2.5 μm . Data were validated using an algorithm available online by the AethLabs company that discards samples associated with measurement errors.



Figure 3.2.4 MicroAeth instrument used for BC continuous measurement.

3.3 Emission inventory

The emission inventory used for modeling includes three types of sources for PM_{2.5} and BC: traffic emissions, industrial/commercial point sources and residential wood combustion. In Sapiranga the industrial/commercial sources are grouped as industrial production (one unit inside the city), charcoal production just north of the city, brick production just south of the city and restaurants of the pizzeria type. All of these industrial/commercial sources emit due to wood combustion.

A combination of bottom-up and top-down approaches has been used to build up the inventory. Bottom-up is the best method when the emissions are known or possible to estimate locally. The top-down approach is necessary for source emissions that are only known or estimated globally over Sapiranga. Top down emissions can be homogeneously distributed over parts or the entire urbanized area, but they can also be heterogeneously distributed by using a distribution proxy such as population density, wood consumption etc.

The inventory was first elaborated for PM_{2.5} emissions and BC emissions were then calculated using BC/PM_{2.5} ratios taken from the literature (Table 3.3.1).

Table 3.3.1 Ratios of BC to PM_{2.5} taken from the literature.

Source	BC/PM _{2.5} ratio	Reference
Wood combustion (RWC, industrial, restaurants)	7%	EMEP/EEA, 2013, air pollutant emission inventory guidebook, Technical report No 12/2013, EMEP/EEA.
Traffic	65%	EMEP/EEA, 2013, air pollutant emission inventory guidebook, Technical report No 12/2013, EMEP/EEA. 1.A.3.b.i, 1.A.3.b.ii, 1.A.3.b.iii, 1.A.3.b.iv Passenger cars, light commercial trucks, heavy-duty vehicles including buses and motor cycles. Table A4-0-2: f-BC values from the COPERT model proposed for Tier 3

The estimated emissions are later re-evaluated as a result of the integrated analysis in section 4.5.

Residential wood combustion

The use of RWC and the wood consumption were estimated from an extensive survey about firing habits, distributed and answered by school children living in Sapiranga's 14 geographical areas (Fig. 3.3.1). Additional information on the burning devices (Figure 3.3.2) was collected by interviewing people at home in several neighbourhoods. To estimate the total use of RWC within the geographical areas, we used the number of inhabitants and households in each city area (data from Prefeitura Municipal, Sapiranga).

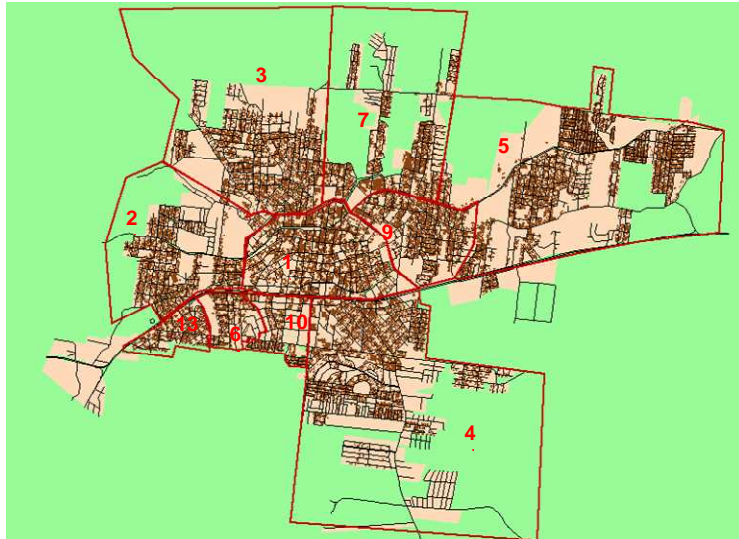


Figure 3.3.1 The 14 different districts used for the wood combustion questionnaire.



Figure 3.3.2 The kitchen stove (left upper and lower) is the most used stove according to the survey. Upper right is the baking stove and lower right the open fireplace.

The survey was answered by 7876 children from 14 geographical areas within Sapiranga (Table 3.3.2). 44% of the respondents reported some kind of wood burning at home. The relative firing habits in each area were assumed to be representative of the habits of the total population of each area. Three different types of wood stoves were identified in

Sapiranga: kitchen stoves (heating and cooking), open fireplaces (heating), and baking stoves (barbeque and baking).

The use of the kitchen stove dominated in all areas followed by the open fire place. The area Centro distinguished from the other areas as the number of open fireplaces was almost the same as the kitchen stoves. In most areas the number of baking stoves was much lower than the two other devices. Cooking and heating were the most common reasons to use the stove but some respondents also used the fire to dry clothes. The survey pointed out the winter as the season for most firing followed by autumn. Only a minor part of the respondents answered that they use wood combustion during spring and summer. The fraction of households using RWC varied from 37 to 96 %, where the higher use of RWC came from areas outside the city itself.

Table 3.3.2 Statistics from the survey of wood combustion habits from school children in Sapiranga.

Question / Area	1. Centro	2. Oeste	3. Centenário	4. São Luiz	5. Amaral Ribeiro	6. Santa Fé	7. São Jacó	8. Morro	9. 7 de Setembro	10. Piquete	11. Quatro Colônias	12. Porto Palmeira	13. Vila Irma	14. Novo Centenário
Do you use wood combustion in your home ?														
Yes	65	468	245	1007	732	109	463	48	129	39	3	5	132	20
No	94	622	421	1360	684	134	637	2	201	46	5	0	188	17
Fraction of fire-using homes	0.41	0.43	0.37	0.43	0.52	0.45	0.42	0.96	0.39	0.46	0.38	1.00	0.41	0.54
What kind of stove do you have ?														
Kitchen stove	35	415	191	881	654	95	440	45	107	29	3	5	116	15
Fire place	32	51	48	98	61	6	33	3	23	5	0	0	14	4
Stove /grill	5	13	12	55	35	10	13	12	7	5	0	0	6	1
Why are you burning wood?														
To cook	34	322	155	718	467	76	352	43	80	26	3	5	97	9
To heat	46	273	173	692	470	71	346	34	94	29	3	2	81	18
To dry clothes	4	27	12	75	53	8	39	12	14	4	0	0	6	0
At what time of the year are you using wood combustion?														
Autumn	17	103	52	244	213	25	132	35	28	10	1	1	30	5
Winter	63	418	237	950	698	106	413	48	126	39	3	5	132	19
Spring	12	43	17	76	76	7	28	15	6	4	1	1	8	1
Summer	11	26	15	62	45	7	20	7	4	1	0	0	8	1
Which days are you using wood combustion?														
All days	10	61	40	274	178	21	137	14	26	10	1	1	20	3
Weekends	9	70	46	171	92	19	47	7	9	7	0	0	21	3
Weekdays	1	21	16	50	41	4	29	7	17	1	0	0	7	1
Anytime	48	296	156	569	437	73	244	25	85	21	2	4	95	16
What time of the day are you using wood combustion?														
Morning	21	161	69	409	318	42	193	31	31	16	2	2	57	3
Mid day	22	135	82	337	251	31	133	28	31	12	1	1	41	8
Afternoon	15	41	30	187	134	15	80	15	18	8	0	0	20	6
Night	54	327	190	737	541	91	364	45	112	30	2	4	90	13

From the survey and the demographic information the total consumption of wood for each area was derived.

The time variation for firing in the open fireplace and the barbeque was taken from the interviews, whereas the time of usage for the kitchen stove was derived from interviews and survey statistics (Tables 3.3.3 and 3.3.4).

Table 3.3.3 Annual time variation in use of burning devices in Sapiranga (% of maximal use).

Seasonal variation	Jan	Feb	Mar	Apr	May	Jun	Jul	Aug	Sep	Okt	Nov	Dec
Kitchen stove	1	1	10	20	30	100	100	100	40	20	10	1
Open fire place	1	1	10	20	30	100	100	100	40	20	10	1
Cooking stove	100	100	100	100	100	100	100	100	100	100	100	100

Table 3.3.4 Relative use (%) of burning devices in Sapiranga during the day.

Diurnal variation	Morning	Noon	Afternoon	Night
Kitchen stove Oeste	61	51	11	100
Kitchen stove Centro	95	100	45	77
Kitchen stove São Luiz	70	58	23	100
Open fire place	0	0	0	100
Cooking stove	0	0	100	100

The total annual emission of PM_{2.5} from each area was calculated considering the number of households, fraction of households using RWC, hours fired annually for an average household, and emission factors for the three different stoves. For modelling purposes, the emission was distributed into 3 point sources at each building of the area, each of them representing one of the three types of fireplaces (this since we do not know which types there are in an individual house). This means that we have more and smaller point sources in the model than what is assumed to exist in reality. This is a good approximation as we do not know the exact location of each chimney. Neighborhoods outside the modeling area and/or with no population were excluded from this calculation, but do not affect the final results since their number in the survey is small and, thus, their contribution to total RWC emission is considered negligible.

The emission factor used for kitchen stoves was 740 gPM_{2.5}/GJ (EMEP/EEA emission inventory guidelines 2013, Tier 2, Table 3-17) and for the open fireplace and baking stove 820 gPM_{2.5}/GJ (EMEP/EEA emission inventory guidelines 2013, Tier 2, Table 3-14). From the interviews we learned that acacia and eucalyptus are the most common types of wood, why we use the heating value 18 MJ/kg. Table 3.3.5 displays the emission factors used in this study.

Table 3.3.5 Emission factors used in the emission inventory (EMEP/EEA emission inventory guidelines 2013, Tier 2, Table 3-14 and 3-17).

			Using heating value of 18 MJ/kg.	
	EF_{BC} BC/PM_{2.5}	EF_{PM_{2.5}} (g/GJ)	EF_{BC} (g/kg)	EF_{PM_{2.5}} (g/kg)
Conventional Stoves	7%	740	0.9	13.3
Open Fireplaces	7%	820	1.0	14.8

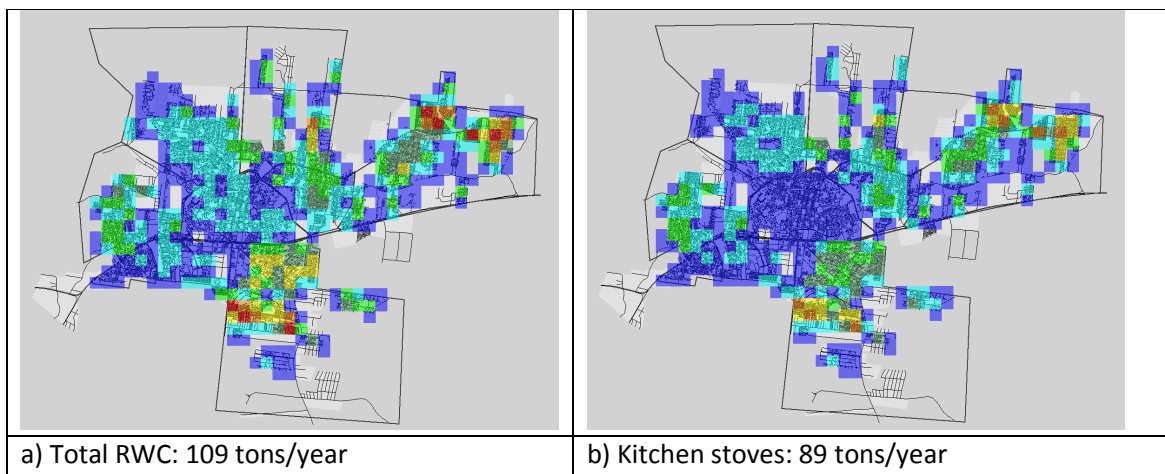
The resulting wood consumption and emission of PM_{2.5} are presented in Table 3.3.6. This estimate of the PM_{2.5} emission from all RWC in Sapiranga is 109 ton/year. The estimated average consumption of wood for a household using RWC is similar between the areas with values from 0.64 to 0.78 tons/year.

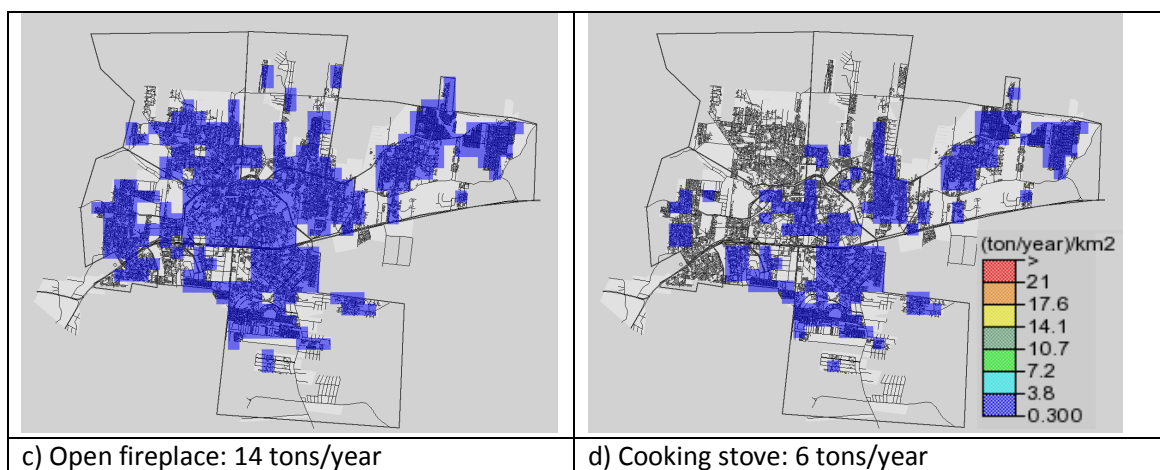
Table 3.3.6 Wood consumption and total emission of PM_{2.5} in Sapiranga.

	<i>Centro</i>	<i>Oeste</i>	<i>Centenário</i>	<i>São Luiz</i>	<i>Amaral Ribeiro</i>	<i>Santa Fé</i>	<i>São Jacó</i>	<i>7 de Setembro</i>	<i>Piquete</i>	<i>Vila Irma</i>
No of households	1687	2590	3007	6813	5842	334	2527	1949	457	307
Total no of households that makes fire	690	1112	1106	2898	3020	150	1064	762	210	127
No of buildings with point sources	2561	2484	3544	4560	5991	612	2007	1897	691	771
Total wood consumption per house [ton/year]	0.78	0.64	0.68	0.75	0.77	0.74	0.75	0.67	0.76	0.71
Total wood consumption in the area [ton/year]	537	713	757	2172	2319	111	799	512	160	90
Total emission of PM_{2.5} [ton/year]	7.55	9.73	10.33	29.05	29.31	1.50	10.85	6.98	2.19	1.20

The spatial distribution of PM_{2.5} emissions from different stoves is presented in Figure 3.3.3. The pattern is a result of the locations of buildings within each area (how close each house is to another) and statistics from the survey.

The total emission from residential wood combustion is estimated to **109 tons/year** for PM_{2.5} and **7.6 tons/year** for BC.





c) Open fireplace: 14 tons/year

d) Cooking stove: 6 tons/year

Figure 3.3.3 Estimated spatial distribution of the annual emission of PM_{2.5} from RWC in Sapiranga: a) all wood burning devices, b) kitchen stoves, c) open fire places, and d) baking stoves. These amounts were re-evaluated in the integrated analysis in Section 4.5.

Restaurants

We identified 17 restaurants in the study area emitting air pollutants when burning wood in the pizza stoves. According to the information from interviews, each restaurant consumes 14 ton wood per month (168 tons/year) and burns wood (acacia and eucalyptus) in the morning (starting at 10:00) until midnight (Table 3.3.7).

Assuming an emission factor for PM_{2.5} of 14.8 g/kg (Table 3.3.4, i.e. the same as for open fireplaces) the total emission for each restaurant per year is 2.48 tons/year. This gives an estimate of totally 42.16 tons/year of PM_{2.5} for all restaurants in Sapiranga. This emission source can be overestimated if the selected restaurants had higher emissions than the non-interviewed.

The total emission for all restaurants is estimated to **42 tons/year** for PM_{2.5} and to **2.9 tons/year** for BC.

Table 3.3.7 Relative use (%) of pizza ovens in Sapiranga during the day.

Hour	1	2	3	4	5	6	7	8	9	10	11	12	13	14	15	16	17	18	19	20	21	22	23	24
Pizzerias	0	0	0	0	0	0	0	0	0	100	100	100	100	75	50	50	100	100	100	100	100	50	10	10

Brick production

Sapiranga has three brick production companies located in the southern part of the municipality. Because of the low-technology burning techniques employed in the manufacturing process and no air pollution control devices, high concentrations of particles can be emitted to the atmosphere.

To estimate the total annual emission of PM_{2.5} by these companies information from a visit to one of the brick production industries was used as well as economic reports from three

brick producers to Sapiranga municipality. The emission factors for open fire (Table 3.3.5) were used and the time variation was set according to Tables 3.3.8 and 3.3.9. The production is largest in the summer as the process depends on good drying conditions for the bricks. There is no production on weekends.

Table 3.3.8 Relative use (%) of brick production ovens in Sapiranga during the day.

Hour	1	2	3	4	5	6	7	8	9	10	11	12	13	14	15	16	17	18	19	20	21	22	23	24
Brick production	70	70	70	70	70	100	100	100	100	100	100	100	100	100	100	100	100	100	100	100	100	100	70	70

Table 3.3.9 Relative use (%) of brick production ovens in Sapiranga along the year.

Seasonal variation	Jan	Feb	Mar	Apr	May	Jun	Jul	Aug	Sep	Okt	Nov	Dec
Brick Production	133	133	83	83	83	34	34	34	83	83	83	133

The three brick production industries are each estimated to emit between 5.8 and 8.0 tons PM_{2.5}/year. The total emission of PM_{2.5} for all three brick industries is estimated to **19.7 tons/year** and the total emission of BC is estimated to **1.4 tons/year**.



Figure 3.3.4 Large wood burning stoves to heat the baking oven for bricks.



Figure 3.3.5 Smoke from a small brick production industry.

Charcoal kilns

There are 45 registered (2012) charcoal producers in Saporanga. They are all located north of the city. By looking at the addresses in "google maps" (www.googlemaps.com) their location was estimated to an area 1 to 10 km from the city border. The terrain in the area is very hilly. It was not possible to get their exact locations from the map, why their emissions were distributed in a large rectangular area source north of the city.

The average production of a charcoal producer is estimated to 3 tons/month (personal communication with a charcoal producer in the area + comparison with his report to Saporanga city). This means that as a total of 135 tons/month is produced.

The emission factor for production of charcoal in a Batch Kiln (EPA-450/4-89-023) is 255.4 lb/tons produced which is 128 kg PM₁₀ /tons produced charcoal, and of this 7% is BC. This gives an emission of 128*135 kg PM₁₀ per month. In the modeling this emission is spread homogenously over the rectangular area source north of Saporanga.

The total emission of PM_{2.5} for all charcoal industries is estimated to **202 tons/year** and the total emission of BC to **14 tons/year**.



Figure 3.3.6 Charcoal kiln in the vicinity of Sapiranga.

Industry within Sapiranga

Sapiranga has no large industry with significant atmospheric emissions derived from burning of wood or fossil fuels. The largest industries are related to footwear, metallurgy and metal treatment. The energy used in these industries is basically electricity. Only Calçados Ramarim Ltda. industry, located in Piquete neighbourhood, uses firewood in the productive process. It consumes about 2.7 ton of the firewood a week (works 8 h during 5 days/week). The emission factor used for non-residential sources, automatic boilers burning wood was 33 g PM_{2.5}/GJ (EMEP/EEA emission inventory guidebook 2013, Tier 2, Table 3-31). Acacia and Eucalyptus are the most common types of wood, why we use the heating value 18 MJ/kg. The emission factor is thus 0,594 g PM_{2.5}/kg wood. This represents an estimated emission of **83 tons/year** for PM_{2.5} and **5.8 tons/year** for BC.

On-road motorized traffic

To estimate traffic emissions, we manually counted vehicles during selected periods in the morning, mid-day and afternoon at 18 locations, since few traffic data were available for the city of Sapiranga. From this counting, three different diurnal patterns were estimated: one for the highway RS-239, one for roads in the northern part of the city, and one for roads in the southern part (Table 3.3.10).

Table 3.3.10 Traffic variation in Sapiranga along the day depending on the geographical sector and day of the week.

Time variation/Time of day	0	1	2	3	4	5	6	7	8	9	10	11	12	13	14	15	16	17	18	19	20	21	22	23
RS 239 (Mon-Fri)	1	1	1	1	1	10	30	30	15	15	25	25	25	15	15	30	30	30	20	20	10	5	5	1
North of 239 (Mon-Fri)	1	1	1	1	1	20	30	20	5	5	5	40	30	10	10	10	30	30	20	20	10	5	5	1
South of RS 239	1	1	1	1	1	20	20	20	5	5	5	40	30	20	10	10	20	15	15	10	10	5	5	1
All roads (Saturday)	1	1	1	1	1	1	5	15	20	30	4	4	20	30	45	45	20	30	20	20	10	5	5	1
All roads (Sunday)	1	1	1	1	1	1	2	7	7	10	20	15	15	10	15	15	15	15	10	3	3	3	2	1

The total traffic on the roads was estimated from the counting at 18 locations. From this counting, the major road links were assigned specific traffic volumes. To quantify the traffic volume on the remaining road network in Sapiranga, we compared the per capita emissions from road traffic (FEPAM, 2010) with the total traffic at the counted roads. This indicates that 30% of the emissions occur on smaller roads and we added this value to the model as a background field.

The traffic was divided into 4 vehicle categories: heavy-duty vehicles fuelled with diesel, light-duty with gasoline, light-duty with ethanol, and motorcycles (MC). The fraction of gasoline is 95% and for ethanol 5% of total light duty vehicles (FEPAM, 2010).

Emissions of coarse particles are negligible in vehicle exhaust why emission factors for total PM can be used for PM_{2.5}. In this study, Brazilian emission factors derived in Sao Paulo (CETESB, 2014) for PM_{2.5} were applied for each vehicle category and the fleet composition was taken from the vehicle registration in Sapiranga (<http://www.detran.rs.gov.br>). These emission factors are for light duty vehicles much lower than the emission standards in PROCONVE (Table 3.3.11), this since PM emissions from gasoline engines are assumed to be low. From this, the total emission of PM_{2.5} from road traffic (exhaust only) is estimated to **12 tons/year**.

Using the same traffic volume counted in Sapiranga but emission factors from Sweden, Chile and PROCONVE limits, the total annual emission of PM_{2.5} amounted to 3 tons/year, 10 tons/year and 30 tons/year, respectively.

The total BC from traffic was estimated from the annual PM_{2.5} emission. The EC/PM_{2.5} ratio was taken from EMEP/EEA emission inventory guidebook 2013 and we compared the Euro- and PROCONVE classes taking into account the knowledge of the age of the vehicle fleet. The total BC emission from traffic is estimated to **7.8 tons/year**, representing 65% of the total PM_{2.5} from traffic exhaust.

Older heavy-duty vehicles emit up to 50 times as much as newer engines (Table 3.3.12). The production year of cars and trucks registered in Sapiranga are presented in Figures 3.3.7 and 3.3.8. Almost 50% of the heavy duty vehicles were manufactured before 1999. Assuming that the vehicle age does not influence the km driven, the emissions from heavy duty from before 1999 contribute with 81% of all PM_{2.5}, the post 1999 heavy duty vehicles 16%, and the light duty vehicles only 3 %.

Table 3.3.11 Emission factors for road traffic. The PROCONVE limits for lights duty vehicles are from PROCONVE L4 and L5 corresponding to the European emission standard Euro 3. PROCONVE limits for heavy duty are PROCONVE P5 for diesel vehicles.

	Brazilian	Swedish		Chilean		PROCONVE
EF PM2.5	0-120 km/h (mg/km)	0-70 km/h (mg/km)	80-120 km/h (mg/km)	0-70 km/h (mg/km)	80-120 km/h (mg/km)	0-120 km/h (mg/km)
MC	3.2	2.3	2.8	3.7	2.7	50
Heavy duty buses	624	114	109	354	333	500 (for 5 kWh/km)
Heavy duty trucks	414	94	92	354	333	700 (for 7 kWh/km)
Light duty ethanol	1.3	9	9	3.7	2.7	50
Light duty gasoline	1.3	2.3	2.8	3.7	2.7	50

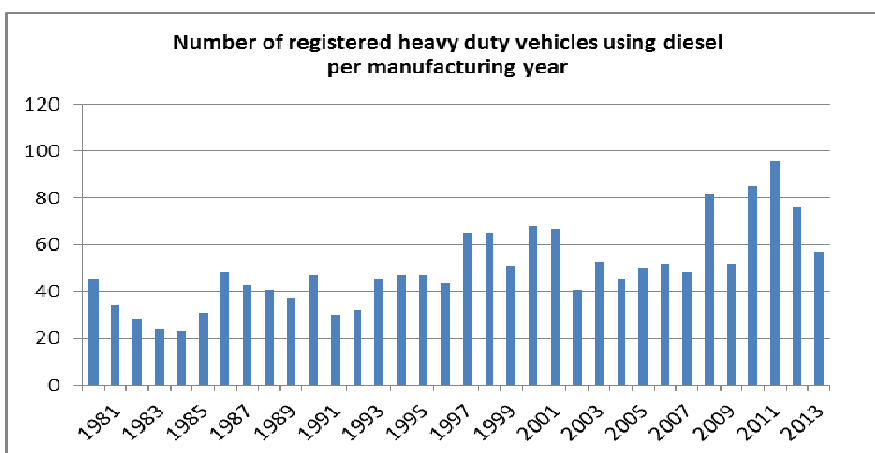


Figure 3.3.7 The age of the heavy duty fleet in Saporanga.

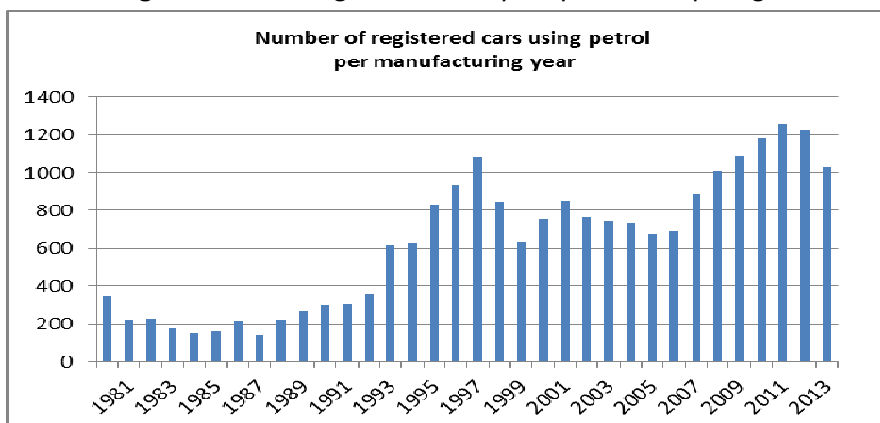


Figure 3.3.8 The age of gasoline cars in Saporanga.

Table 3.3.12 Simplified high estimation of emission factors for each manufacturing year. (CETESB, 2014).

Maximum EF PM _{2.5} (g/km)		
	Heavy Duty	Bus
before 1999	0.715	1.071
2000-2001	0.355	0.533
2002-2003	0.139	0.209
2004-2007	0.111	0.166
2008	0.09	0.16
2009	0.09	0.15
2010	0.095	0.154
2011	0.08	0.15
2012	0.015	0.021
2013	0.016	0.021

Emissions outside Sapiranga, used as input to the regional scale model

Figure 3.3.9 (left panel) shows the anthropogenic emissions from the Porto Alegre – Novo Hamburgo area. During the Sapiranga monitoring campaign, there were also emissions from biomass burning taking place at different locations, generating time-limited emissions that sometimes took place close to Sapiranga. The PM_{2.5} emissions during August 2014 were, according to the regional scale model, **24 528 tons/year** from anthropogenic sources and **53 431 tons/year** from biomass burning.

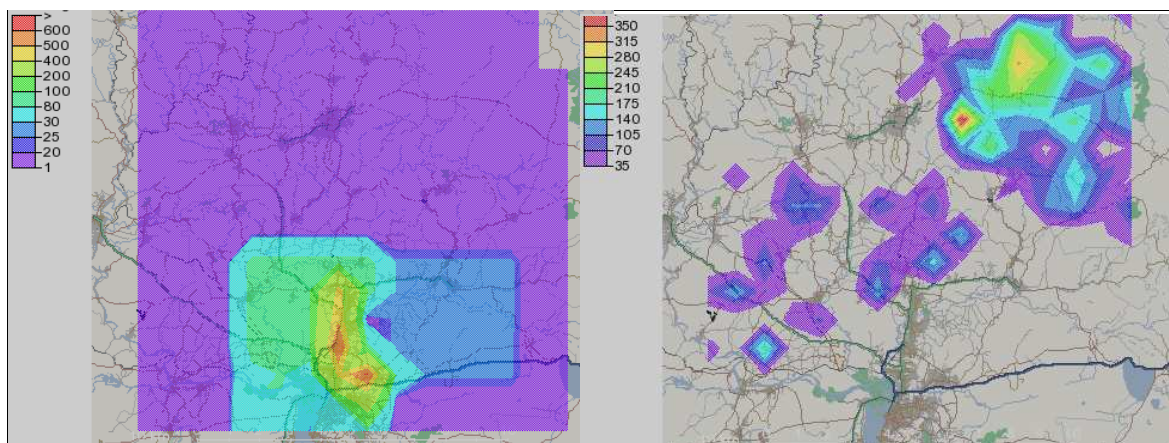


Figure 3.3.9 Urban (left) and biomass burning (right) emissions in the region (10^{-7} kg/m²,day). Average emissions from July 15 to August 29, 2014.

3.4 Regional dispersion modeling

The regional dispersion modeling chosen for the background numerical studies was the CCATT-BRAMS modeling system (Longo et al., 2013), which consists of an atmospheric chemistry transport model (CCATT) coupled on-line with a limited-area atmospheric model (BRAMS). The BRAMS model is the Brazilian version (with specific development for the tropical and subtropical regions) of the non-hydrostatic time-split compressible model RAMS (Regional Atmospheric Modeling System), developed at the University of the State of Colorado (Tripoli and Cotton, 1982).

The CCATT is an Eulerian model of atmospheric transport that simulate the trace gases mixing rate through the solution of the mass conservation equation, which includes advection, turbulent mixing in planetary boundary layer, dry and wet deposition, ascension plume associated with fires, and vertical transport associated with the shallow (not precipitant) and deep convection. In addition, the model includes chemical reactions and aerosol processes, solar radiation and terrestrial interactions.

The pollutants transported by convection in the model CCATT-BRAMS uses the formalism of mass flow, based on Grell and Devenyi (2002) deep convection scheme, which accounts for the mass transport in the updrafts and downdrafts (only deep convection) within the cumulus cloud and the environmental subsidence. There are two important updates in the 4.5 version: the introduction of a monotonic formulation (Walcek, 2000) for the advective transport, as an additional option to the second order scheme proposed by Tremback (1987) and the use of observational information from AERONET (AErosol RObotic NETwork) as input to calculate the optical properties required by Community Aerosol and Radiation Model for Atmosphere (CARMA) included in the model (Longo et al., 2013; Rosario et al., 2011, 2013).

The CCATT-BRAMS can be configured with any chemical mechanism, using the M-SPACK pre-processor (Modified Simplified Preprocessor for Atmospheric Chemical Kinetics) (Djouad, 2002; Longo et al., 2013). The M-SPACK automatically pre-processes the chemical species aggregation and creates the Fortran90 routine files to use in the model. There are two options for the rates of photolysis: standard conditions from lookup tables or updated at each timestep using the model FAST-TUV (Tie et al., 2003). The numerical integrator of chemical mechanisms is based on the Rosenbrock method. The simulations performed in this work use the RODAS 3 version, with four stages and third order, described in Longo et al. (2013).

The emission pre-processor (PREP-CHEM-SRC, Freitas et al., 2011) provides emission fields interpolated to serve as input to regional and global transport models and considers urban/industrial, biogenic, biomass burning and volcano sources. The biomass burning sources (for CO, CO₂, CH₄ and NO_x and PM_{2.5}) can be estimated directly from satellite remote sensing fire detections using the Brazilian Biomass Burning Emission Model (3BEM, Longo et al., 2009). The organic and black carbon, SO₂ and Dimethylsulfide

(DMS) are obtained from the system GOCART (Goddard Chemistry Aerosol Radiation and Transport).

Biogenic Emissions are obtained from MEGAN (Model of Emissions of Gases and Aerosols from Nature, Guenther et al., 2006) used to estimate gases and aerosols emissions from terrestrial ecosystems. The urban emissions are provided from a South America regional inventory that aggregates local inventories vehicular emissions with RETRO (RETRO, <http://retro.enes.org>) and EDGAR (<http://edgar.jrc.ec.europa.eu>, Olivier et al., 1996, 1999) anthropogenic global database (Alonso et al., 2010).

The biomass burning emissions have daily temporal resolution and the fire detection maps are merged with 1 km resolution land cover data. The biogenic emissions covers the entire world with a $0.5^\circ \times 0.5^\circ$ spatial resolution. The RETRO emissions have $0.5^\circ \times 0.5^\circ$ / month resolution and the EDGAR database has $1^\circ \times 1^\circ$ / year (v4.1) and $0.1^\circ \times 0.1^\circ$ / year (v4.2) resolution.

With aim to simulate the background influence of fires, urban plumes from nearby cities and long range transported pollutants, a numerical experiment covering the campaign period was performed, using emissions from PREP-CHEM-SRC without the Sapiroanga contribution. Figure 3.4.2 shows the selected grid. This simulation uses the RELACS chemical mechanism (Crassier et al., 2000), atmospheric initial and boundary conditions from T126L42 Global model (CPTEC/INPE – Brazil) and chemical initial and boundary conditions from MOCAGE (Josse et al., 2004; Teyssèdre et al., 2007), included in the model system by the DPREP-CHEM module.

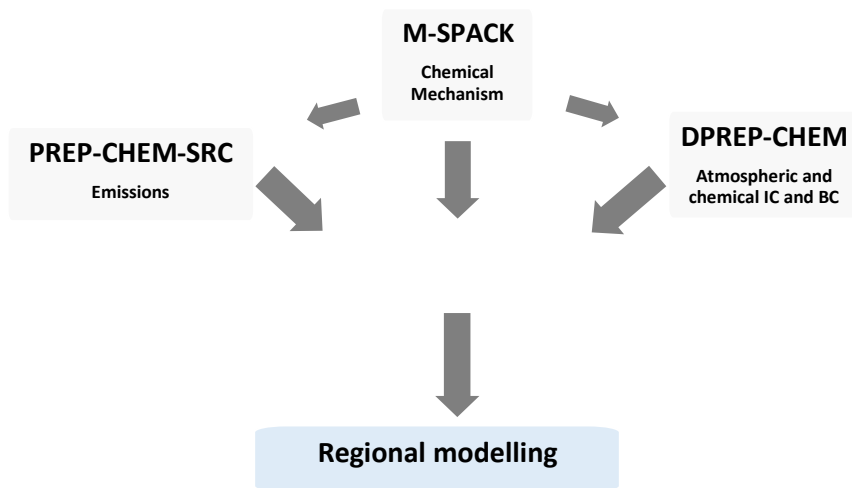


Figure 3.4.1: Schematic diagram of CCATT-BRAMS system.

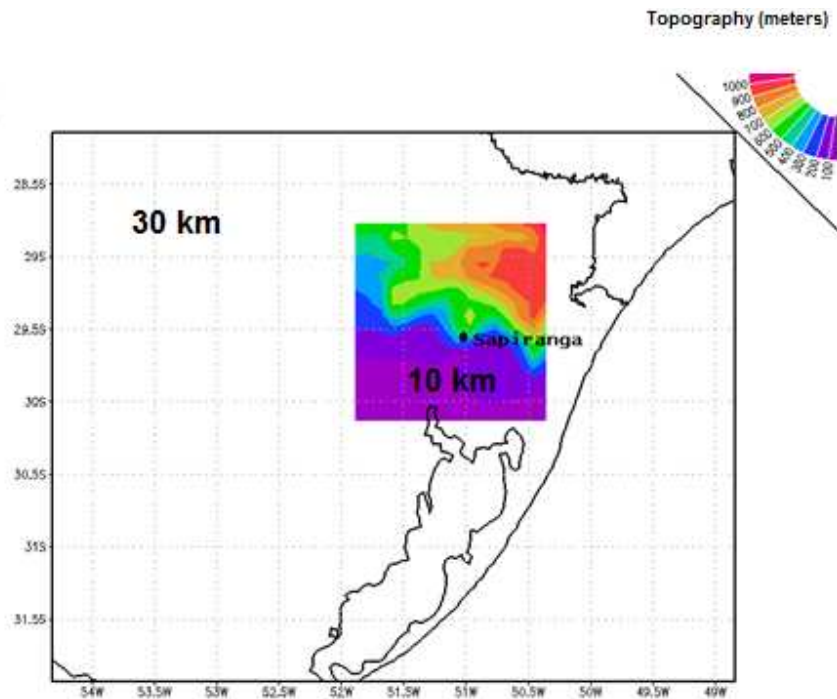


Figure 3.4.2: Simulation grids and topography (meters) in the second grid.

3.5 Local dispersion modeling

Two types of dispersion models are used for the local scale, one Gaussian model to simulate the spatially distributed impact of local emissions within Sapiranga at high resolution and another semi-empirical street canyon model to simulate the impact of the traffic inside a specific street canyon like e.g. the street where the monitoring station T was located. Both models use meteorological information pre-processed in a wind model. The dispersion models and the wind model are part of the Airviro system (<http://www.smhi.se>).

The wind field calculation is based on the concept first described by Danard (1976), where mesoscale winds are generated by using the horizontal momentum equation, the pressure tendency equation and the first thermodynamic equation. This concept assumes that small-scale winds can be seen as a local adaptation of large scale winds (free winds) due to local fluxes of heat and momentum from the sea or earth surface.

The large-scale winds as well as vertical fluxes of momentum and temperature are estimated from profile measurements in one or several meteorological masts. Boundary scaling parameters are determined from one or several profile measurements in the area, giving estimates of boundary layer heights, diabatic heating and potential temperature distribution at ground level. A free wind, i.e. an estimate of a wind at the location of the mast, at the level where the wind is not affected by surface fluxes of heat and momentum, is estimated based on the profile measurements and extrapolation procedures suggested by Holtslag (1984). When the free wind field is estimated, the initial surface pressure field is determined in accordance with a geostrophic balance.

The determination of turbulence scaling parameters like e.g. the Monin-Obukhov length (L) follows the profile method discussed by Berkowicz and Prahm (1982). When vertical temperature gradient data are missing – as is the case for this Sapiranga application – it is possible to determine the same scalars using ordinary synoptic data and the resistance method (van Ulden & Holtslag, 1985).

The Gaussian model simulates one hour average concentration plumes from multiple point sources, each one with an individual plume rise. Area or grid sources are converted to a number of point sources at surface level and without plume rise. Line sources (road traffic) are as well converted to a number of surface point sources along the line, here the initial dispersion is linked to traffic intensity and the turbulence created by the vehicles.

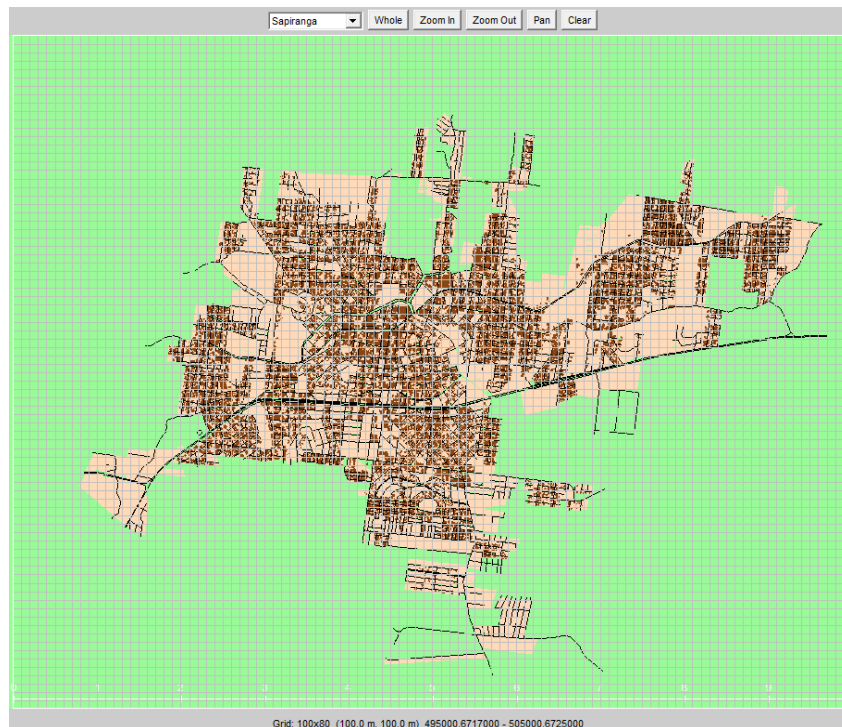


Figure 3.5.1: Modeling domain and spatial resolution for the Gaussian dispersion model.

To determine the impact on air pollutant concentrations caused by vehicle emission inside street canyons, we used the OSPM model (Berkowicz, 2000). The model requires the dimensions of the street canyon, expressed in road width, number of lanes, the width between the surrounding houses and heights of the surrounding houses. The OSPM model has one part, which is a direct plume model, following the estimated wind direction at the bottom of the street canyon. The other part, taking care of the contribution from the re-circulation, is calculated by a simple box model. OSPM assumes stability conditions inside the street canyon to be neutral. The two receptor points are located at each side of the road and in the middle of the block (road link), i.e. they express the concentration levels at the pavement caused by local traffic. The contribution from the urban background as well as from the long range transported pollution arriving to the city must be added to the OSPM output to obtain the actual concentration at the street canyon.

4 Results

4.1 Meteorological measurements

Figure 4.1.1 shows the ambient air temperature registered at the meteorological stations (Health Clinic and Bombeiros stations). The variations and the average values are close to identical. We identified four cold episodes: June 20, July 9, July 26 and August 14, the latter being the most intense. These episodes in Sapiranga were characterized by cold fronts passages that carried polar air over Southern Brazil (Fig. 4.1.2). On August 13/14 an intense cold front caused a cold wave in Brazil, with episodes of moderate to severe frost in the south.

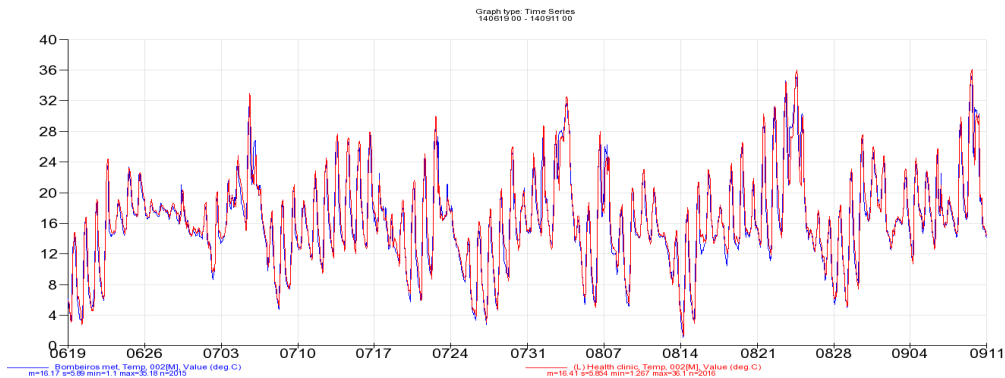
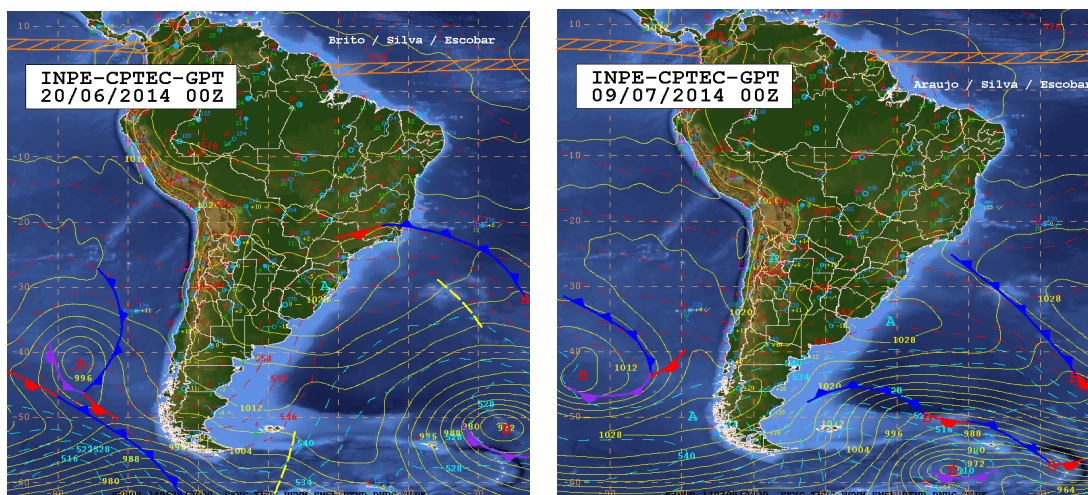


Figure 4.1.1 Temperature (Celsius) from the two meteorological stations located at Bombeiros (blue) and the Health Clinic monitoring station L (red). Period: June 19 to September 10.

While temperature data were successfully collected for the entire period, records of wind direction and speed were scarce (Fig. 4.1.3). Non-zero wind speed at Health Clinic was registered only during 69% of the time, i.e. the wind speed was too low to be detected by the instrument during 31% of the time. Moreover, the instrument at Bombeiros had a failure that lead to a large gap in data up to August 8.



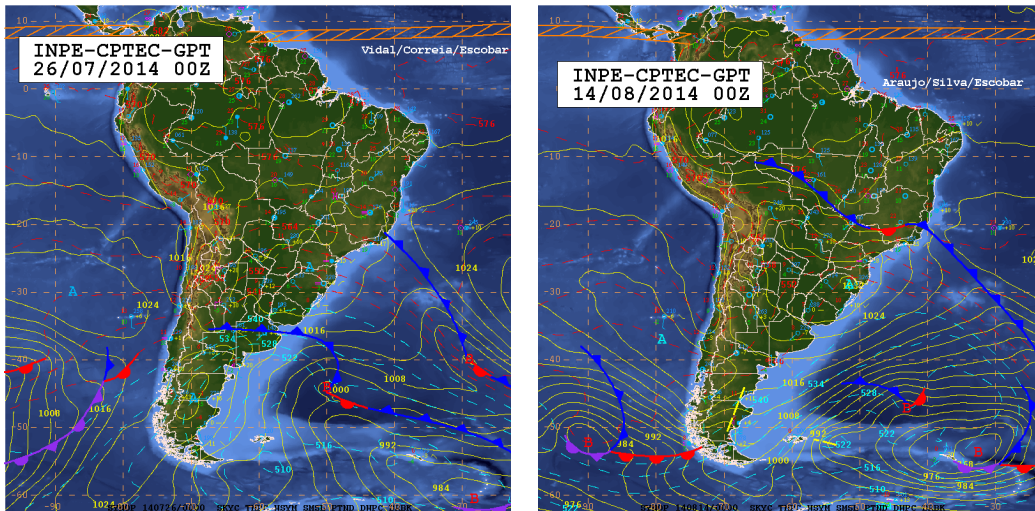


Figure 4.1.2 Synoptic chart from CPTEC/INPE showing the four intense cool episodes observed in Saporanga city.

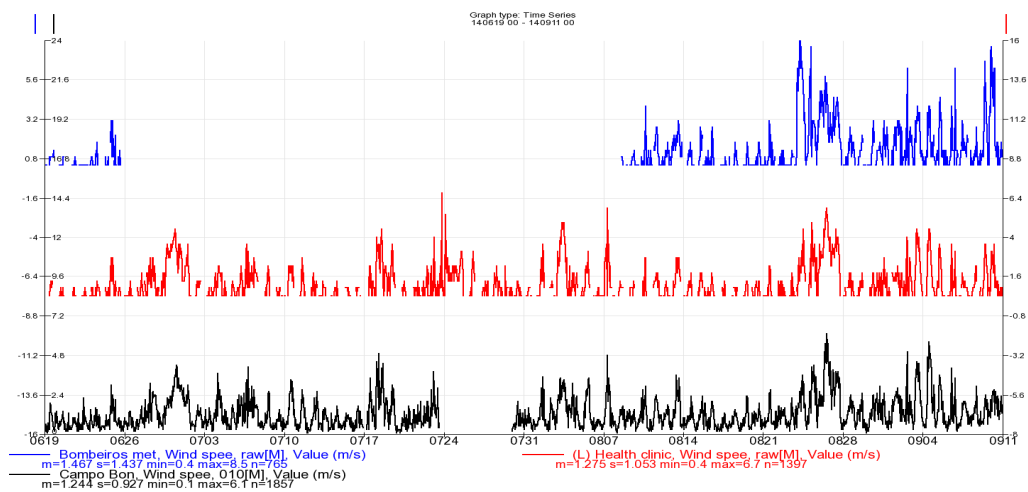


Figure 4.1.3 Raw wind speed data from station Bombeiros (blue), Health Clinic station L (red) and INMET station Campo Bom (black).

The wind direction was predominantly from northeast and southwest at the Health Clinic station and from north and from southeast at the Bombeiros station. There is a strong influence of local topography because Saporanga is located close to mountains and with hills inside the urban area, and this could explain the different wind patterns at the two sites.

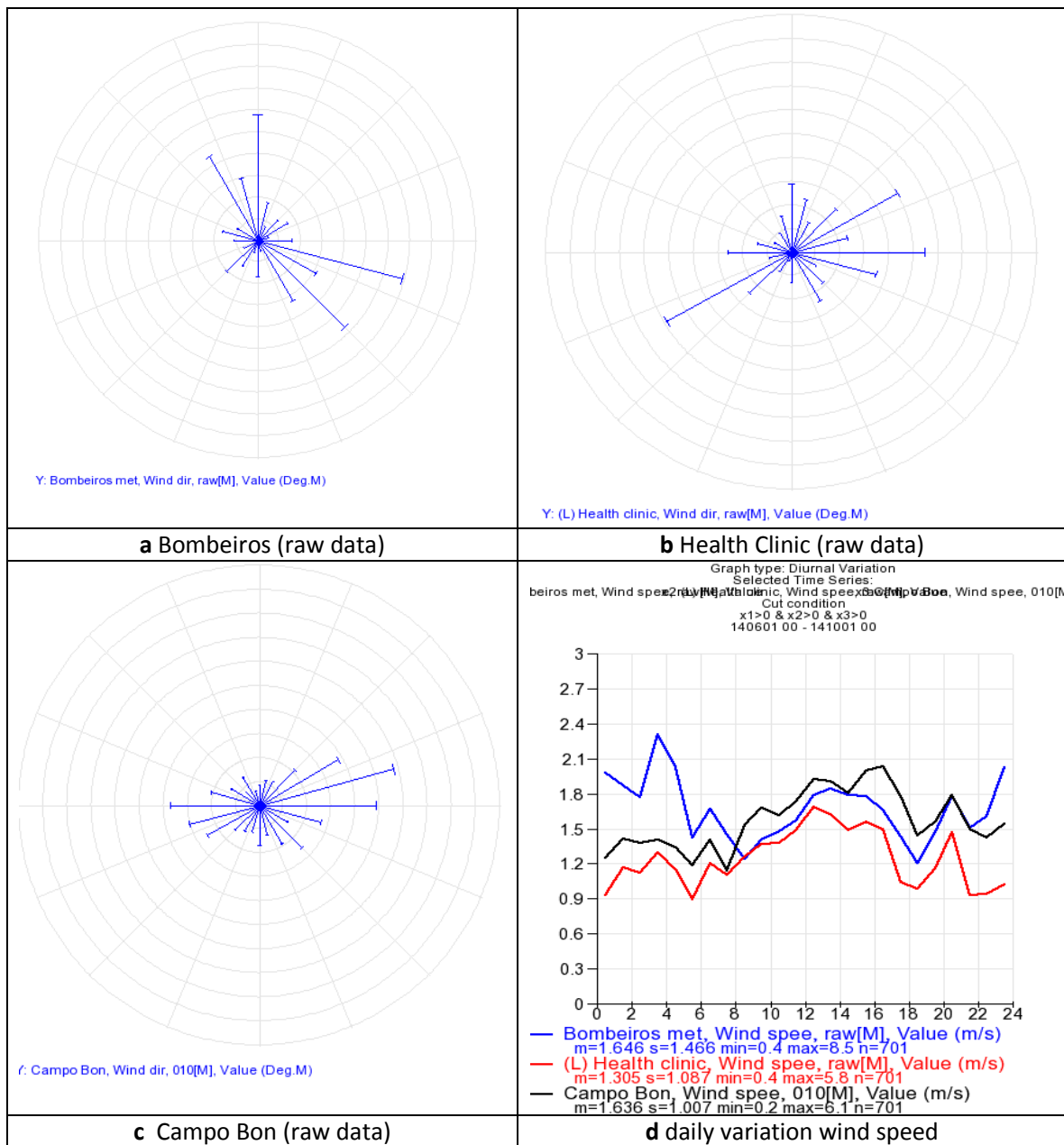


Fig. 4.1.4 Wind direction at three stations (a-c) and daily variation in wind speed (d) during the period June to September, 2014 (only included hours where data exist from all three stations).

In order to have consistent input data to the dispersion model during the monitoring campaign (most data collected July 31 – August 28, 2014), we also used the Campo Bom data together with the two stations above. As part of the project we simulated the entire year of 2014 and for the periods outside the field campaign only Campo Bom data were available. There is a consistency between Campo Bom and Health Clinic wind speed and wind direction data. The wind rose at Bombeiros showed a somewhat different pattern and also larger wind speeds during the night (Fig. 4.1.4).

4.2 Air Quality monitoring results

The Sapiranga assessment focuses fine particulate matter and its composition. The principle variables studied are PM2.5, BC, EC/OC and particle number concentration (total number and size distribution of particles < 1 µm). We also report elemental composition. The results will be presented per station.

The regulation valid in Rio Grande do Sul state is the national air quality standards (NAQS, CONAMA Resolution 003/90) which have limit values for inhalable particles (PM10) of 50 µg m⁻³ (annual average) and 150 µg m⁻³ (maximum daily average). However there is no limit value for PM2.5 in the national legislation. Of interest for referencing the levels registered in Sapiranga are the São Paulo state legislation, which has a stricter legislation for PM10 and also includes the limit levels for PM2.5. Finally it is of interest to compare with European Union (EU) legislation, based on WHO recommendations. Table 4.2.1 summarizes the different regulations of inhalable particle concentration values.

Table 4.2.1 Air quality standards for aerosol mass in Brazil and Europe.

Unit: µg m ⁻³	PM10 annual	PM10 90-percentile	PM10 max value	PM2.5 annual	PM2.5 max value
Brazilian NAQS	50	-	150	-	-
Sao Paulo AQS	40	-	120	20	60
EU Air Quality Directive	40	50	-	25	-

Table 4.2.2 displays reference concentrations reported in the literature, e.g. the survey of PM2.5 mass concentrations in six Brazilian cities (Maura de Miranda et al., 2012) and results from the automatic air quality monitoring network published by FEPAM (2014).

Table 4.2.2 Average annual concentration levels reported from other cities

Unit: µg m ⁻³	PM10 annual	PM2.5 annual	Black smoke (BS) annual	reference
Sao Paulo	-	28.1	10.6	Maura de Miranda et al., 2012 Measurement period: June 2007 – August 2008
Rio	-	17.2	3.4	
Belo Horizonte	-	14.7	4.5	
Curitiba	-	14.4	4.4	
Porto Alegre	-	13.4	3.9	
Recife	-	7.3	1.9	
Canoas/PU 2010	38.9	-	-	FEPAM, 2014
Canoas/PU 2011	34.7	-	-	
Canoas/PU 2012	36.9	-	-	
Esteio/VE 2010	23.2	-	-	
Esteio/VE 2011	26.3	-	-	
Esteio/VE 2012	27.1	-	-	

In what follows we discuss the characteristics of the observed pollutants, looking for evidences, or at least indications, of the impact of the two local sources - road traffic and wood combustion – on the air quality. Obviously there is an important background of pollution arriving to Sapiranga. By integrating the results of the measurements with dispersion modeling output, we will discuss further the size of the local contribution.

Background station B

Figure 4.2.1 shows the PM2.5 levels measured with the BAM-1020 instrument installed at Station B, after discarding very high peaks, clearly caused by measurement failure. From the remaining observations the average level in this location was found to be around 17 $\mu\text{g}/\text{m}^3$, but an influence of local sources is likely. This area is located in the city periphery, almost entering the rural zone, but there are residences around the school. In fact, analysing the average concentrations during the different days of the week (Fig. 4.2.2), is notable that the higher values are registered on Sundays. With relation to hourly variability, there is a small tendency for higher values of PM2.5 in the morning and at the night (Fig. 4.2.3).

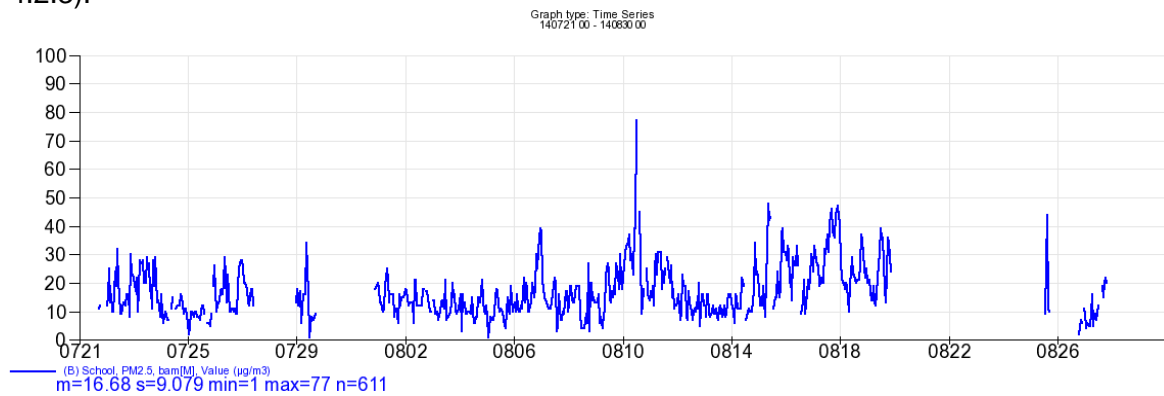


Figure 4.2.1 PM2.5 hourly levels registered by the BAM-1020 monitor at Station B. Some isolated extreme values have been excluded, since they were associated with an instrument error.

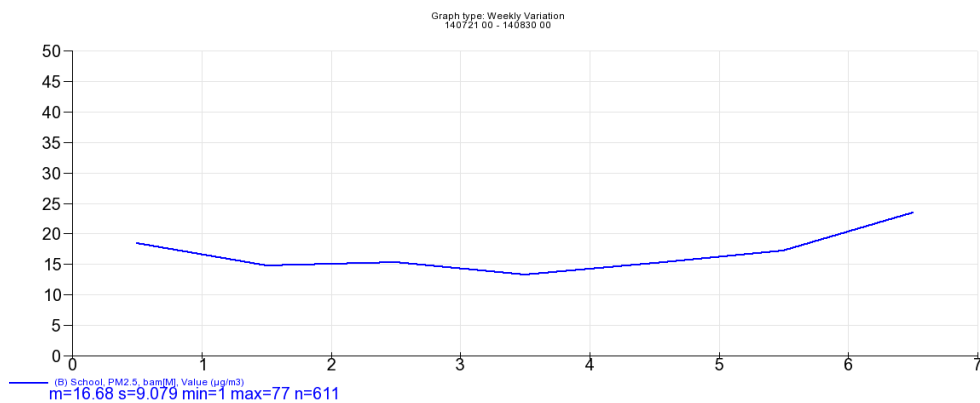


Figure 4.2.2 PM2.5 average concentrations at station B for different days of the week (first value left is Monday, last value right is Sunday)

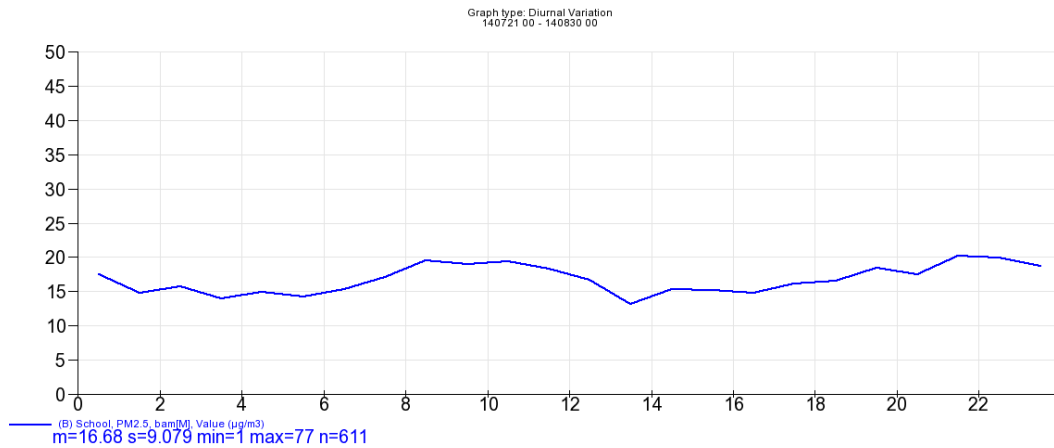


Figure 4.2.3 Daily mean cycle of PM2.5 concentrations at station B

In summary the monitored values at station B indicate a background PM2.5 level of up to $15 \mu\text{g m}^{-3}$. However, there were repeated problems with the feeding of the filter, leading to measurement errors which may not have been completely removed. The installation also required the inlet to be bent, which was obtained by using a plastic (PVC) tube as part of the intake tube. The plastic tube introduces particle mass losses that are difficult to quantify. As a result, we will use the BAM data at station B as a minimum baseline of PM2.5 concentrations.

PM2.5, OC, EC and BC measured at stations T and L

The results of the filter samplings using the Harvard Impactor (HI) will be presented first, since it is considered that the mass monitoring technique is most close to the reference method and we will use it as “true concentration levels”. The HI sampling resulted in a month long time series at both station T (Fig. 4.2.4) and L (Fig. 4.2.5).

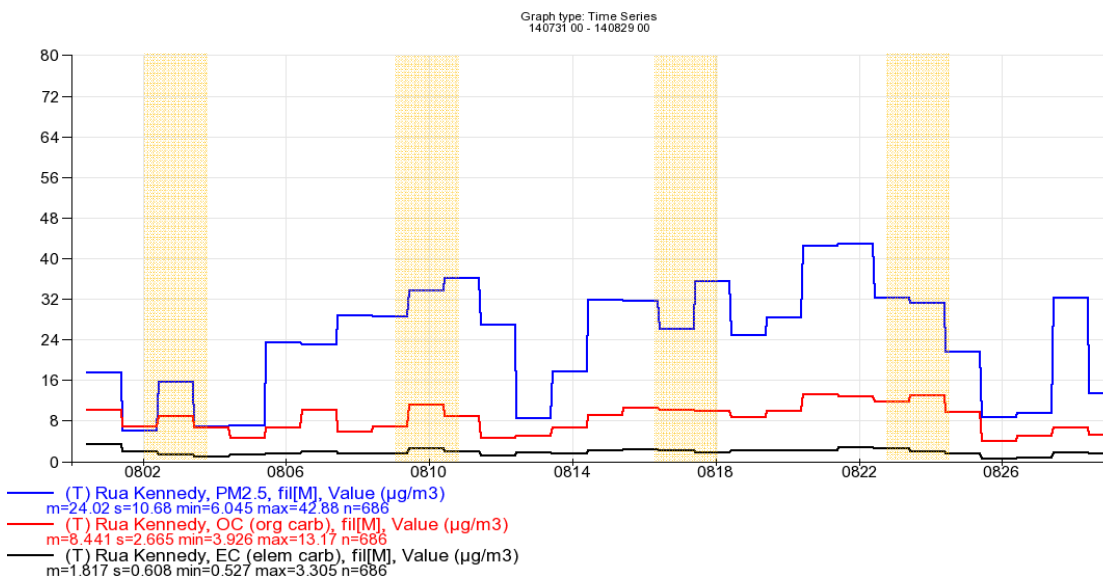


Figure 4.2.4 PM2.5 (blue), OC (red) and EC (black) levels registered at station T. The filters were changed at 11:00 hours every morning. Weekends are marked in yellow.

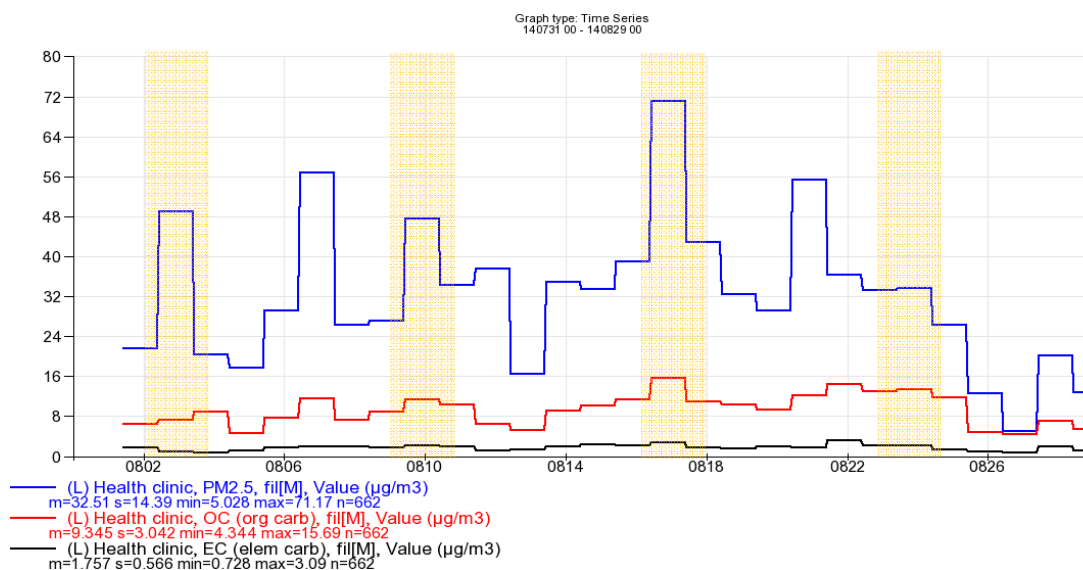


Figure 4.2.5 PM2.5 (blue), OC (red) and EC (black) levels registered at station L. The filters were changed at 11:00 hours every morning. Weekends are marked in yellow.

Table 4.2.4 Observed average levels during the period July 31 – August 29, 2014.

	PM2.5 (µg ^{m-3})	OC (µg ^{m-3})	EC (µg ^{m-3})	OC/PM2.5	EC/PM2.5	OC/EC
station T	24.0	8.4	1.8	35%	8%	4.6
station L	32.5	9.3	1.8	29%	5%	5.3

The month long average values (Table 4.2.4) indicate PM2.5 levels at or slightly above the limit values (annual mean) of São Paulo state and the EU legislation. The levels at the residential station L are considerably higher than those measured at station T, despite that the latter was located in one of the most trafficked streets of the city center.

The August 2014 average PM2.5 levels reported here are higher than the annual average PM2.5 reported in Porto Alegre by Maura de Miranda et al. (2012), however the authors report a seasonal effect for this city where PM2.5 levels are higher during July-August. A visual inspection of the daily values published in the same article, provides a monthly mean estimation of ~20 µg/m³ in August. Thus the station T monthly average may be comparable to the Porto Alegre annual mean, but the station L level may indicate higher annual average values as compared to the Porto Alegre reference.

The rather high OC/EC ratios are, if compared to values reported in the literature (Pio et al., 2012) typical for biomass burning. The OC portion of PM2.5 in Sapiranga is also comparable to the ratio observed in the Chilean city Osorno (31%, pers. comm. Matías Tagle), a city completely dominated by huge PM2.5 contributions from local wood combustion. The EC to PM2.5 ratios in Sapiranga are slightly higher than those observed in Osorno (3%), i.e. traffic may be a somewhat more important source to PM2.5 in Sapiranga.

There are some common temporal variations in PM2.5 levels at the two stations, e.g. the low levels registered on August 3-4, 12-13 and 25-26. During the days in between these periods both stations have increased levels, but station L shows a larger variability with higher peak values.

In parallel with the HI sampling of PM2.5, a DustTrak monitor registered hourly data. The DustTrak monitor was installed two weeks at station T and then moved to station L. In order to have consistent PM2.5 levels, the DustTrak data were corrected so that the running 24h mean values compare with the HI levels. The two graphs of Figs. 4.2.6 and 4.2.7 show how the DustTrak raw data (red line) was adjusted (black line) to fit the HI levels. Since the DustTrak data sometimes show high peak values, there is a need to compensate with levels down to zero. The correction procedure was specified to not go below 2 μgm^{-3} .

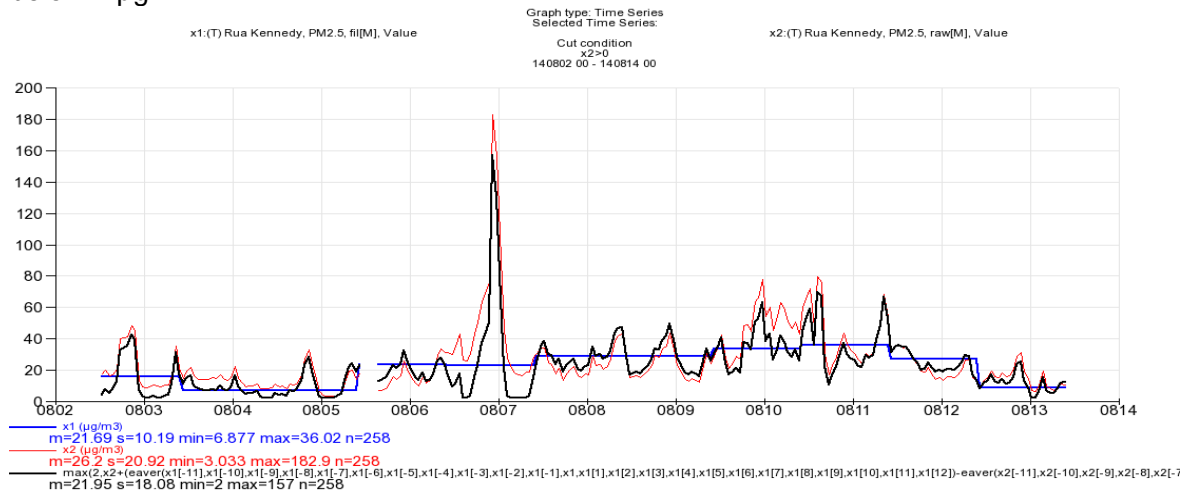


Figure 4.2.6 PM2.5 HI (blue), PM2.5 DustTrak raw (red) and corrected (black) levels registered at station T. Period: August 02-13, 2014.

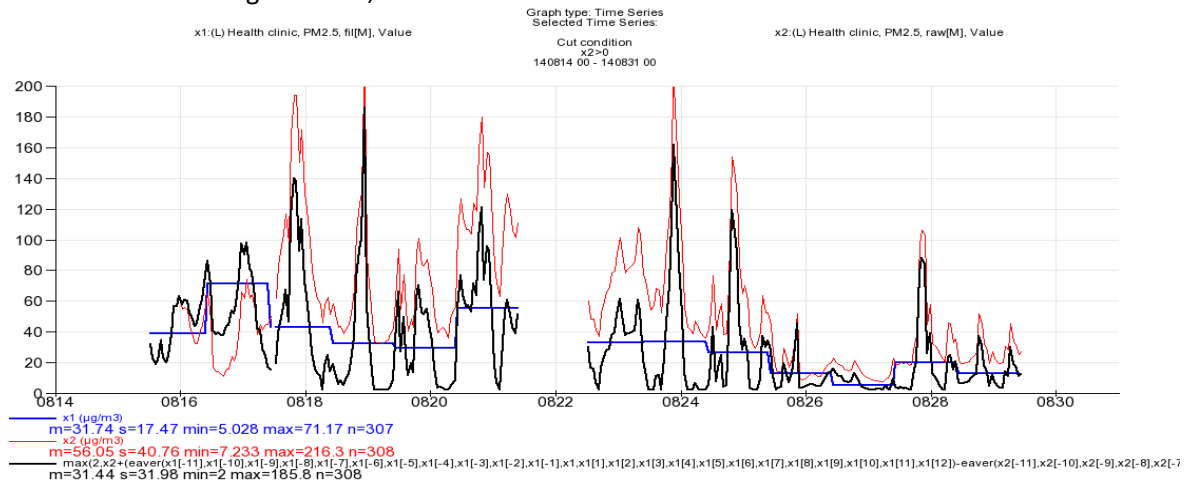


Figure 4.2.7 PM2.5 HI (blue), PM2.5 DustTrak raw (red) and corrected (black) levels registered at station L. Period: August 14-29, 2014.

The BC levels at station T (Fig. 4.2.8) are higher during weekdays because road traffic is a major BC source and traffic volume is lower on weekends. At station L (Fig. 4.2.9) there is also a tendency for slightly higher BC levels during weekdays. OC levels are higher on

weekends (although a peak appears also during the week). This can be an indication of a stronger impact from other sources than traffic - e.g. wood combustion - on weekends.

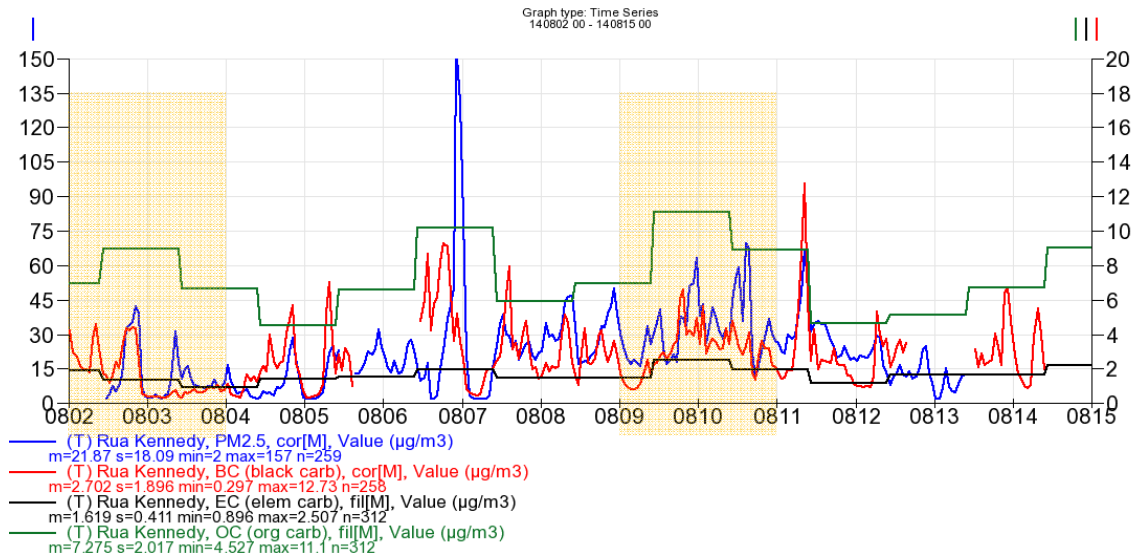


Figure 4.2.8 PM2.5 DustTrak corrected (blue), BC microAeth (red), EC HI (black) and OC HI (green) at station T. Period: August 02-14, 2014.

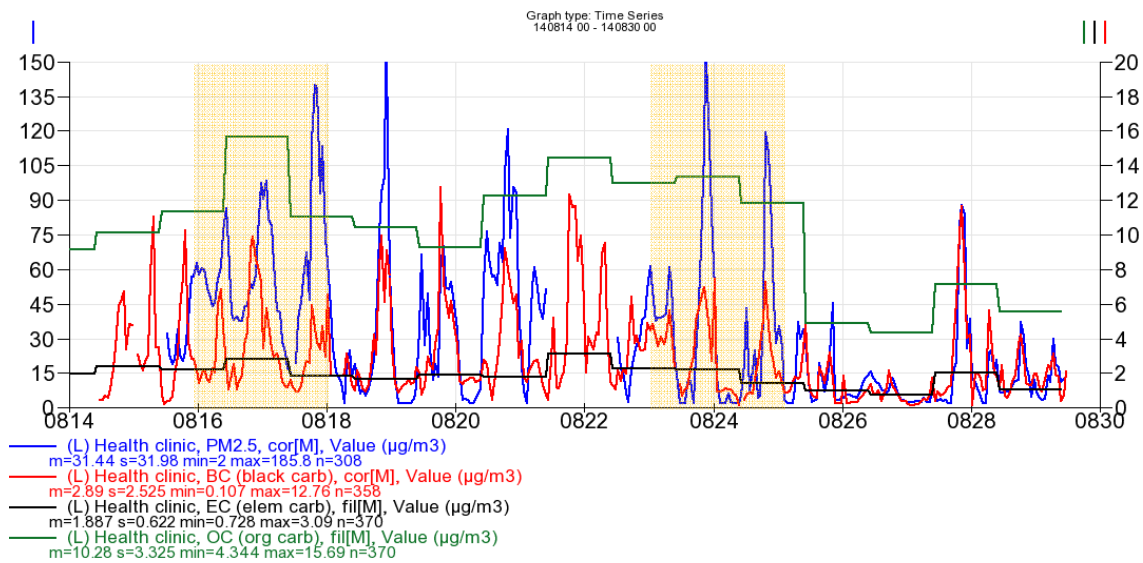


Figure 4.2.9 PM2.5 DustTrak corrected (blue), BC microAeth (red), EC HI (black) and OC HI (green) at station L. Period: August 02-14, 2014.

BC levels and BC/PM2.5 ratios (Table 4.2.5) are lower than those reported from Porto Alegre by Maura de Miranda et al. (2012), but since the Porto Alegre data were determined with optical reflectance (black smoke) it is not straight forward to compare with BC data measured with aethalometer (optical absorption).

The ratios of BC (aethalometer) to EC (filter and thermic analysis) are close to 1.5 at the two stations. The ratio of 1.5 will be used while estimating the emissions in the integrated analysis (Section 4.5).

Table 4.2.5 Observed average BC levels during the period July 31 – August 29, 2014.

<i>Site</i>	<i>BC</i> (μgm^{-3})	<i>BC/PM2.5</i> (%)	<i>BC/EC</i> (-)	<i>Period</i>
T	2.70	14	1.67	Aug 02 – 14, 2014
L	2.89	10	1.52	Aug 15 – 29, 2014

Particle number & size distribution at stations B, T and L

The Table 4.2.6 presents the Particle Number Concentrations (PNC) average for the different sites considered in this study. For the B and L sites only measurements during weekdays are available. At site T it is observed that the PNCs were generally higher during the weekend than on weekdays. The short monitoring periods imply that the relations between the mean PNCs can be more due to meteorological conditions and does not necessarily reflect emission intensity. Instead it is of more interest to analyze the temporal variations and the size distributions.

Table 4.2.6 Mean particle number concentrations (PNC) and the mean concentrations for the nucleation, Aitken and accumulation modes.

<i>Site</i>		<i>PNC</i>	<i>Nucleation</i>	<i>Aitken</i>	<i>Accumulation</i>
B	Weekdays	1.00E+04	3.43E+03	4.62E+03	1.98E+03
L	Weekdays	2.16E+04	5.93E+03	1.02E+04	5.44E+03
T	Weekdays	2.71E+04	7.61E+03	1.35E+04	5.91E+03
	Weekends	3.59E+04	6.96E+03	1.91E+04	9.79E+03

All results are expressed as particle/cm³.

Figure 4.2.10 shows the daily variation for at the different sites. It is possible to see two well defined peak concentrations at 9 h and 19 h, corresponding to periods when many vehicles are in circulation. For the weekend stands out the maximum PNC at 21 h. This can be due to both the increased circulation of vehicles during weekends, especially from people going to parties or going home on Sunday, as many travel to nearby cities as well

as a contribution of nanoparticles derived from wood or coal burning, used in barbecue, typical for this region.

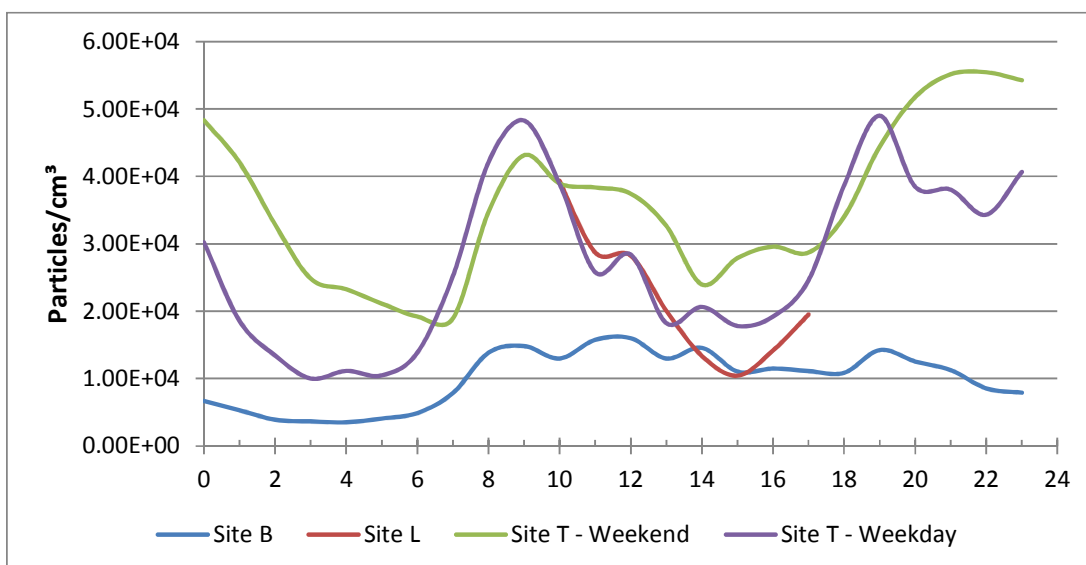


Figure 4.2.10 Daily variation of the nanoparticles concentrations.

For all locations (B, L and T), trimodal distributions were adjusted for the average nanoparticles concentrations (Figures 4.2.11-14). Table 4.2.7 presents the modes (D_g) and the contribution fraction (N_i) for each of the modes. The mode 1, centered on ~ 14 nm, corresponds to the nucleation mode, the mode 2 is centered between 32 and 36 nm, corresponds to the Aitken mode, and mode 3, corresponding to the accumulation mode, was centered on ~ 99 nm. Although the modes are concentrated in similar particle diameters, as can be seen in Table 4.2.7, the contribution of each mode (N_i) are different for each of the evaluated areas. Through this modal contribution it is possible to get some clues of the origin of nanoparticles.

Table 4.2.7 Lognormal parameters of the mean particle number size distributions.

Site		σ_{g1}	D_{g1} (nm)	σ_{g2}	D_{g2} (nm)	σ_{g3}	D_{g3} (nm)	N_1	N_2	N_3
B	Weekdays	0.155	13.8	0.491	32.4	0.457	99.8	0.087	0.524	0.389
L	Weekdays	0.183	15.0	0.523	32.2	0.466	99.7	0.049	0.460	0.491
T	Weekdays	0.141	14.1	0.536	34.1	0.428	99.2	0.039	0.550	0.410
	Weekends	0.127	14.3	0.576	36.9	0.425	97.0	0.018	0.446	0.536

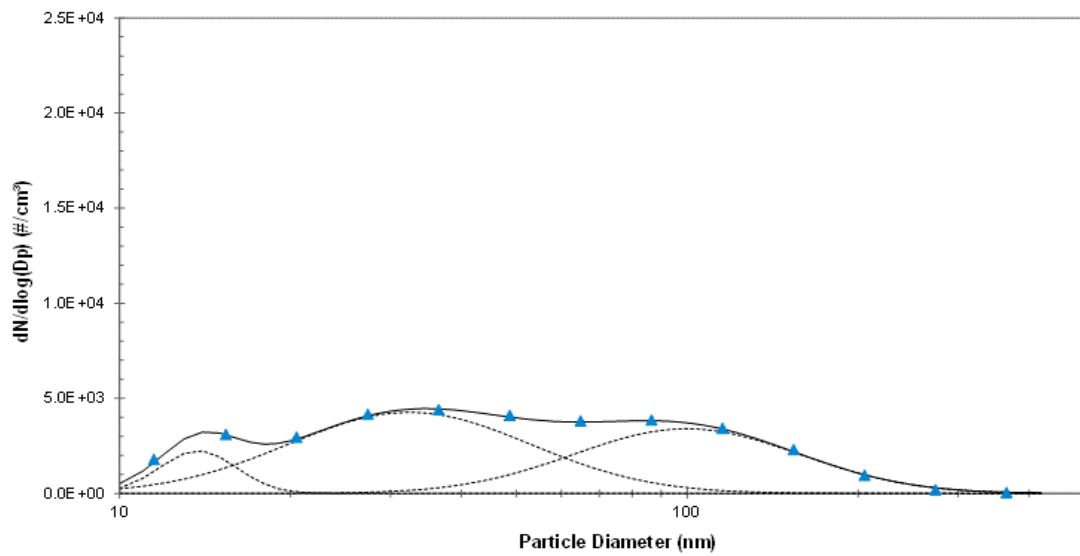


Figure 4.2.11 Fitted multimodel particle size distribution. Average model (solid line), lognormal model components (dotted lines) and average observed concentrations (triangles) - Site B - Weekdays

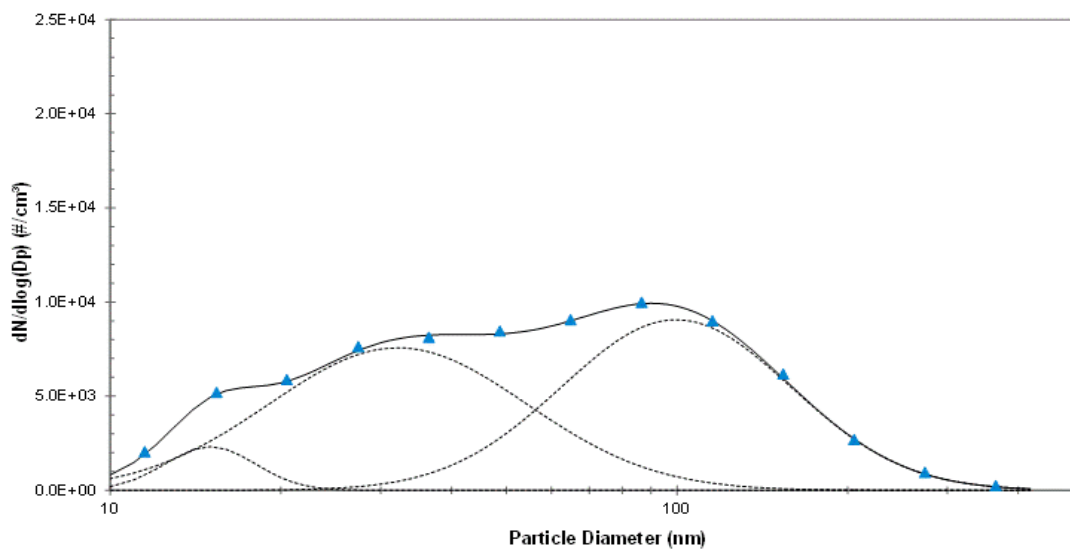


Figure 4.2.12 Fitted multimodel particle size distribution. Average model (solid line), lognormal model components (dotted lines) and average observed concentrations (triangles) - Site L - Weekdays

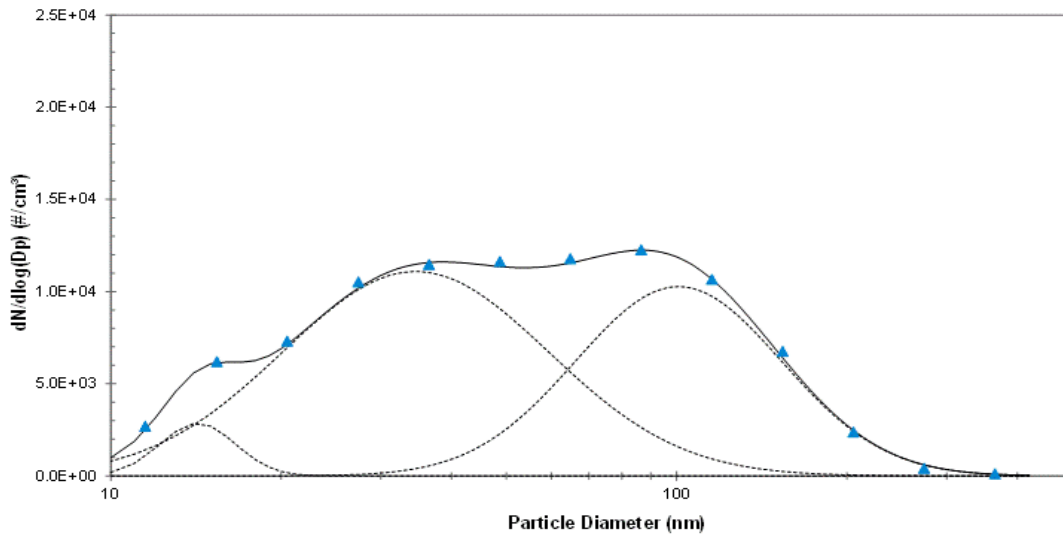


Figure 4.2.13 Fitted multimodel particle size distribution. Average model (solid line), lognormal model components (dotted lines) and average observed concentrations (triangles) - Site T – Weekdays

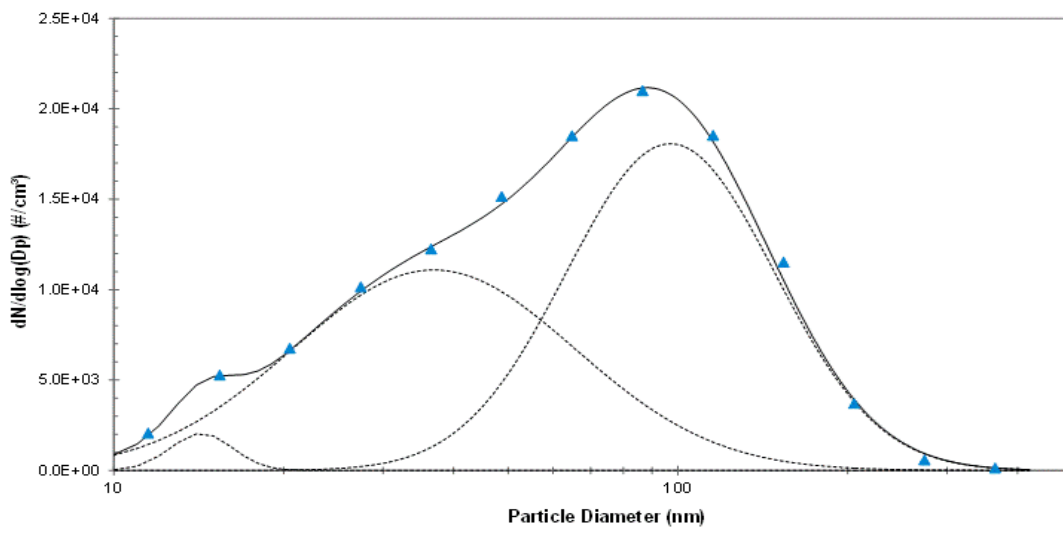


Figure 4.2.14: Fitted multimodel particle size distribution. Average model (solid line), lognormal model components (dotted lines) and average observed concentrations (triangles) - Site T – Weekend

Mode 1 can be attributed to the particles formed in the atmosphere through the gas-to-particle conversion after rapid cooling and dilution of semi-volatile species from the exhaust gases with ambient air when the saturation ratio of gaseous compounds of low volatility reaches a maximum (Charron and Harrison, 2003; Kittelson et al., 2006a; Kumar et al., 2010). The particles in modes 2 and 3 may be attributed to particles formed in the combustion chamber (or shortly thereafter), with associated condensed organic matter

(Kittelson et al., 2006b; Kumar et al., 2008; Kumar et al., 2010). They derive mainly from the combustion of engine fuel and lubricant oil by diesel-fuelled or direct injection petrol-fuelled vehicles (Wehner et al., 2009), as well as from the coagulation of nucleation mode particles.

Particles from mode 2 and mainly mode 3 can be also associated with biomass burning or other source not related to vehicles emissions. If we consider the measurements only made on weekends in the T site, when little influence of vehicle traffic is expected, it can be observed that the particles from modes 2 and 3 are still in high concentration (Figure 4.2.14).

Although anthropogenic biomass combustion for residential purposes can have important contributions to ambient particle concentrations, the emissions of nanoparticles from biomass combustion are not well characterized and they depend on biomass type and combustion temperature. Particle size distributions for fast and slow burning of the wood samples typically have a unimodal distribution. The diameter is larger during the ignition process and varies from 50 to 70 nm for fast burning depending on the species of the wood. Also, the size distributions of particles from burning of the leaves and branches were unimodal, with the exception of the ignition phase of the slow burning of Spotted Gum samples, which showed bimodal size distribution behavior (Wardoyo et al. 2006).

The temporal variation of mode 2 (traffic and some wood combustion) and mode 3 (dominated by wood combustion) as plotted in Fig. 4.2.15 show differences in the evening and night levels. This may be explained by more wood combustion impact during nights. Note also that PM2.5 levels are highest in the late night, when traffic emissions are expected to be low.

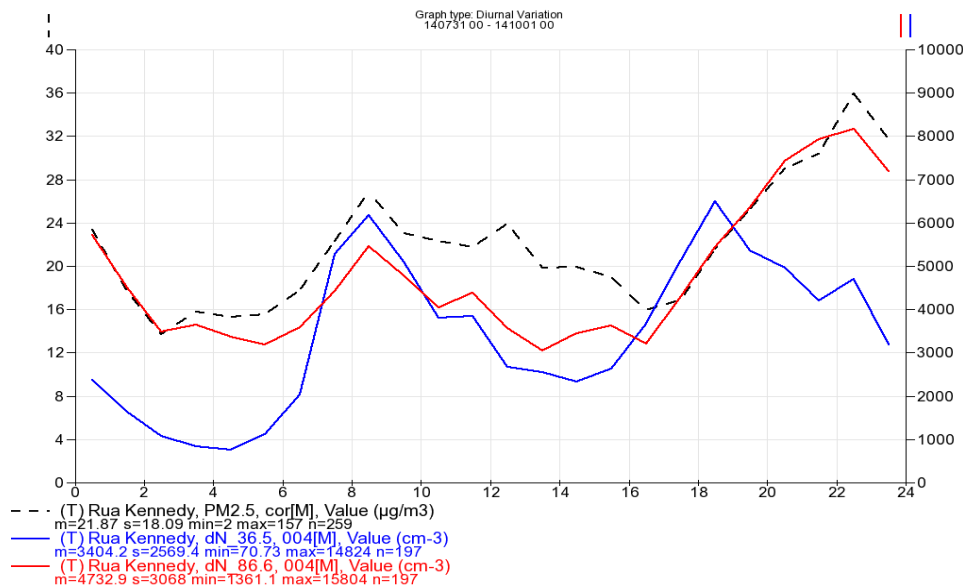


Figure 4.2.15 Daily variation in mode 2 (blue) and mode 3 (red) in comparison with PM2.5 (black) at station T (both weekday and weekend data included).

Particle elemental composition

Receptor models, as the Positive Matrix Factorization (PMF), are statistical methods for quantifying the contribution of different emission sources, based on the time variation of characteristic inorganic elements associated with various sources or processes (fingerprint). The composition of PM_{2.5} determined by using the analytical methods mentioned previously, delivers a data matrix X of *i* by *j* dimensions, in which *i* represents the number of samples and *j* the chemical species measured, associated with uncertainties *u*. The goal of PMF is to solve a chemical mass balance equation between measured species concentrations and sources profiles, with a determined number of factors. The factor profiles resolved by PMF are interpreted to identify the sources that contribute to PM_{2.5} mass, according to a review of relationships between measured species by Calvo et al. (2013).

A total of 22 variables were finally retained during the analysis:

EC, OC, Na, Al, Si, S, Cl, K, Ca, Ti, V, Cr, Mn, Fe, Ni, Zn, Br, Zr, Mo, In, Hg and Pb.

The PMF analysis was performed separately for the two sampling sites (29 filter samples per site), and 4 factors were resolved according to their characteristic tracers. Tables 4.2.8 and 4.2.9 present the PMF analysis solution for the data collected at stations T and L, respectively. We identified and connected each PMF factor to a particular emission source – or in some cases to a mix of sources - according to the literature.

Table 4.2.8
Elemental contribution to each PMF factor (in percentage of total element mass) at station T. Predominant elements for each factor are boldfaced.

	% of species				Species conc. (µg/m ³)
	Soil	Biomass/ Heavy Industry	Metallurgy	Vehicles	
MP2.5	18.0	25.7	42.2	14.1	25.2
OC	28.9	36.5	25.0	9.6	8.27
EC	25.2	34.7	32.1	8.0	1.71
Na	20.5	36.1	29.4	14.0	0.10
Al	53.8	25.8	16.5	3.9	0.11
Si	63.1	11.5	21.9	3.5	0.16
S	1.5	33.3	0.0	65.3	0.45
Cl	0.0	60.9	24.5	14.7	0.018
K	26.3	52.9	20.8	0.0	0.37
Ca	52.0	9.3	34.1	4.6	0.035
Ti	65.1	32.7	0.0	2.2	0.0056
V	17.1	38.5	4.7	39.6	0.0005
Cr	15.7	49.0	32.8	2.5	0.0009
Mn	95.4	4.6	0.0	0.0	0.0011
Fe	42.9	26.5	22.4	8.2	0.137
Ni	13.8	80.7	5.5	0.0	0.0012
Zn	0.0	46.8	5.3	47.9	0.010
Br	21.9	36.1	0.0	42.0	0.002
Zr	13.7	0.0	67.4	19.0	0.003
Mo	20.8	76.9	2.3	0.0	0.001
In	36.8	0.0	23.8	39.3	0.015
Hg	39.8	4.8	41.2	14.1	0.0078
Pb	5.9	18.8	27.7	47.7	0.0072
Mass (µg/m ³)	4.53	6.48	10.65	3.56	

Major concentrations were found in carbonaceous fraction (EC and OC), which were slightly higher at L station. The emission sources identified by the PMF analysis were soil, biomass burning, heavy industry, metallurgy, traffic vehicles, and waste burning/incineration.

The PM_{2.5} aerosol sampled at the two stations showed S and K as predominant inorganic species, those being tracers for diesel combustion (diesel fuel in Brazil has a sulfur content of 500 to 2000 ppm) and wood burning, respectively. The soil source was clearly identified at both stations, showing a high percentage of crustal material (Al, Si, Ca, Ti and Fe). At the city center station T, vehicular traffic stands out as one of the four factors. At station L, the impact of local traffic is expected to be low and vehicular emissions enter in a factor mixed with industrial impact. The biomass burning source, commonly associated with high K levels, was not clearly separated in any of the stations, instead it appears together with industrial/metallurgical elements like Ni, Br, Hg and Mo.

Table 4.2.9

Elemental contribution to each PMF factor (in percentage of total element mass) at station L. Predominant elements for each factor are boldfaced.

	% of species				Species conc. (µg/m ³)
	Soil	Biomass/ Metallurgy	Vehicles/ Heavy Industry	Waste burning/ incineration	
MP2.5	7.7	46.0	20.2	26.2	31.03
OC	24.4	35.6	19.0	21.0	9.12
EC	22.7	37.2	14.0	26.1	1.686
Na	25.1	26.8	35.9	12.2	0.091
Al	65.8	13.9	11.7	8.5	0.103
Si	81.8	3.4	4.2	10.5	0.146
S	12.6	11.6	75.6	0.2	0.420
Cl	0.0	6.8	0.0	93.2	0.052
K	28.1	39.7	14.4	17.8	0.387
Ca	66.6	12.4	5.5	15.4	0.029
Ti	84.1	2.0	1.4	12.5	0.005
V	35.2	0.0	22.6	42.2	0.0003
Cr	40.1	0.0	47.4	12.4	0.001
Mn	19.1	37.1	37.2	6.6	0.001
Fe	58.9	15.0	13.1	13.0	0.099
Ni	38.8	12.4	18.0	30.8	0.001
Zn	0.0	0.2	77.8	22.0	0.011
Br	3.5	70.6	0.0	25.9	0.002
Zr	0.0	43.4	52.6	4.1	0.003
Mo	22.3	21.0	41.6	15.1	0.003
In	49.4	8.6	34.1	7.9	0.014
Hg	2.5	68.8	28.7	0.0	0.010
Pb	15.5	11.8	42.5	30.2	0.007
Mass (µg/m ³)	2.39	14.27	6.26	8.12	

It is noteworthy that this mixed factor shows the highest contribution of EC and OC at both stations, which indicates burning of organic material, possibly from industrial processes using biomass combustion. The Cl appearing at station T in the mixed biomass/industry factor and also, in higher absolute levels, in the fourth “incineration” factor of station L, can indicate local waste burning with plastic materials.

A large part of the PM aerosol in Sapiranga is of regional origin. Braga et al. (2005) characterized the elemental profile in the Metropolitan Area of Porto Alegre by using factor analysis on sampled PM filters. They identified several industrial sources: oil refinery (Refinaria Alberto Pasqualini), two steel plants (Siderúrgica Riograndense and Gerdau-Aza S.A), a petrochemical complex (III Complexo Industrial Petroquímico), and two coal-fired power plants in Charqueadas (60 km to Porto Alegre), see map in Figure 4.2.16. They also found the contribution of vehicular and waste burning activities, and highlighted the contribution of elements as V, Cr, Ni, Cu, Zn along with S and Cl.

Although the PMF analysis could be a good tool to identify and apportion PM2.5 emission sources, there is a large uncertainty associated with the reduced number of samples (29) per site collected during the Sapiranga pilot study. The results should rather be used as an independent information source to be put together with the integrated (measurement data and model simulation results) analysis presented in Section 4.5. From the PMF analysis of PM2.5, we highlight the larger contribution of biomass burning at station L, as compared to station T (Fig. 4.2.17).

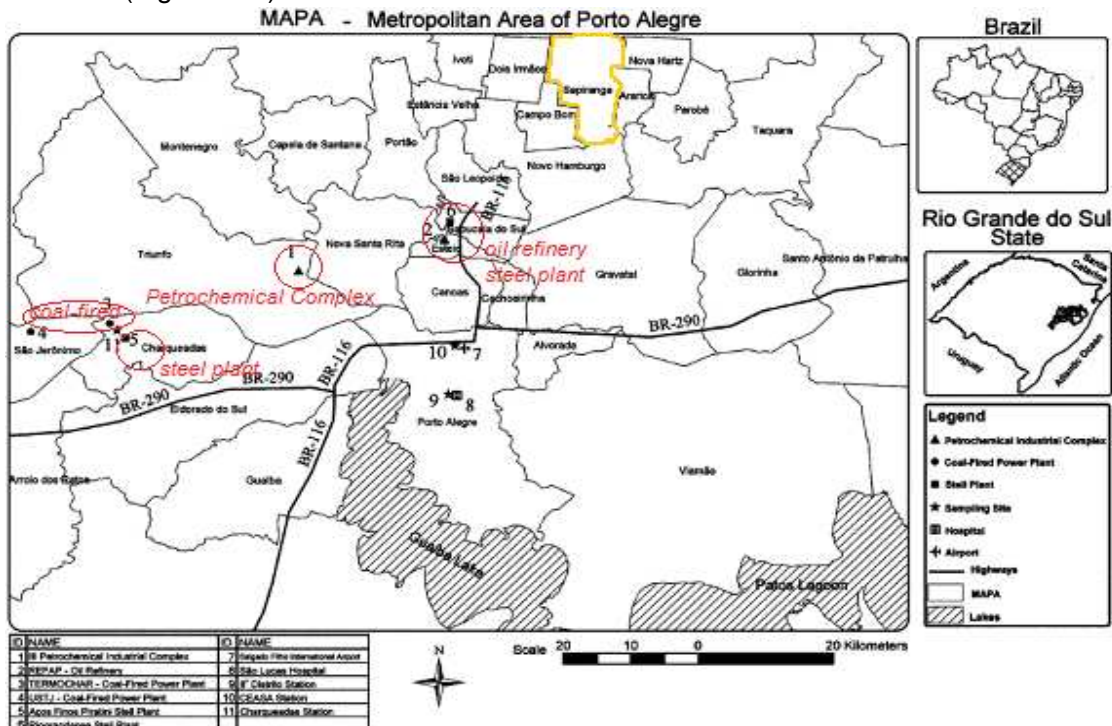


Figure 4.2.16 Location of main industrial sources in the Porto Alegre Metropolitan region. Map source: Braga et al. (2005).

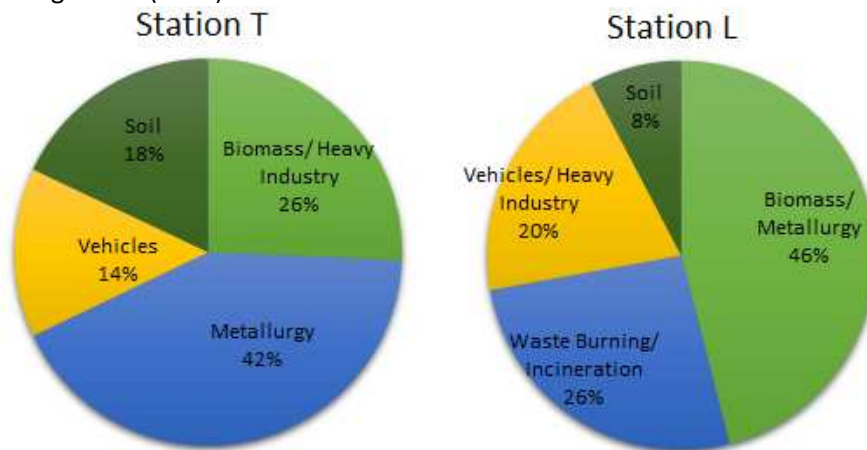
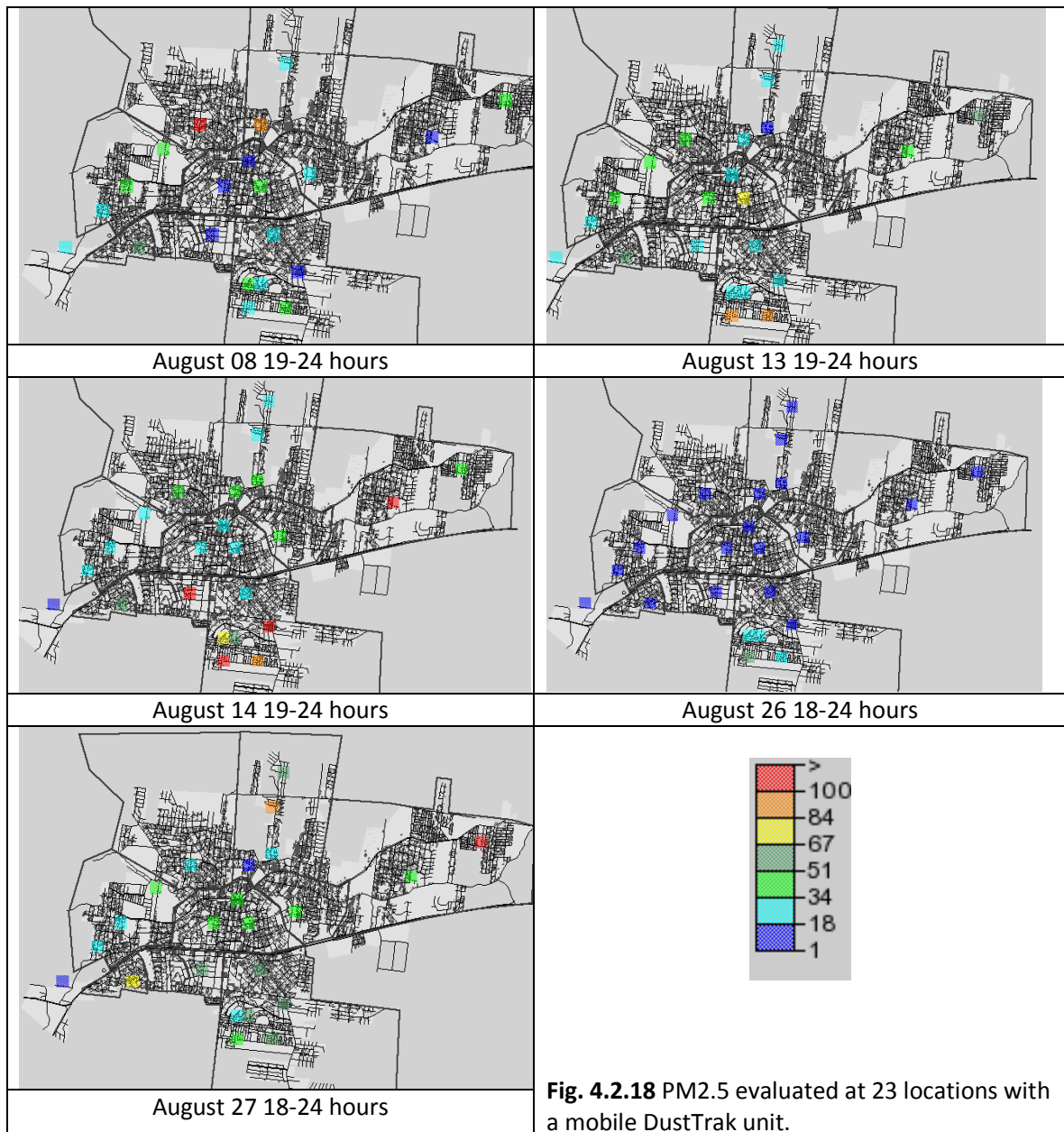


Figure 4.2.17 PMF-estimated contribution to total PM2.5 mass at station T and L. The dominant sources were associated with biomass burning and metal or heavy industry (mixed factor).

Mobile measurements of PM2.5 and BC

Mobile measurements of PM2.5 (DustTrak monitor) and BC (microAeth) are illustrated in Figs. 4.2.18 and 4.2.19, respectively. The mobile data collected with this second DustTrak monitor was not corrected with the concurrent Harvard Impactor filter data. Instead the raw DustTrak data was reduced by 30%, as indicated in the latest calibration of the instrument made in Chile one month before the Sapiiranga campaign. Even though there is a larger uncertainty of absolute levels, it should be noted that the objective of the mobile measurements is to look for spatial gradients and variability across the city.



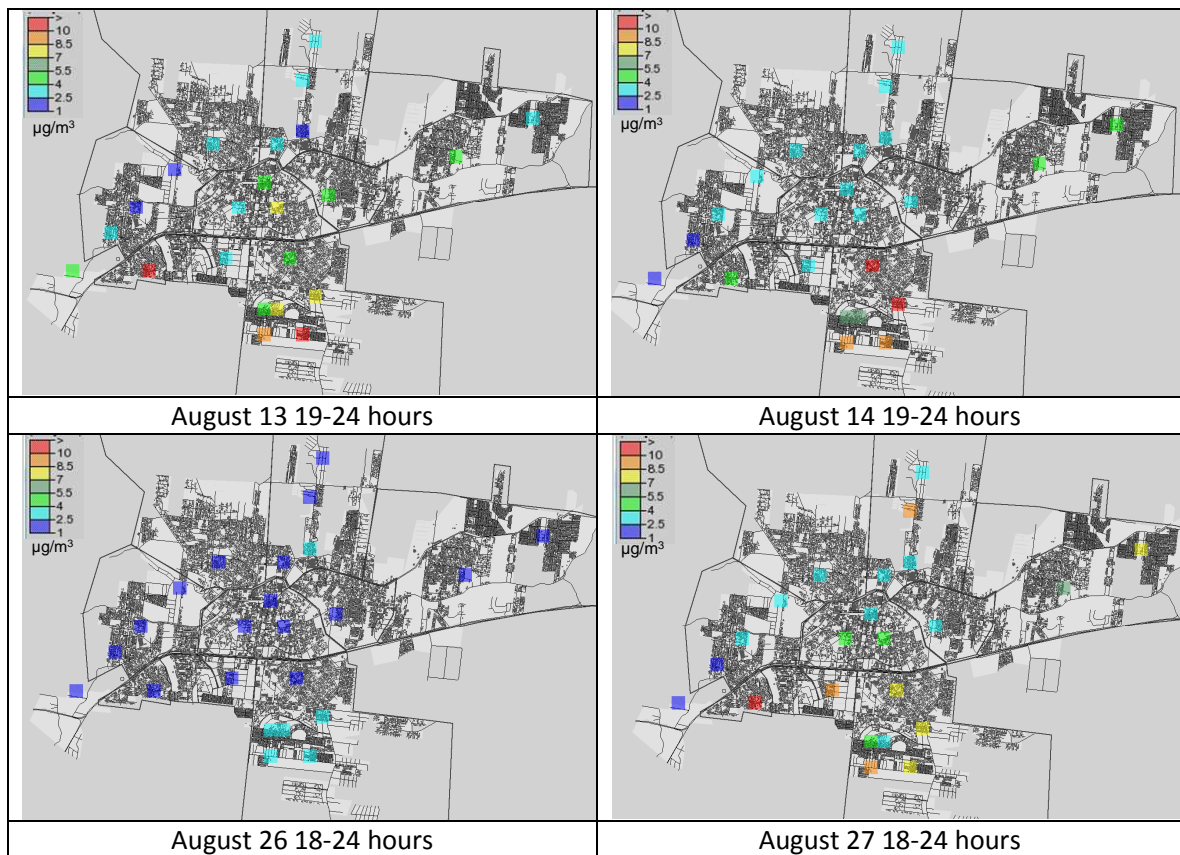


Fig. 4.2.19 BC levels evaluated with the mobile microAeth instrument.

The averaged PM_{2.5} and BC distributions in Fig. 4.2.20 indicate that the westernmost part of the city, north of RS239 highway, is a relatively clean area, whereas pollution levels rise towards the east and to the south. The distribution also indicates the presence of local sources that create large gradients in relatively small areas, e.g. in northwest (district 3 Centenário) and in southwest (district 13 Vila Irma). The mobile PM_{2.5} data also confirm high average levels during these evenings, with 5 locations with PM_{2.5} levels >50 µg/m³ (temporal average over all nights), this to be compared with a minimum temporal average of 16 µg/m³ at one of the stations. During the evening August 14 a spatially averaged concentration over all 23 receptor locations was found to be 58 µg/m³, while the same average during the evening of August 26 was only 11 µg/m³ (Figure 4.2.21). Although the absolute PM_{2.5} concentration measurements have a larger uncertainty, the mobile campaign clearly show both the large variations between different locations in Sapiranga, as well as the large day-to-day variability.

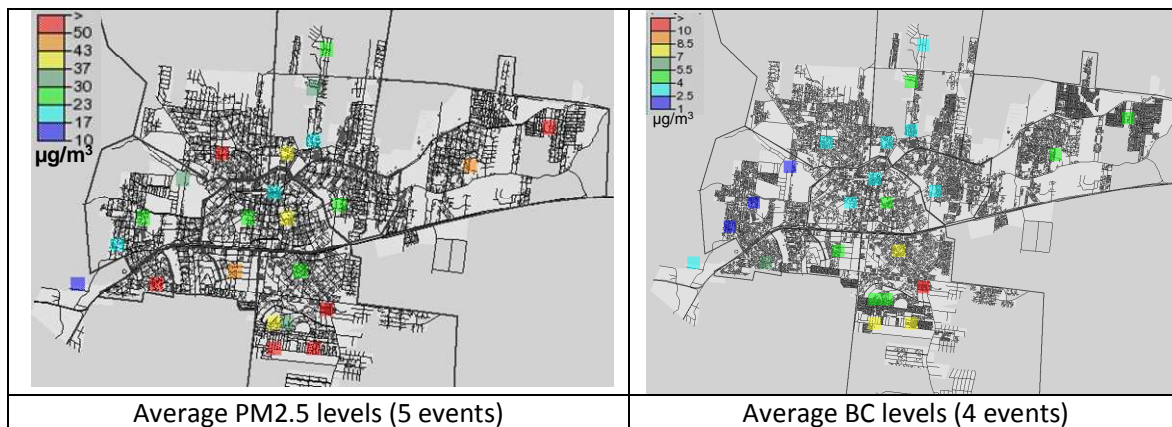
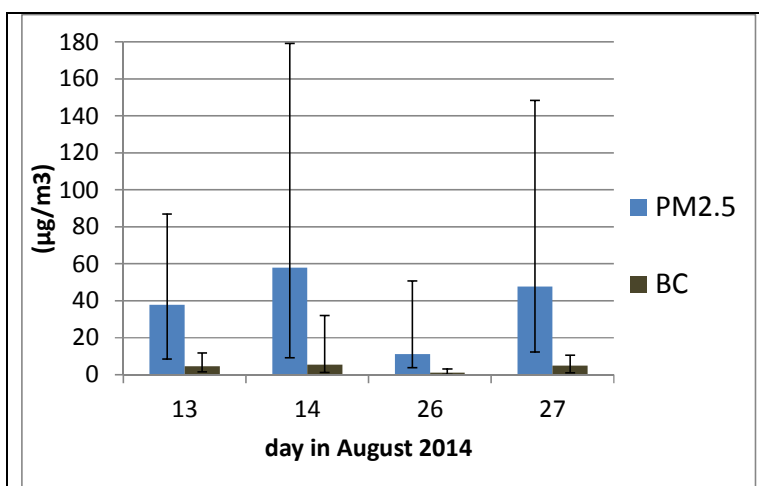


Fig. 4.2.20 Average levels from mobile measurements.

Fig. 4.2.21

Spatially averaged levels from all 23 monitored stations during 4 evenings of PM_{2.5} (blue) and BC (black) from mobile measurements. Maximum and minimum values indicated as error bars. BC to PM_{2.5} ratios vary between 9 and 12%, for all four nights an average of 10%.



4.3 Regional dispersion modeling

The regional simulation estimates the background contribution to the PM_{2.5} concentrations inside Saporanga. Figure 4.3.1 shows the concentration of fine particles over the Rio dos Sinos Valley, emitted from urban and biomass burning sources during the field campaign period. The results show that the Saporanga city was influenced by neighbouring larger cities located west (Porto Alegre and Novo Hamburgo). We can also notice that during the study period, there was an influence (below 30%) from vegetation fires in the vicinity (Fig. 4.3.2 and 4.3.3).

Comparing the PM_{2.5} simulated over Saporanga (pixel with 10 km spatial resolution) with the values observed at Station B (BAM-1020), it is possible to see that the model consistently represents the temporal variability but overestimate the average background (ratio of simulated to monitored average PM_{2.5} is 242%, Fig. 4.3.4). The biomass burning has a relatively low impact on Saporanga's mean PM levels, but some fire foci were

registered in the vicinity of Sapiroanga urban area in the period August 20 to 22, giving strong peaks in the local observations. The thinner blue line in Fig. 4.3.4 shows the PM_{2.5} contribution from biomass burning sources.

Figures 4.3.5 and 4.3.6 display the background contributions simulated with the regional model in comparison to monitored PM_{2.5} concentrations at station T and L, respectively. Here the average levels are more similar to monitored, but still overestimating, giving a relation simulated/measured PM_{2.5} of 173% at station T and 128% at station L. An overview of simulated and monitored averaged PM_{2.5} levels is found in Table 4.3.1.

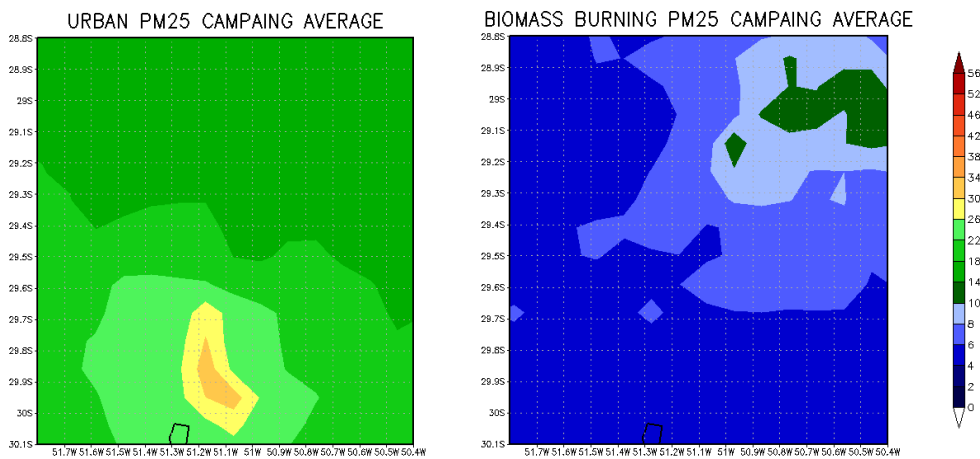


Figure 4.3.1 PM_{2.5} urban and biomass burning concentration ($\mu\text{g}/\text{m}^3$) – Average over campaign period.

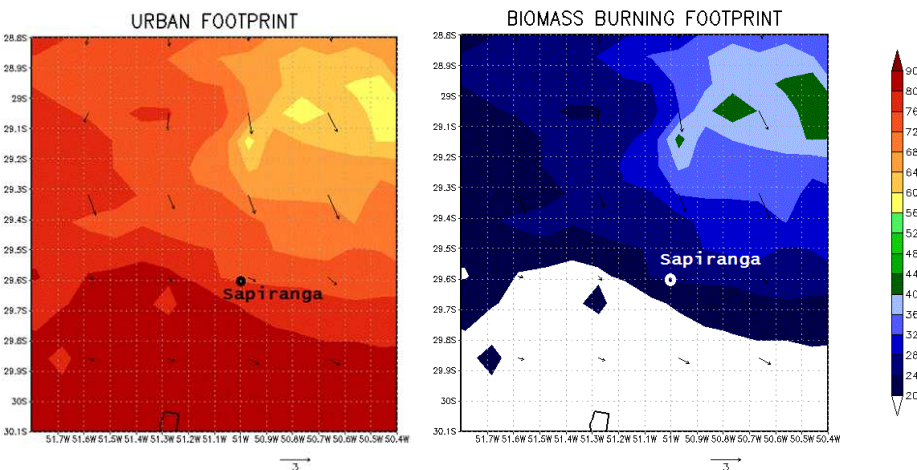


Figure 4.3.2 Urban and Biomass burning footprint (contributions) to PM_{2.5} (%) and average wind (m/s).

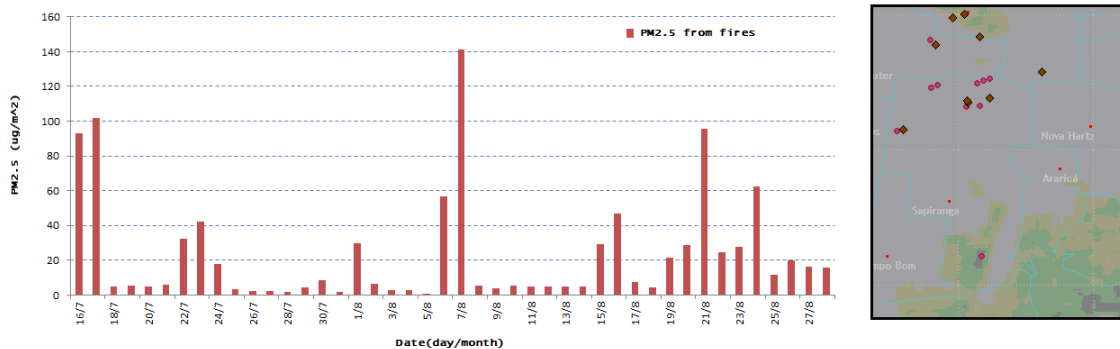


Figure 4.3.3 PM2.5 contributions from biomass burning sources simulated in station B. Fires for august 2014 (the spots are representative of period from august 21 to 22), adapted from BDQueimadas database [<http://www.dpi.inpe.br/proarco/bdqueimadas/>]

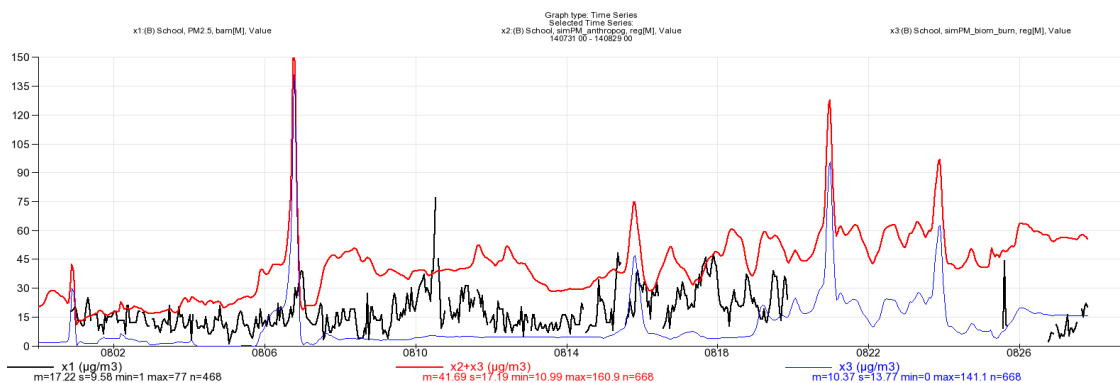


Figure 4.3.4 Simulated background PM2.5 (total = red, biomass burning = blue) and monitored PM2.5/BAM (black) at station B.

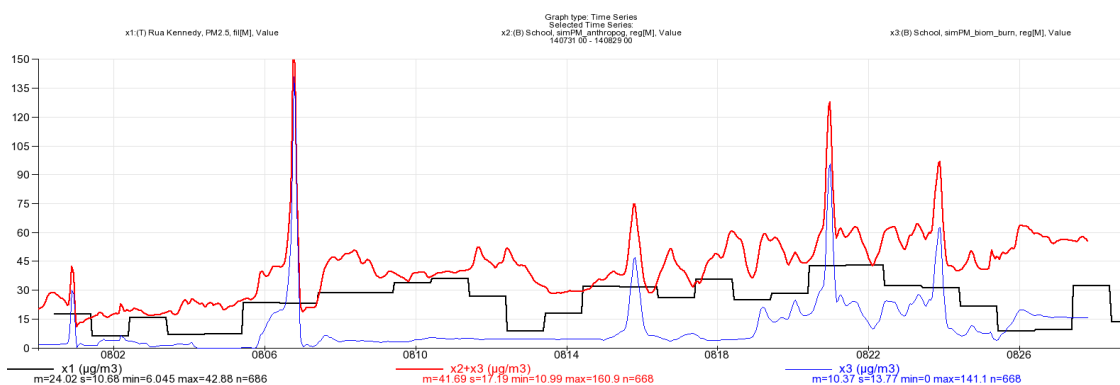


Figure 4.3.5 Simulated background PM2.5 (total = red, biomass burning = blue) and monitored PM2.5/BAM (black) at station T.

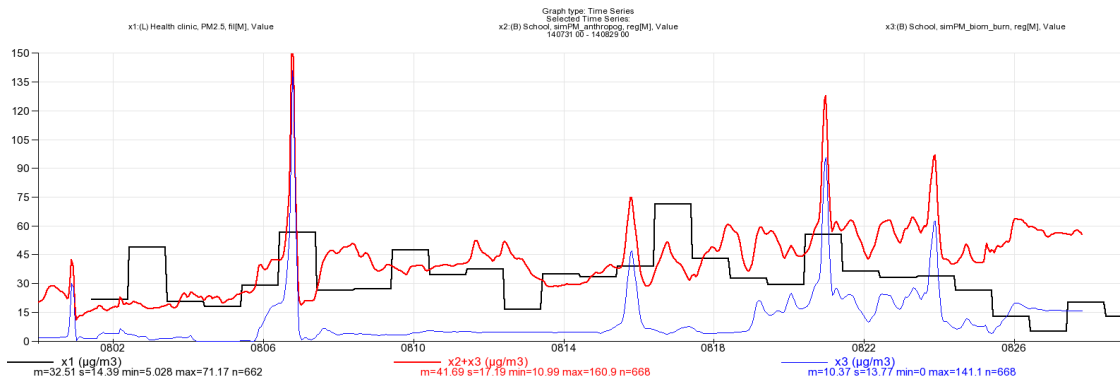


Figure 4.3.6 Simulated background PM2.5 (total = red, biomass burning = blue) and monitored PM2.5/BAM (black) at station L.

Table 4.3.1 Simulated background contributions to PM2.5 at station B, T and L
Period: July 31 – August 29, 2014. Monitored concentrations are given in the last column.

Site	anthropogenic sources	biomass burning	total background from regional model	monitored	simulated / monitored
B	31.3	10.4	41.7	17.2 ¹	242%
T	31.3	10.4	41.7	24.0	173%
L	31.3	10.4	41.7	32.5	128%

¹ Uncertain level as data capture was only 67% and losses during peak values are suspected.

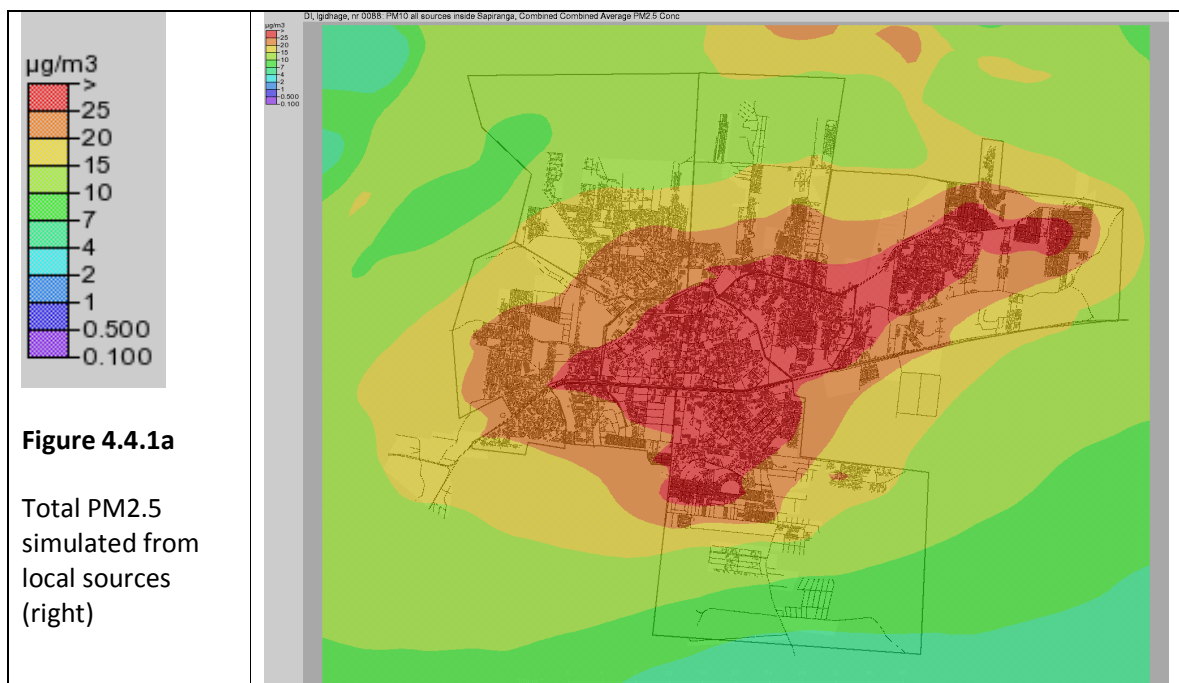
4.4 Local dispersion modeling

Model simulations of PM_{2.5} contributions were performed with a Gaussian model, using a 100x100 m grid covering the city area and emissions were taken from the inventory (Section 3.3). The following simulations were calculated for the period July 31 – August 28:

1. Only emissions from restaurants/pizzerias (mostly wood combustion)
2. Only emissions from one industrial source inside Sapiranga (wood combustion)
3. Only emissions from residential wood combustion
4. Only emissions from road traffic
5. Only emissions from charcoal and brick production (both sources in rural areas just outside Sapiranga, both due to wood combustion)

Also the OSPM street canyon model was run for the road link of station T (Rua Kennedy), with emissions only from road traffic at that particular road link.

The average concentration results for the monitoring period are displayed in Fig. 4.4.1a-b and listed in Table 4.4.1. Note that the simulations calculated in this Section 4.4 are based on the emission inventory presented in Section 3.3 and no background concentrations were added. Table 4.4.1 shows that the impact of the RWC source is one magnitude larger than for the other sources.



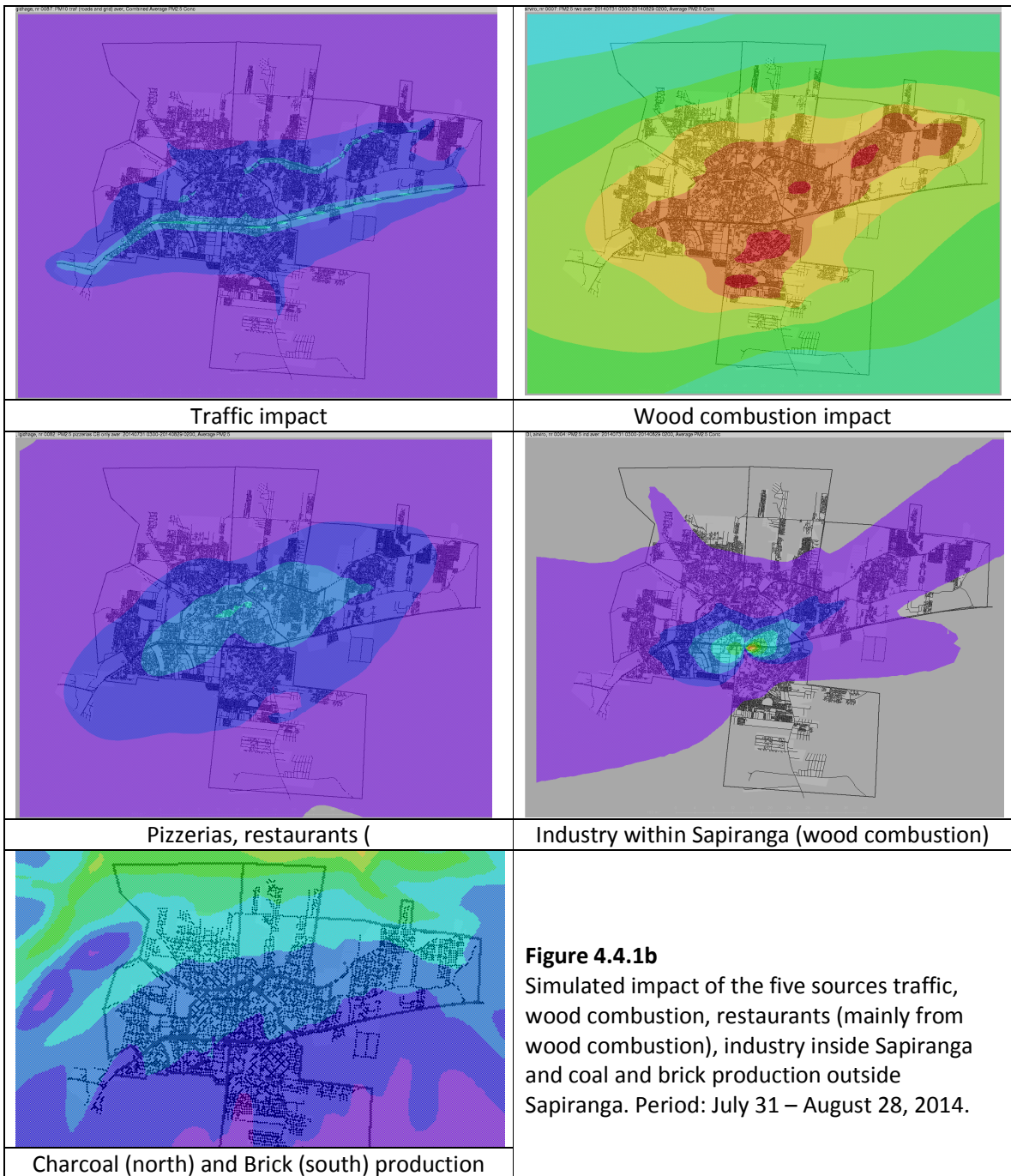


Table 4.4.1 Simulated average local contributions to PM2.5 at station B, T and L (traffic_OSPM indicate local contribution from street canyon, traffic_UB is contribution from all other streets in the city. Period: July 31 – August 29, 2014. Note: No background has been added.

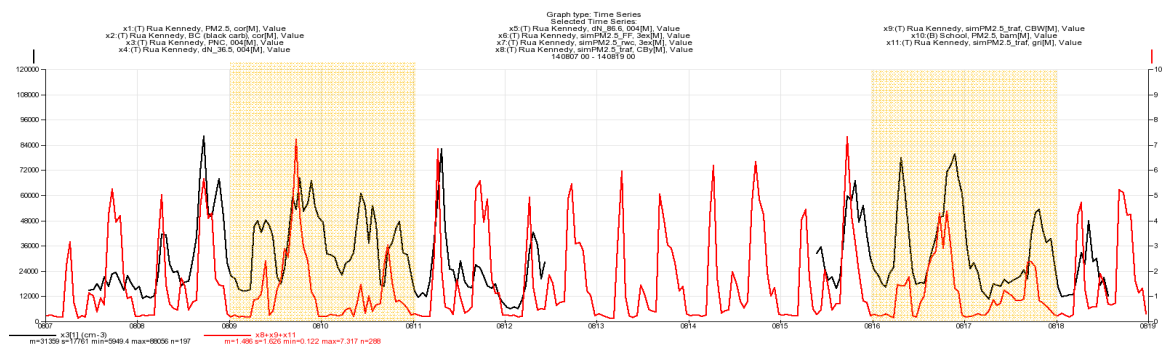
Site	traffic_ OSPM	traffic_ UB	pizzerias	Industry	RWC	Charcoa + brick	total simulated	Monitored
B	-	0.60	0.59	0.27	15.1	1.23	17.8	17.2 ²
T	0.64	0.96	1.08	1.34	23.2	0.93	28.2	24.0
L	-	0.46	0.45	0.41	20.2	0.63	22.2	32.5

The simulated concentrations were calculated using emission factors taken from the literature and international assessments. There is, thus, a rather large uncertainty in the simulated absolute levels and especially for wood combustion since the emissions factor may vary hundreds of percent. There is also a considerable uncertainty in the distribution of the use of residential wood combustion (RWC), both in space and in time. The impact of the traffic source is small and there exist good grounds to increase the emission factors to include not only exhaust particles but also road dust.

We can, by comparing the two last columns of Table 4.4.1 conclude that it is not possible to achieve consistent levels of simulated and monitored levels by only introducing a rural background, uniform over the city. There are likely errors in the distribution of the wood combustion contribution, with too high impact at station T and B.

To identify larger errors in the simulated contributions, we will systematically look at the characteristics of monitored and simulated data. First, we analyze the simulated hourly time series at the station where monitored data have the best quality and volume, i.e. the station T.

Fig. 4.4.2 shows that the simulated traffic impact varies in similar way as monitored PNC, at least during weekdays (only possible to compare the temporal variation, not the amplitude). On Friday nights and weekends, the measured PNC signal shows broader peaks that extend longer into the nights.



Figur 4.4.2 Comparison at station T between monitored PNC (particle number concentration, black) and simulated PM2.5 from traffic exhaust (street canyon plus surroundings, in red).

² Uncertain level as data capture was only 67% and losses during peak values are suspected.

Fig. 4.4.3 compares the monitored PM2.5 with simulated PM2.5 contributions from RWC. The model results show that wood combustion, with its late night emissions, can explain the high measured PM2.5 and PNC levels that extend until midnight (although simulated peak levels are too high). From the baseline of monitored PM2.5, one can see that there is certain background concentration lifting the PM2.5 levels on August 7-11, 2014.

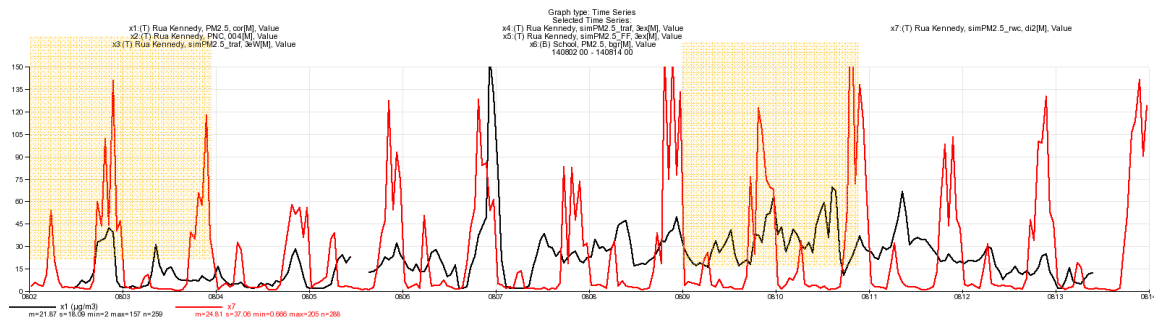


Figure 4.4.3 Comparison at station T between monitored PM2.5 (black) and simulated PM2.5 from residential wood combustion (red).

The background PM2.5 contribution arriving to Sapiranga from sources outside the city can be estimated from the baseline (lower nighttime concentrations) of the station B data, considering that there are relatively few local emissions sources around this station (Fig. 4.4.4). There is however a gap in monitored data from August 20 to 25, i.e. the period with a marked biomass burning impact according to Fig. 4.3.3. The interpolated background for these days is likely not realistic. In Section 4.5 we will compare this interpolated background with the regional model output.

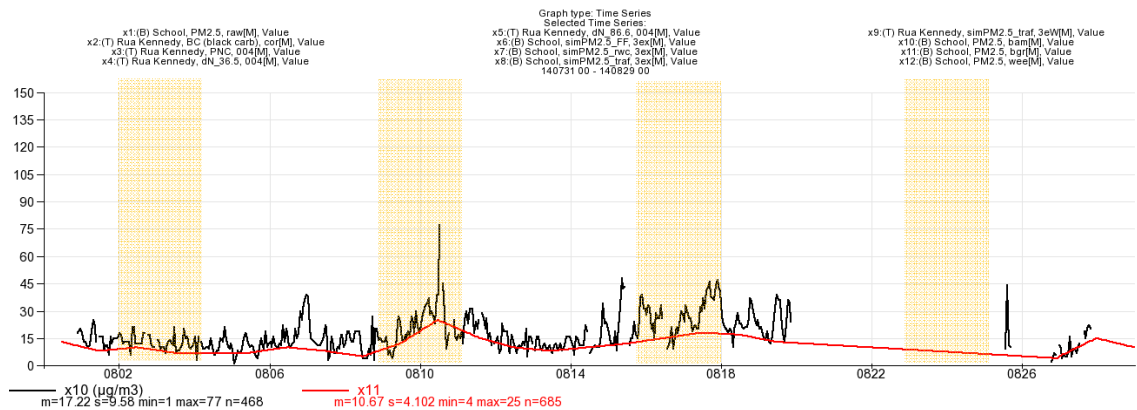


Figure 4.4.4 Monitored PM2.5 concentrations (BAM instrument) at station B. An estimated background PM2.5 concentration in incoming air is given by the red line.

Figure 4.4.5 shows the total simulated PM2.5 at station B, i.e. the sum of pizzerias, industry (inside and just outside the city), RWC, traffic and the interpolated background concentration of Fig. 4.4.4. The high simulated peaks are mainly built up by RWC and they rise to $\sim 150 \mu\text{g m}^{-3}$ during shorter periods, which is much higher than the BAM PM2.5 values. However, the BAM instrument had an intake tube which was partly plastic (PVC), a fact that must have implied losses of particle mass.

One of the DustTrak monitors was installed in parallel and that data showed concentration peaks much higher than the BAM values and not so far from the simulated peaks. This particular DustTrak monitor was not calibrated against the Harvard Impactor; instead a correction factor from an earlier calibration in Chile was used. Thus, the absolute levels of the DustTrak data from station B are more uncertain when compared to stations T and L.

In summary, the simulated PM2.5 levels are too high, likely due to overestimated RWC emissions. Note that the DustTrak monitor, which measures over the August 20-25 gap in BAM data, indicates high peak values which may be connected to the Aug 21 biomass burning signal (Fig. 4.3.3).

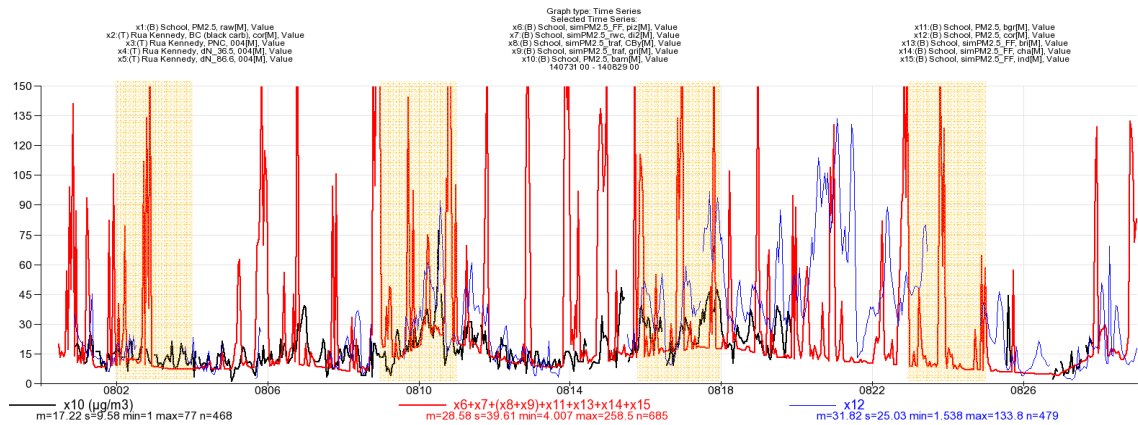


Figure 4.4.5 Comparison at station B between monitored PM2.5 (BAM instrument = black, DustTrak instrument = blue) and total simulated PM2.5 including restaurants, industry, RWC, traffic, brick and coal production and the interpolated background concentration of Fig. 4.4.4 (red).

Figure 4.4.6 shows the comparison between the monitored PM2.5 and sum of the simulated contributions at station T, including background of Fig. 4.4.4. As can be seen the impact of RWC – the source emitting during evening-night - is overestimated in the model simulation.

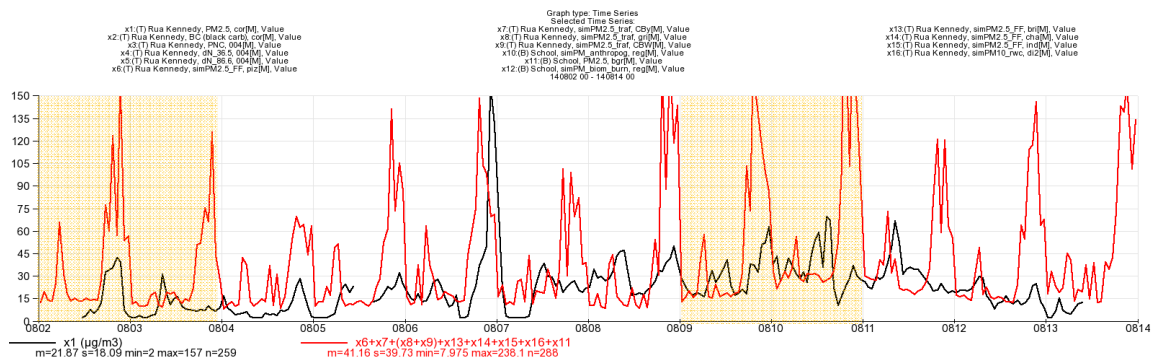


Figure 4.4.6 Comparison at station T between monitored PM2.5 and simulated total PM2.5 from pizzerias, industry (inside and outside the city), RWC, traffic and the background contribution of Fig. 4.4.4 (red).

The final comparison is made at station L, a residential area in the southern part of Sapiranga (Fig. 4.4.7). Here we can see that the model is no longer overestimating the levels, measured and simulated peaks are of the same size. However, the model simulated peaks are narrower and show a larger temporal variation, as compared to monitored PM2.5.

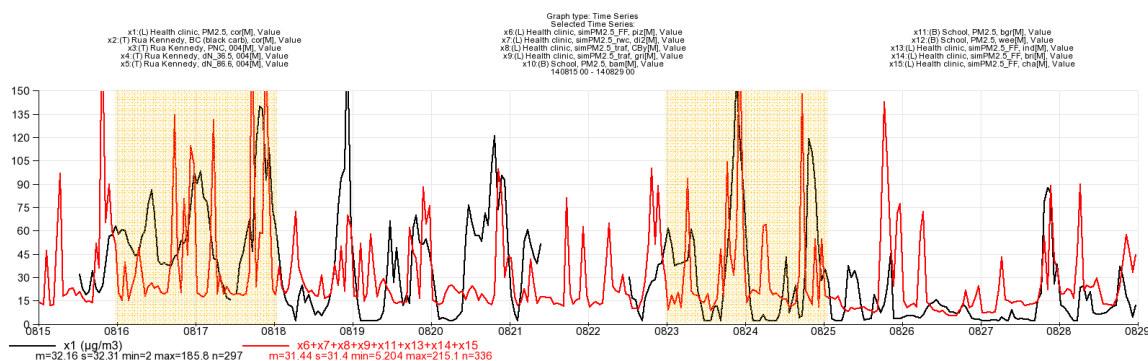


Figure 4.4.7 Comparison at station L between monitored PM2.5 (black) and total simulated PM2.5 including pizzerias, industry (inside and outside the city), RWC, traffic and the background concentrations of Fig. 4.4.4 (red).

The comparison between measured and simulated levels, including a background concentration from incoming air estimated from the baseline of station B PM2.5 BAM data, has given the averaged levels of Table 4.4.2 (the simulated values excluding background are those of Table 4.4.1). We can thus see that the simulated PM2.5 levels show

- an overestimation at station B
- an overestimation at station T
- more similar levels at station L

In Section 4.5 we will analyze possible reasons for these deviations between simulated and monitored data.

Table 4.4.2 Simulated contributions to PM2.5 at station B, T and L.
Period: July 31 – August 29, 2014.

Site	simulated excl. background	simulated incl. background	monitored BAM & Harvard Impactor
B	17.8	34.5	17.2 ³
T	28.2	44.8	24.0
L	22.2	38.8	32.5

It is also possible to compare the 5 mobile monitoring events presented in Fig. 4.2.22. First we compare the spatial average concentrations all over the city (23 monitoring points), per

³ Uncertain level as data capture was only 67% and losses during peak values are suspected.

event (Fig. 4.4.8). As can be seen the simulated levels are considerably higher than the monitored levels, at least during the first two nights.

The temporal averages at each of the 23 mobile stations are shown in Fig. 4.4.9, both according to measurements and to model simulations. The tendency for high levels in the southern district 4 (São Luiz) is found both in measurements and in the model. However, in the city centre the simulated levels are too high and in general the monitored PM2.5 levels show stronger spatial gradients. There is no spatial correlation found between monitored and simulated levels at the 23 locations. This indicates that a much more detailed study is required to establish the spatial gradients in emissions (i.e. the residential wood combustion, the source that dominates the local impact).

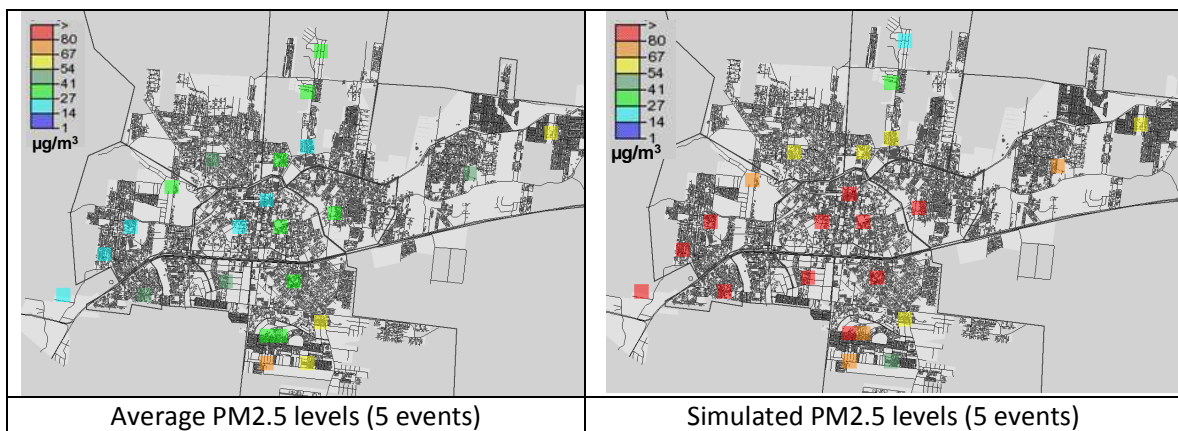
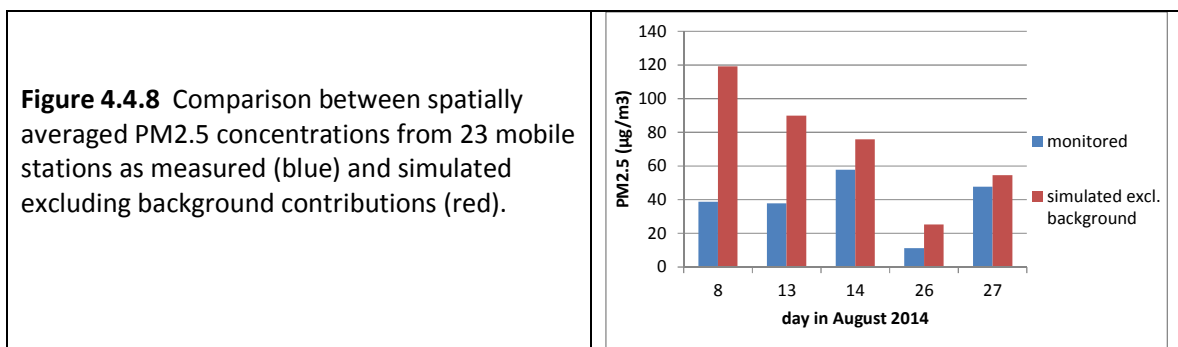


Fig. 4.4.9 PM2.5 average levels from mobile measurements during 5 nights (left) and from simulations of the same nights (right).

4.5 Integrated analysis of emissions and impact

The emission inventory provided PM_{2.5} emissions for different sectors, as well as their temporal and spatial distributions. During August 2014 the different sources contributed to emissions estimated as:

Regional area (northern RS):

- Anthropogenic: 24 528 tons/year
- Biomass: 53 431 tons/year

Local area (Sapiranga):

- Charcoal production (north Sapiranga): 202 tons/year
- Brick production (south Sapiranga): 20 tons/year
- Road traffic (exhaust particles): 12 tons/year
- Pizzerias, restaurants: 42 tons/year
- Industrial (wood combustion): 83 tons/year
- Residential wood combustion: 109 tons/year

From the model results presented earlier, we can find inconsistencies between measured and simulated levels. Our main assumption will be that there are errors in the emissions in terms of emission magnitude, but also in their spatial and temporal distribution. These errors may be found both outside Sapiranga (regional model) and inside (local model). We will discuss here if we can identify more specifically for which emission sources those errors are found, in order to come to a conclusion on PM_{2.5} and BC emissions and levels in Sapiranga.

From the analysis of particle number size distributions (Section 4.2), we identified size modes of fresh vehicle exhausts and wood combustion. There was also a slightly larger size mode that could have originated from RWC during certain conditions, and this mode had its maximum during the late night, matching the hours when RWC is mostly used.

The analysis of the elemental composition and the PMF model output also identified wood combustion as a source, but mixed with industrial emissions (Fig. 4.2.21). The elemental composition analysis pointed on a higher biomass/wood combustion impact at station L. Other tracers of anthropogenic sources like vehicles, metal industry and waste burning/incineration were also found.

The regional model assessed the strength and temporal variation of the long-range PM contribution in Sapiranga, both from anthropogenic emissions in the nearby cities as well as certain events of biomass burning in the vicinity of the city. Clearly the simulated background concentrations are too high, likely caused by overestimated anthropogenic emissions in the Porto Alegre area. However we will investigate whether a modified output of the regional model can be used together with local model output to achieve better performance at stations T and L (where good quality data are available). Of special

interest is the intermittent biomass burning signal, which seems to have affected Sapiranga during the campaign.

We will then analyze the local model output where the wood combustion impact is the dominating one, however with overestimated levels in station B and T. Possible ways of adjusting the Sapiranga emissions will be discussed, to achieve a better similarity with measured particle levels.

Finally, we will use the knowledge gained on particle and BC levels during the campaign period, to extend to annual average levels.

Regional background

Two ways of estimating the PM2.5 levels in incoming air have been presented, the regional model output and the estimate taken from the baseline of the BAM monitoring at station B. Fig. 4.5.1 shows that a reduction of the regional model contribution to 40% of the original output, will give a signal consistent with the background estimated from the station B measurement. Given the uncertainty (and data losses) of the monitored data in station B, the use of the regional model output is to be preferred; it will also provide a separation of the impact of urban emissions from that of biomass burning. The regional model will also provide a regional signal for the entire year of 2014, to be used later in the estimation of annual average PM2.5 levels in Sapiranga.

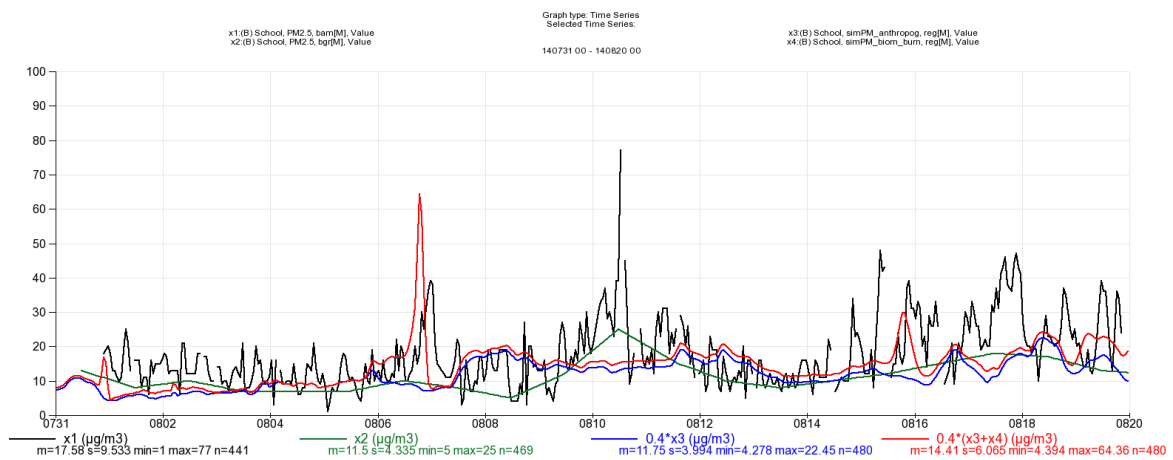


Figure 4.5.1 PM2.5 levels at station B: monitored BAM PM2.5 (black), estimated background from baseline of BAM measurement at station B (green), regionally modelled contributions from anthropogenic sources outside Sapiranga (blue) and total regionally modelled contribution including biomass burning (red). Note that the regional model output has been reduced to 40%.

The regionally simulated background signal is consistent with the lowest registered PM2.5 concentrations at station T (August 2, 4-5, 12), however a bit too high for August 25-26 (Fig. 4.5.2). The short and strong peak registered by the DustTrak instrument in the night of August 6-7 can be, as the model indicates, attributed to biomass burning.

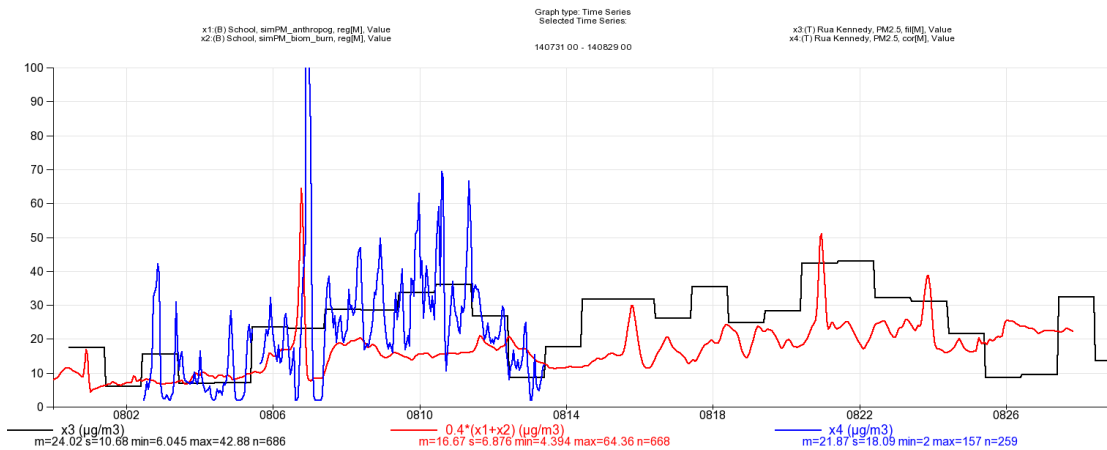


Figure 4.5.2 PM2.5 levels at station T: monitored daily PM2.5 from filter sampling (black), monitored daily values according to the (corrected) DustTrak instrument (blue) and regionally modelled long-range contribution from sources outside Sapiranga (red).

Simulated contributions from sources in Sapiranga

When adding the contributions from the local model to the regional background (red line in Fig. 4.5.2), there is a large overestimation of simulated PM2.5. Hence, we reduce the largest contribution, the one from wood burning (Table 4.4.1) to only 10%. As can be seen, this gives at station T both a comparable average PM2.5 level ($24 \mu\text{g}/\text{m}^3$) and also hourly variations with peaks comparable to the ones measured by the DustTrak instrument (blue line in Fig. 4.5.3).

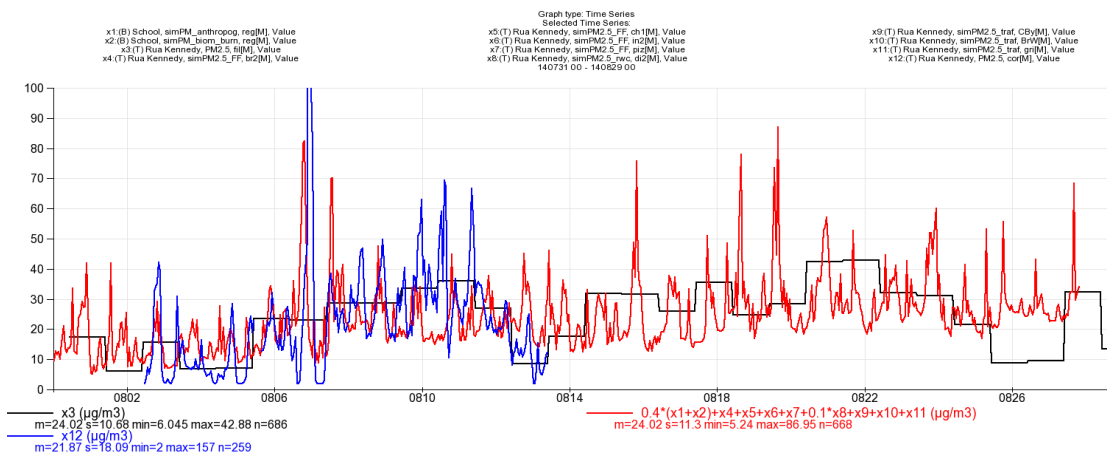


Figure 4.5.3 Measured daily PM2.5 at station T (black), measured hourly DustTrak PM2.5 (blue) and model simulated (red). The simulation includes both regional and local model output, with the impact of RWC heavily reduced to 10%.

We now compare monitored levels with the sum of the regional and local model outputs at station L. Here the reduction of the wood combustion impact was set to 70%, to achieve an average value and peak levels similar to the measured ones. Fig. 4.5.5 shows the monitored and simulated daily averages.

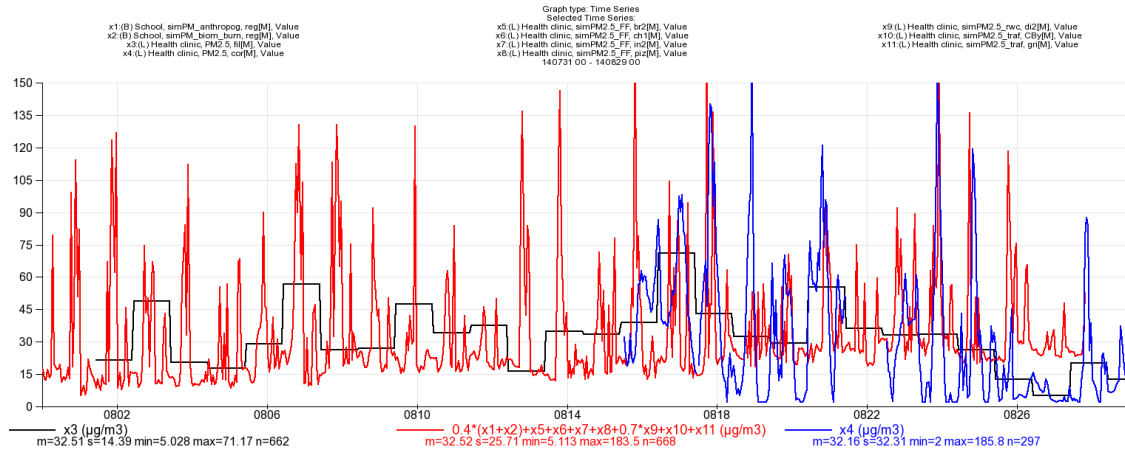


Figure 4.5.4 Measured daily PM2.5 at station L (black), measured hourly DustTrak PM2.5 (blue) and model simulated (red). The simulation includes both regional and local model output, with the impact of RWC reduced to 70%.

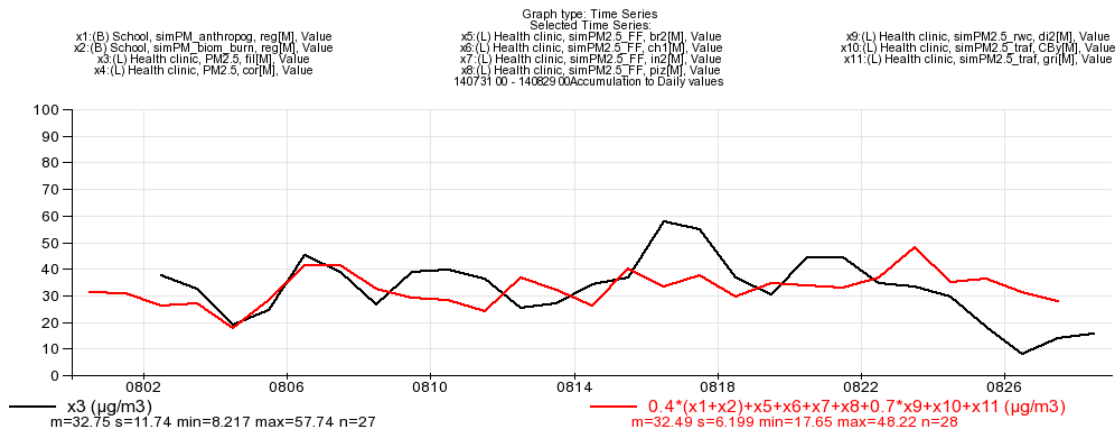


Figure 4.5.5 Daily averaged PM2.5 at station L: monitored levels (black) and model simulated (red). The simulation includes both regional and local model outputs. Here the RWC contribution was reduced to 70%, as in Fig. 4.5.4.

Emissions according to integrated analysis

We now know that the RWC source, as given by the emission inventory, is highly overestimated – 10 times - in the central area of the city (station T). However, at station L we find a monitored signal that corresponds to RWC emission of 70% of that given by the emission inventory. It is not possible to simply reduce emissions in one area, since the

impact pattern of a certain source is over the entire city (compare the distribution of the RWC emissions in Fig. 3.3.3a) and the averaged impact in Fig. 4.4.1b (upper right). Therefore we will rather consider an estimated range of emissions, even if it is clear that RWC sources close to station L are likely to emit more closer to what the inventory indicates and RWC sources in the city centre less. We learned from the mobile PM2.5 monitoring (Fig. 4.2.24) that there are various locations with similar pollution levels as around the station L, indicating a strong spatial variation in RWC.

Table 4.5.1 summarizes the analysis we performed by comparing the model outcome with monitored data.

Table 4.5.1 PM2.5 emissions during August 2014, after the integrated analysis.

source of PM2.5	factor (compared to emission inventory)	typical contribution within city (max in August, μgm^{-3})	emissions in August (tons/year)	comments
regional anthropogenic	0.4	12.5	9 800	Mainly from the Porto Alegre area
regional biomass burning	0.4	14.2	21 400	Largest emissions were found in the northeastern part of Rio Grande do Sul state.
traffic	1.0	2.0	12	Road dust not included (can typically be the same magnitude as exhaust)
pizzerias	1.0	2.5	42	From wood combustion
RWC	0.1-0.7	15 (with the 0.7 factor)	11-76 (in August, lower as an annual mean)	The geographical distribution is not correct, but total emission levels are at these magnitudes. Also temporal variation requires further research.
charcoal production	1.0	2.5	202	Highly uncertain, both in emission strength and geographical location.
brick production	1.0	<0.1	20	Uncertain, but do not show impact over the city.

Local emissions of BC are estimated through BC/PM2.5 ratios taken from the literature (Table 4.5.2). Figure 4.5.6 shows the bar diagrams for the estimated emissions in Sapiranga. The uncertainty interval for RWC is large, however the mobile measurements indicate that there are various areas of the city with similar emissions as those close to

station L. It is therefore likely that the Sapiranga RWC emissions are more in the middle or upper part of the estimated interval.

Note that wood combustion includes not only RWC emissions, but also those from restaurants and industry. Thus, wood combustion is the major source of both PM2.5 and BC within Sapiranga.

Table 4.5.2 Estimated emissions of PM2.5 and BC in Sapiranga for August 2014 (tons/year)

Source	PM2.5	BC	Ratio BC/PM2.5	comments
brick production	20	1.4	7%	<i>outside the city</i>
charcoal production	202	14.1	7%	<i>outside the city</i>
traffic exhaust	12	7.8	65%	<i>inside the city</i>
residential wood combustion	11-76	0.8-5.3	7%	<i>inside the city</i>
restaurants	42	2.9	7%	<i>inside the city</i>
industry	83	5.8	7%	<i>inside the city</i>
Total inside city:	148-213	17-22		
Total Sapiranga:	370-435	33-37		

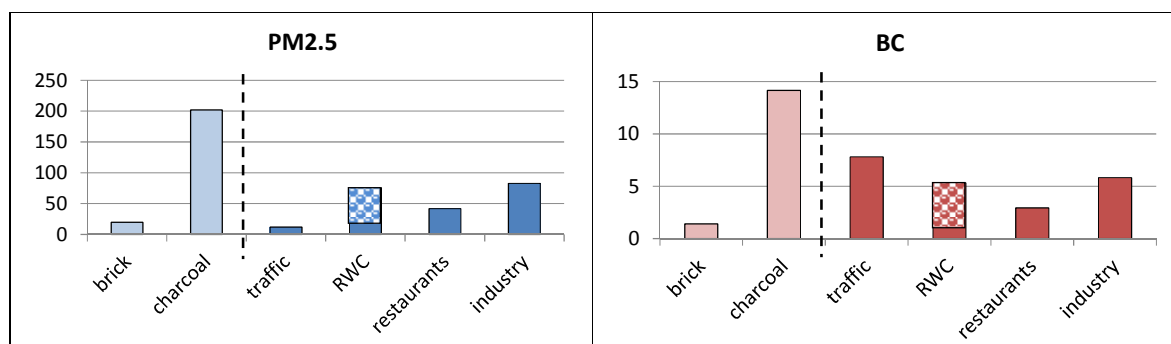


Figure 4.5.6 Estimated emissions of PM2.5 and BC for August 2014, after the integrated analysis, expressed as tons/year. The first two sources are located outside the residence areas of Sapiranga. The uncertainty of the RWC source is indicated as an interval, as in Table 4.5.2.

Source contributions to monitored levels at station T and L

Figure 4.5.7 shows the source contributions to monitored PM2.5 levels at stations T and L in August 2014, according to the integrated analysis. The regional background PM2.5 explains 69% in station T and 51% in station L. Although the charcoal production north of Sapiranga has large emissions, its impact on these two stations is minor. Even at station T, the RWC source is the largest local contributor and it is the completely dominating local source at station L.

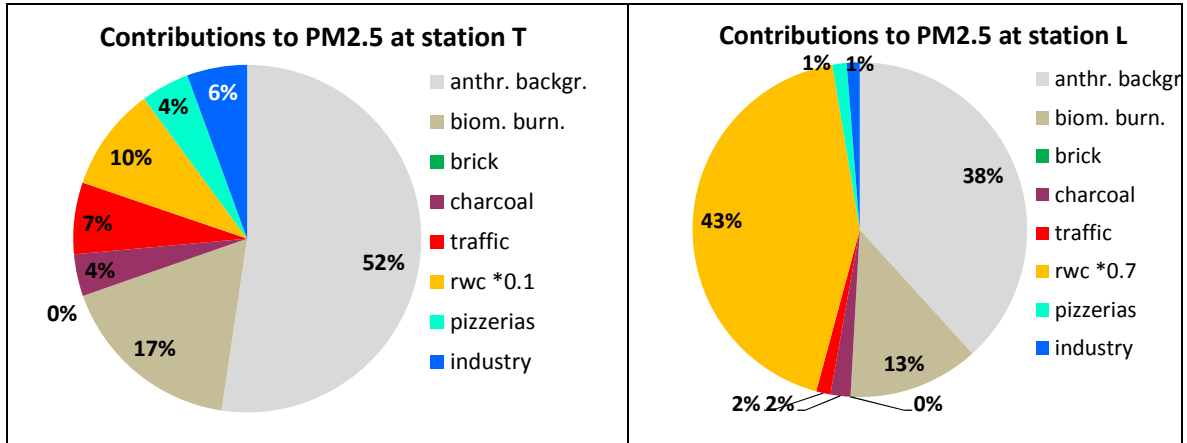


Figure 4.5.7 Contributions of different PM2.5 sources during August 2014, according to the integrated analysis of monitor data and model simulations. Monitored PM2.5 levels were 24.0 $\mu\text{g}/\text{m}^3$ (station T) and 32.5 $\mu\text{g}/\text{m}^3$ (station L).

Figure 4.5.8 shows the source contributions to BC levels. In areas where traffic is intense, like in the city centre and station T, road vehicle emissions are the dominating local source. In residential areas like station L, the RWC source dominates.

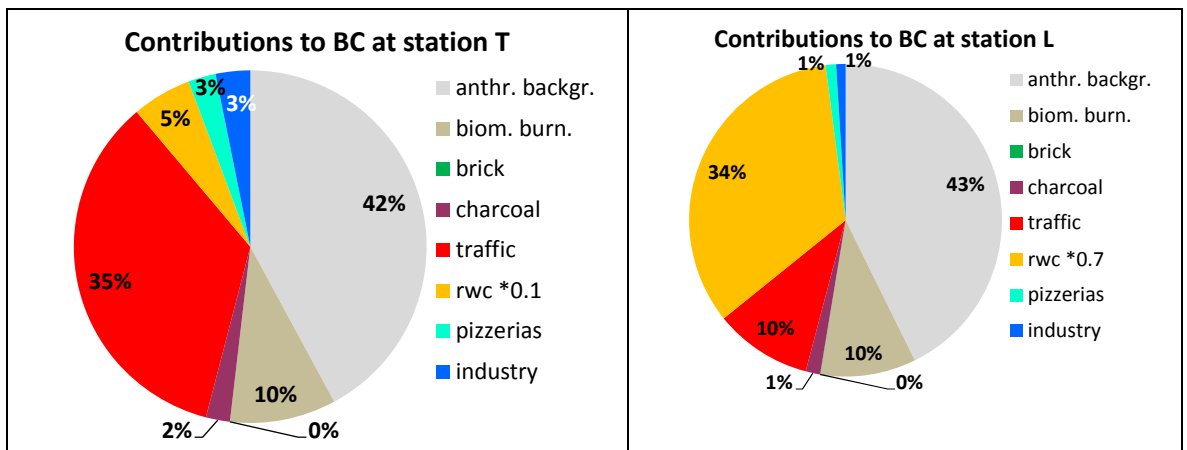


Figure 4.5.8 Contributions of different BC sources during August 2014, according to the integrated analysis of monitor data and model simulations. Monitored EC levels were 1.8 $\mu\text{g}/\text{m}^3$ at both stations. We use a BC/EC ratio of 1.5 (Table 4.2.5) to estimate a BC level of 2.7 $\mu\text{g}/\text{m}^3$ at both stations as an average concentration for August 2014.

Transformation to annual average emissions and concentrations

The results presented so far described the conditions during the monitoring campaign in August 2014. We now extrapolate the August 2014 values to annual averages for 2014 with the support from regional and local model results. Figure 4.5.9 is used to estimate the annual variability of source contributions. The anthropogenic contribution during the full year 2014, as compared to the contribution in August 2014, was 85%. The estimation for biomass burning was 55% and for local RWC in Sapiranga was 34% (the last low percentage is a consequence of the assumed variation in wood burning, Table 3.3.2). For other sources, the emissions were assumed to be constant over the year.

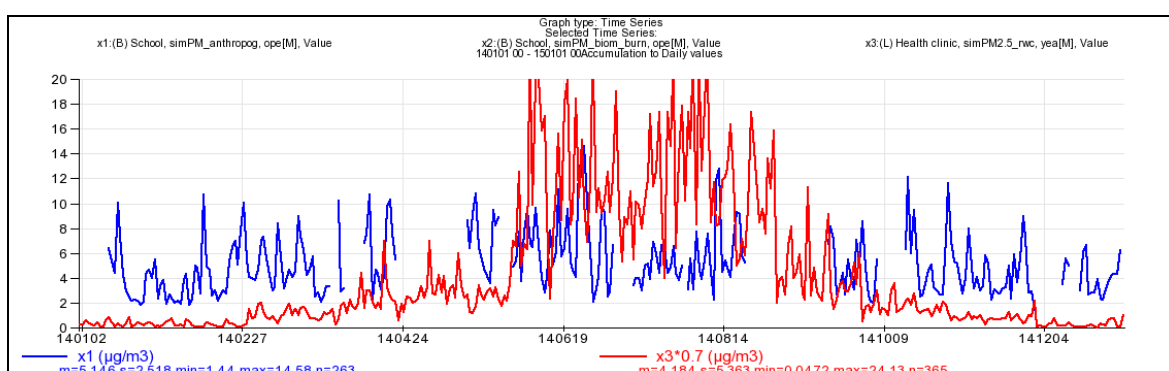


Figure 4.5.9 Simulated daily average values for the entire year 2014 taken from the CCATT-BRAMS operational model with model domain covering the entire South America (blue) and local simulation of the RWC source within Sapiranga (red).

With support from those relationships, we estimate the average emissions in 2014 as listed in Table 4.5.3 and Fig. 4.5.10.

Table 4.5.3 Estimated annual average emissions of PM2.5 and BC in Sapiranga during 2014 (tons/year)

Source	PM2.5	BC	Ratio BC/PM2.5	comments
brick production	20	1.4	7%	<i>outside the city</i>
charcoal production	202	14.1	7%	<i>outside the city</i>
traffic exhaust	12	7.8	65%	<i>inside the city</i>
residential wood combustion	4-26	0.3-1.8	7%	<i>inside the city</i>
restaurants	42	2.9	7%	<i>inside the city</i>
Industry	83	5.8	7%	<i>inside the city</i>
Total inside city:	140-163	16-18		
Total Sapiranga:	363-385	32-34		

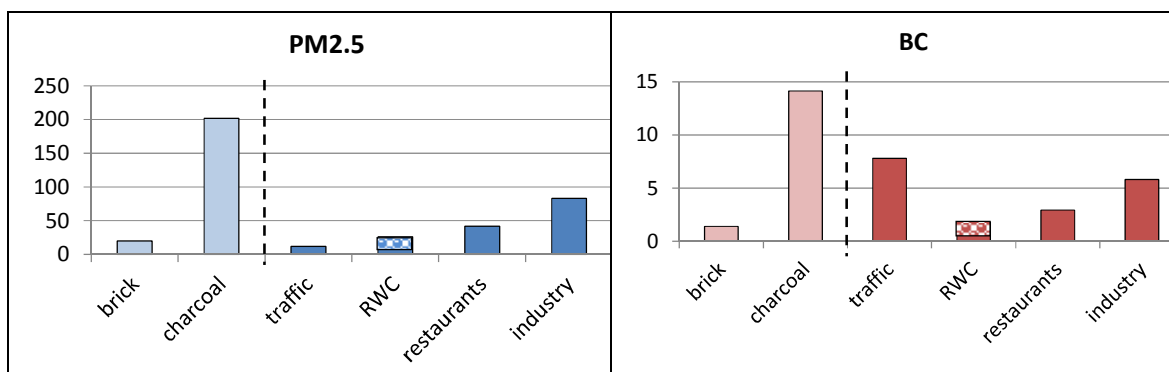


Figure 4.5.10 Estimated annual average emissions of PM_{2.5} and BC during 2014, after the integrated analysis, expressed as tons/year. The first two sources are located outside the residence areas of Sapiranga. The uncertainty of the RWC source is indicated as an interval, as in Table 4.5.3.

The corresponding annual average concentrations and source contributions to PM_{2.5} and BC at station T and L are displayed in Figs. 4.5.11 and 4.5.12. The PM_{2.5} concentrations are now just below 20 µg/m³ at both stations, which is still rather high when compared with the reported values from Porto Alegre and other Brazilian cities (Table 4.2.2) and it is also at the level of the São Paulo state limit value for PM_{2.5}.

The local contribution to PM_{2.5} levels from RWC is small at station T, although total impact of wood combustion – RWC, charcoal, restaurants and industry – sum up to 22% (Fig. 4.5.11). At station L, the RWC source is still the largest local source.

For BC the traffic is the dominating source at station T, but at station L the contribution from RWC is of the same magnitude as traffic. The annual mean BC levels in Sapiranga are estimated to 2.3 at station T and 1.8 µg/m³ at station L.

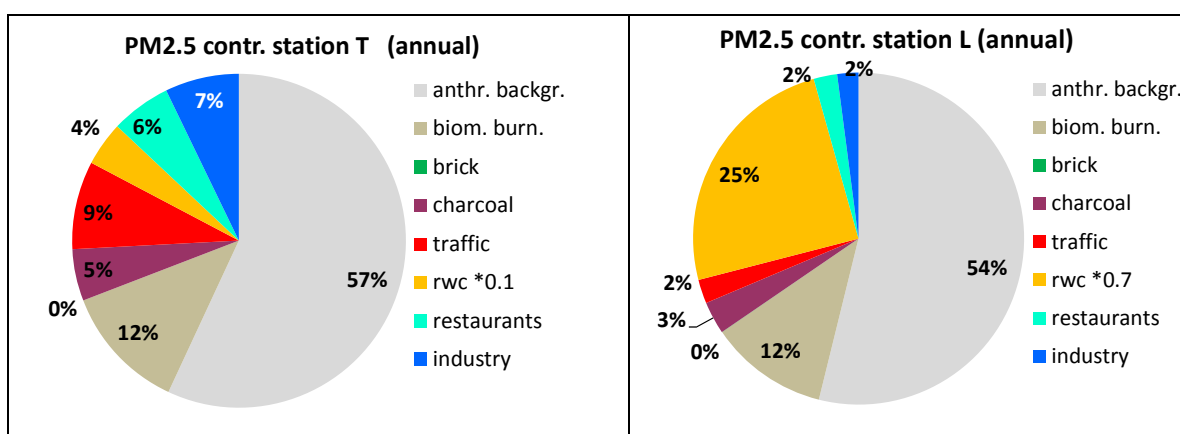


Figure 4.5.11 Estimated contributions of different PM_{2.5} sources for the year 2014, according to the integrated analysis of monitor data and model simulations. Simulated annual average for PM_{2.5} were 18.6 µg/m³ (station T) and 19.7 µg/m³ (station L).

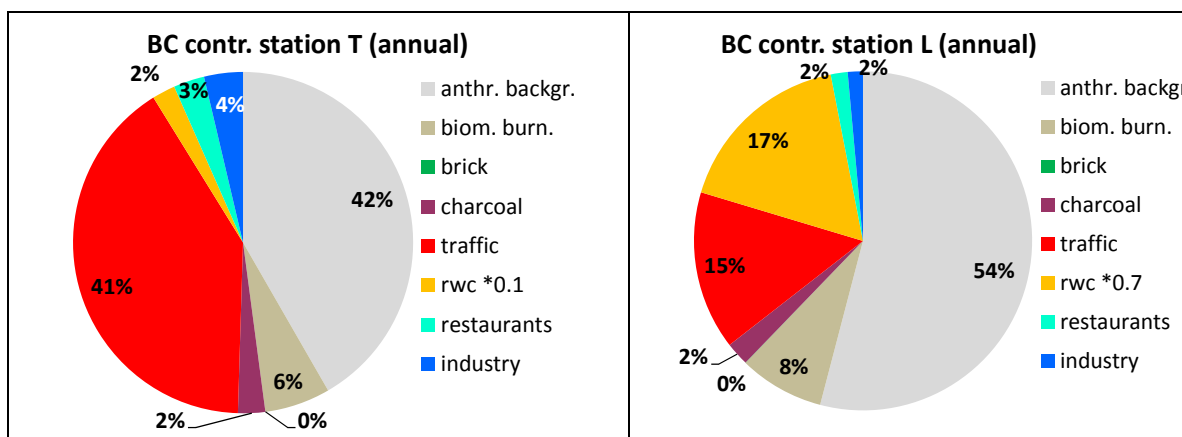


Figure 4.5.12 Estimated contributions of different BC sources for the year 2014, according to the integrated analysis of monitor data and model simulations. BC levels were estimated to $2.3 \mu\text{g}/\text{m}^3$ at station T and $1.8 \mu\text{g}/\text{m}^3$ at station L.

5 Conclusions

Levels of fine particles in Sapiranga are comparable or slightly higher than those reported from the Metropolitan area of Porto Alegre. There is no limit value for fine particles in Rio Grande do Sul state, but the annual average PM_{2.5} levels determined for Sapiranga are at the limit value for the São Paulo state legislation ($20 \mu\text{g}/\text{m}^3$). Therefore it is of interest to identify the main sources of the fine particle pollution in Sapiranga.

The measurements and model simulations show that the background air arriving to Sapiranga is responsible for 65-70% of the annual mean pollution within the city. Sources outside Sapiranga are found in particular in the urbanized areas between Porto Alegre and Sapiranga, but there are also frequent vegetation fires to the north of the city that generates significant particle pollution during parts of the year. In Sapiranga center (station T) wood combustion, used in connection with commercial/industrial activities as well as for heating and cooking in residential areas, contribute to about 22% and local traffic exhausts for the remaining 9% of the measured PM_{2.5} level. In some residential areas, exemplified with São Luiz where station L was located, the residential wood combustion is the dominating local source (25% contribution to measured PM_{2.5} level for RWC, 32% for all local wood combustion sources), even more accentuated during winter conditions (43% for RWC). The mobile monitoring campaign indicates that conditions can be similar in other residential areas of Sapiranga.

For BC the annual mean levels are estimated to be between 1.5 and $2.5 \mu\text{g}/\text{m}^3$, with a more dominating contribution from local traffic exhausts, although RWC also contributes significantly in residential areas like at station L.

6 Recommendations

The main objectives with the Sapiranga pilot project were to estimate the emissions of fine particles and black carbon, and determine the impact of those emissions on the air quality in the city. With those results as a basis, there are possibilities to identify actions and measures that can reduce both emissions and pollution levels. We will briefly discuss some areas where actions could contribute to lower the air pollution levels in Sapiranga.

1. Actions in the Porto Alegre Metropolitan area: About half of the air pollution in Sapiranga is caused by sources in Porto Alegre, Novo Hamburgo and other urbanized areas outside Sapiranga itself. Improved technology of the vehicle fleet, a stricter annual inspection of the maintenance programs and status of the vehicles and especially a renewal of the heavy duty diesel vehicles of the Rio Grande do Sul state would lower the contribution from road traffic. The chemical analysis of particles sampled in Sapiranga indicates rather large contributions from industrial sources, especially metallurgic industry and waste burning. Open biomass burning is also a significant contributor and possible ways of controlling those should be considered.
2. Industrial/commercial sources in Sapiranga: All of those, representing charcoal and brick production as well as restaurants, use wood combustion with a rather old technology and without cleaning the exhaust gases. Emissions are large for the industrial sources, however they are mostly situated outside the residential part of Sapiranga and have less effect on population exposure. The small scale of the industry - typically family own plants - can possibly make it difficult to demand a change to a new and improved technology (which may be comparatively expensive), however improved operation and use of dry wood could have positive effects on the emissions and should be requested. The restaurant sources are inside the city and their impact is larger, but obviously the use of wood for baking pizzas are deeply traditional and not easily changed by, e.g., a switch to electric ovens. Reporting wood consumption/supplier and controlling wood quality (dryness) could have a certain positive effect on wood-burning sources.
3. Residential sources: This study did not quantify the burning of waste and garden residues outside. Still this could be an important source of pollutants and should be minimized. Especially waste may contain toxic elements which could be cleaned out if burned in efficient waste incineration plants.

The pilot project focused the use of residential wood combustion for heating and cooking, which according to the questionnaire is fairly common in many residential areas. It is clear that actions to improve the operation and technology of those fireplaces, as well as to replace the wood combustion with cleaner fuels like pellets, gas and electricity, would imply efficient ways to reduce particle pollution in the city. Here are some examples to illustrate what can be done:

A traditional open fireplace has an efficiency of less than 15%. A change to a more modern solution, which has an efficiency of up to 75%, will reduce the fuel consumption with 80%. This means that by burning 1/5 of wood you will get the same heat. The main technology that a modern fireplace benefits from is the control of air. In a traditional fireplace the fire sucks air from the room, warms it, but loses most of the heat through the chimney. This process also implies that cold air from the outside is sucked into the room through leaky windows and doors. Also when there is no fire the warm air from indoor can escape through the chimney that is often completely open. The modern fireplace uses doors to control the inlet of air and a damper in the chimney that can be closed when there is no or little fire. Another way to increase the efficiency is to increase the transport of warm air from the fireplace to the rest of the house. Obviously an improved house isolation will lower the wood consumption and emissions, reducing the cold outside air to enter and maintaining the heated indoor air for a longer time.

Particle emissions from a fireplace is highly depending on wood moisture. The burning efficiency increases and emissions decreases with the use of dry (<20% moisture content) wood. Good quality of the wood can be obtained by storing it indoors (ventilated) or at least under roof for about a year, before its use as a fuel.

4. Road traffic: In this project we have identified that the fleet of heavy duty includes a large fraction of old vehicles produced before year 2000. We cannot say how much these are used but assume that they are driven as much as newer vehicles. This is an assumption that lies behind the reported result in emissions and concentrations in Sapiranga. The use of older diesel vehicles is known to be a dominant source of particles and especially Black Carbon. California has, as an example, implemented local and state regulations on diesel vehicles and thereby decreased the BC emissions on diesel-dominated southern California freeways by 40% between 2009 and 2011 (Kozawa et al., 2014). Diesel exhaust is proved to be carcinogenic in high concentrations (Silverman et al., 2012; Attfield et al., 2012).
5. Phasing out highly emitting old diesel vehicles in Sapiranga can reduce the particulate matter and BC in the ambient air of the city. A brand new heavy duty vehicle emits about 2% of an old vehicle and the emission reduction among vehicles produced before the year of 1999, as compared to those produced after 1999, is at least 50% (CETESB, 2014). If all heavy duty vehicles from before 1999 were replaced by vehicles from 2000 the reduction of the traffic PM emission would be 40%, if they were replaced by vehicles produced after 2012 the reduction would be 80%.

7 Acknowledgements

This project has been initiated as an activity within the framework of the Memorandum of Understanding to cooperate in the fields of environmental protection, climate change and sustainable development, signed between the Swedish and Brazilian Ministries of Environment. The technical cooperation has been achieved with support from the Swedish Ministry of Environment, Fundação Estadual de Proteção Ambiental Henrique Luiz Roessler (FEPAM), Universidade Federal de Pelotas, Universidade Tecnológica Federal do Paraná (UTFPR), Centro Mario Molina Chile and the Prefeitura Municipal de Saporanga.

We also acknowledge the collaboration offered by Instituto Nacional de Meteorologia (INMET) for offering meteorological data from the Campo Bom station, and other local entities and individuals in Saporanga that allowed the project team to complete the monitoring campaign and perform the recompilation of activities and information required for the emission inventory.

8 References

- Alonso, M. F., Longo, K. M., Freitas, S. R., Fonseca, R. M., Marecal, V., Pirre, M., Gallardo, L., 2010. An urban emissions inventory for South America and its application in numerical modeling of atmospheric chemical composition at local and regional scales. *Atmospheric Environment*, 44, 5072-5083.
- Attfield, MD., Schlieff, PL., Lubin, JH., 2012 The diesel exhaust in miners study: a cohort mortality study with emphasis on lung cancer. *J Natl Cancer Inst.* March 2, 2012. doi:10.1093/jnci/djs035.
- Berkowicz, R., 2000. OSPM – a parameterised street pollution model. *Environmental Monitoring and Assessment*, 65, 323-331.
- Berkowicz, R. and Prahm, L. P., 1982. Evaluation of the Profile Method for Estimation of Surface Fluxes of Momentum and Heat. *Atmos. Environ.* 16, 2809-2819
- CETESB 2014 (São Paulo). Emissões veiculares no estado de São Paulo 2013 [recurso eletrônico] CETESB ; Coordenação técnica Marcelo Pereira Bales ; Elaboração Antônio de Castro Bruni [et al.]. - - São Paulo : CETESB, 2014. 1 arquivo de texto (150 p.) : il. color., PDF ; 3,77MB. - - (Série Relatórios / CETESB, ISSN 0103-4103)

- Charron, A., Harrison, R.M., 2003. Primary particle formation from vehicle emissions during exhaust dilution in the roadside atmosphere. *Atmospheric Environment* 37, 4109-4119.
- Crassier, V.; Syhre, K.; Tulet, P.; Rosset, R., 2000. Development of a reduced chemical scheme for use in mesoscale meteorological models, *Atmospheric Environment*, v. 34, 2633–2644.
- Danard, M., 1977. A Simple Model for Mesoscale Effects of Topography on Surface Winds. *Monthly Weather Review*, 99, 831-839.
- Djouad R., Sportisse B., Audiffen N., 2002. Numerical simulation of aqueous phase atmospheric models: use of a non-autonomous Rosenbrock method. *Atmospheric Environment*, v. 36, n. 5, 873-879.
- EMEP/EEA, 2013, Emission inventory guidebook 2013, EEA Technical report NO 12/2013, EEA.
- FEPAM, 2010. 1º Inventário de emissões atmosféricas das fontes móveis do estado do Rio Grande do Sul- ano base -2009.
- FEPAM, 2014. Diagnóstico da qualidade do ar no Rio Grande do Sul no period de 2003 a 2012. FEPAM report, 99 pp.
- Freitas, S. R., Longo, K. M., Alonso, M. F., Pirre, M., Marecal, V., Grell, G., Stockler, R., Mello, R. F., Sánchez Gácita, M., 2011. PREP-CHEM-SRC 1.0: a preprocessor of trace gas and aerosol emission fields for regional and global atmospheric chemistry models. *Geoscientific Model Development*, v. 4, p. 419-433.
- Grell G.A., Dévényi D., 2002. A generalized approach to parameterizing convection combining ensemble and data assimilation techniques. *Geophysical Research Letters*, v. 29, n.14, 38.1-38.4.
- Guenther, A., Karl, T., Harley, P., Wiedinmyer, C., Palmer, P.I., Geron, C., 2006. Estimates of global terrestrial isoprene emissions using MEGAN (Model of Emissions of Gases and Aerolos from Nature), *Atmos. Chem. Phys*, 6, 3181-3210.
- Holtslag A. A. M., 1984. Estimates of Diabatic wind Speed Profiles from Near Surface Weather Observations. *Boundary Layer Meteorology* 29, 225-250.
- Hossain, A.M.M.M., Park, S., Kim, J.-S., Park, K., 2012. Volatility and mixing states of ultrafine particles from biomass burning. *Journal of Hazardous Materials* 205-206, 189-197.
- Hussein, T., Hämeri, K., Aalto, P.P., Paatero, P., Kulmala, M., 2005. Modal structure and spatial-temporal variations of urban and suburban aerosols in Helsinki-Finland. *Atmospheric Environment* 39, 1655-1668.

- Josse, B. ; Simon, P.; Peuch, V-H., 2004. Radon global simulations with the multiscale chemistry and transport model MOCAGE. *Tellus*, v. B 56, 339-356.
- Kittelson, D.B., Watts, W.F., Johnson, J.P., 2006a. On-road and laboratory evaluation of combustion aerosols – Part 1: Summary of diesel engine results. *Aerosol Science* 37, 913-930.
- Kittelson, D.B., Watts, W.F., Johnson, J.P., Schauer, J.J., Lawson, D.R., 2006b. On-road and laboratory evaluation of combustion aerosols - Part 2: Summary of spark ignition engine results. *Aerosol Science* 37, 931-949.
- Kozawa, K.H Park, S.S., Mara, S.L., Herner, J.D. 2014. Verifying Emission Reductions from Heavy-Duty Diesel Trucks Operating on Southern California Freeways. *Environmental Science & Technology*, Volume:48 Issue:3 Pages:1475-1483 DOI:10.1021/es4044177
- Kumar, P., Fennel, P., Britter, R., 2008. Effect of wind direction and speed on the dispersion of nucleation and accumulation mode particles in an urban street canyon. *Science of the Total Environment* 402, 82-94.
- Kumar, P., Robins, A., Vardoulakis, S., Britter, R., 2010. A review of the characteristics of nanoparticles in the urban atmosphere and the prospects for developing regulatory controls. *Atmospheric Environment* 44, 5035-5052.
- Longo, K M., Freitas, S. R., Andreae, M. O., Yokelson, R., Artaxo, P., 2009. Biomass burning, long-range transport of products, and regional and remote impacts. *American Geophysical Union*, v. 186, 207–232.
- Longo, K. M., Freitas, S. R., Pirre, M., Marécal, V., Rodrigues, L. F., Panetta, J., Alonso, M. F., Rosário, N. E., Moreira, D. S., Gácita, M. S., Arteta, J., Fonseca, R., Stockler, R., Katsurayama, D. M., Fazenda, A., Bela, M., 2013. The Chemistry CATT-BRAMS model (CCATT-BRAMS 4.5): a regional atmospheric model system for integrated air quality and weather forecasting and research. *Geoscientific Model Development*, v. 6, p. 1389-1405.
- Maura de Miranda, R., de Fatima Andrade, M., Fornaro, A., Astolfo, R., Afonso de Andre, P., Saldiva, P., 2012. Urban air pollution: a representative survey of PM2.5 mass concentrations in six Brazilian cities. *Air Qual Atmos Health*, 5, 63-77. DOI 10.1007/s11869-010-0124-1.
- MIDEPLAN-SECTRA, 2010. Implementación del Modelo Cálculo de Emisiones Vehiculares (MODEM) en Ciudades con Planes de Transporte y Planes de Gestión de Tránsito.

- Morawska, L., Ristovski, Z., Jayaratne, E.R., Keogh, D.U., 2008. Ambient nano and ultrafine particles from motor vehicle emissions: Characteristics, ambient processing and implications on human exposure. *Atmospheric Environment* 42, 8113-8138.
- Paatero, P., and Hopke, P. K., 2003. Discarding or downweighting high-noise variables in factor analytic models, *Anal. Chim. Acta*, 490, 277-289, 10.1016/s0003-2670(02)01643-4.
- Rosário, N. E., Longo, K. M., Freitas, S. R., Yamasoe, M. A., and Fonseca, R. M., 2013. Modeling the South American regional smoke plume: aerosol optical depth variability and surface shortwave flux perturbation, *Atmos. Chem. Phys.*, 13, 2923—2938, doi:10.5194/acp-13-2923-2013.
- Rosário, N. M. E.: Variability of aerosol optical properties over South America and the impacts of direct radiative effect of aerosols from biomass burning, Ph.D. thesis, Institute of Astronomy, Geophysics and Atmospheric Sciences, University of São Paulo, São Paulo, 2011 (in Portuguese).
- Olivier, j.g.j.; Berdowski, j.j.m., 2001. Global emissions sources and sinks. in: Berdowski, j.; Guicherit, r.; b.j. heij (eds.) *the climate system, lisse, the netherlands.balkema publishers/swets & zeitlinger publishers*,2001. p. 33-78. a.a. isbn 90 5809 255 0.
- Pio, C., Cerqueira, M., Harrison, R.M., Nunes, T., Mirante, F., Alves, C., Oliveira, C., Sanchez de la Campa, A., Artíñano, B., Matos, M., 2011. OC/EC ratio observations in Europe: Re-thinking the approach for apportionment between primary and secondary organic carbon. *Atmos. Environ.*, 45, 6121-6132.
- Silverman, DT., Samanic, C.M., Lubin, J.H., 2012. The diesel exhaust in miners study: a nested case-control study of lung cancer and diesel exhaust. *J Natl Cancer Inst.* March 2, 2012. doi:10.1093/jnci/djs034.
- Teyssède, H.; Michou, M.; Clark, H. L.; Josse, B.; Karcher, F.; Olivé, D.; Peuch, V.-H; Saint-Martin, D.; Cariolle, D.; Attié, J.-L.; Nédélec, P.; Ricaud, P.; Thouret, V.; Van der, A R. J.; Volzthomas, A.; Chéroux F., 2007. A new tropospheric and stratospheric Chemistry and Transport Model MOCAGE-Climat for multi-year studies: evaluation of the present-day climatology and sensitivity to surface processes. *Atmospheric Chemistry and Physics*, v. 7, 5815-5860.
- Tie, x.; Madronich, s.; Walters, s.; Zhang, r.; Rasch, p.; Collins, w., 2003. Effect of clouds on photolysis and oxidants in the troposphere. *journal of geophysical research*, v. 108, n. d20, 4642-4664.

Tremback, c.; Powell , j.; Cotton , w.r.; Pielke, r., 1987. The forward in time upstream advection scheme: extension to higher orders, monthly weather review, v. 115, 540-555.

Tripoli, g.j.; Cotton w.r., 1982. The colorado state university three-dimensional cloud/mesoscale model -- 1982. part i: general theoretical framework and sensitivity experiments. journal de recherches atmospheriques,v. 16, 185-220.

van Ulden, A.P. and Holtslag, A.A.M., 1985. Estimation of atmospheric boundary layer parameters for diffusion applications. J. of Climate and Applied Meteorology, Vol. 24, 1196-1207.

Wardoyo, A.Y.P., Morawska, L., Ristovski, Z.D., Marsh, J., 2006. Quantification of particle number and mass emission factors from combustion of Queensland trees. Environmental Science & Technology 40, 5696-5703.

Wehner, B., Uhrner, U., von Lowis, S., Zallinger, M., Wiedensohler, A., 2009. Aerosol number size distributions within the exhaust plume of a diesel and a gasoline passenger car under on-road conditions and determination of emission factors. Atmospheric Environment 43, 1235-1245.